Investigation into the underlying mechanisms of diabetic cardiomyopathy using a mouse model of diabetes

A thesis submitted to The University of Manchester for the degree of Doctor of Philosophy in the Faculty of Medical and Human Sciences

2015

Riyad Adnan Al-Maimani

School of Medicine

List of contents

Word count 28,497

List of figures

List of tables

List of abbreviations

ABCC8	ATP-binding cassette, sub-family C, member 8
Adra1a	Adrenergic receptor, alpha 1a
Adrb3	Adrenergic receptor, beta 3
AGEs	Advanced glycation end products
ANGII	Angiotensin II
Aqp2	Aquaporin 2
AT1R1a	Angiotensin type 1a
AT1Rs	Angiotensin type 1 receptors
ATLAS	Assessment of Treatment with Lisinopril and Survival
ATP	Adenosine triphosphate
BAS	Bile acid sequestration
BCA	Bicinchoninic acid
BCAA	Branched-chain amino acid
BLK	Tyrosine kinase, B-lymphocyte specific
BNP	Brain natriuretic peptide
BP	Blood Pressure
BSA	Bovine serum albumin
Ca^{2+}	Calcium
CAD	Coronary artery disease
cDNA	Complimentary DNA
Cebpa	CCAAT/Enhancer Binding Protein (C/EBP), Alpha
CEL	Carboxyl-ester lipase
CHCl3	Chloroform
CHD	Coronary heart disease
CIRKO	Cardiac insulin receptor knockout
COL1A1	Collagen 1 alpha 1
COL3A1	Collagen III alpha 1
CSA	Cross sectional area
Ctla4	Cytotoxic T-lymphocyte-associated protein 4
Cu^{1+}	Copper sulphate ions
CVD	Cardiovascular disease
db/db mice	Diabetic/diabetic mouse model
ddH_2O	Double-distilled water
DEPC	Diethylpyrocarbonate
dIVS	Intraventricular septum in diastole
dLVD	Left ventricle end diastolic

DM	Diabetes mellitus
DNA	Deoxyribonucleic acid
DOCA	Deoxycorticosterone acetate
dP/dt_{max}	Maximum rate of pressure change in left ventricle
dP/dt_{min}	Minimum rate of pressure change in left ventricle
dPW	Posterior wall thickness in diastole
DPX	Distyrene, plasticizer and xylene
Echo	Echocardiography
EDTA	Ethylenediaminetetracetic acid
EF	Ejection fraction
ENU	N-ethyl-N-nitrosourea
Fbp1	Fructose-1,6-bisphosphatase 1
FBPase1	Fructose 2,6-bisphosphate
FBS	Fasting blood sugar
FFAs	Free fatty acids
FoxO	Forkhead box-containing protein, O subfamily
FS	Fractional shortening
FXR	Farnesoid X receptor
G6pc	Glucose-6-phosphatase
GAPDH	Glyceraldehyde-3-Phosphate Dehydrogenase
GC	Gas chromatography
Gcgr	Glucagon receptor
GCK, GK	Glucokinase
GLUT1,2,3,4	Glucose transporter 1,2,3,4
Gpd1	Glycerol-3-phosphate dehydrogenase 1 (soluble)
GSK3	Glycogen synthase kinase 3
H&E	Heamatoxylin and eosin
HF	Heart Failure
HMDB,	Human Metabolome Database
HNF-1α	Hepatocyte nuclear factor 4α
HNF1A	Hepatocyte nuclear factor 1α
HNF1B	Hepatocyte nuclear factor 1β
Hnf4a	Hepatic nuclear factor 4, alpha
HO	Homozygous
HR	Hazard ratio
HRP	Horse-radish peroxidise
HT	Heterozygous
HTN	Hypertension
HW/BW	Heart rate/ body weight ratio
IDF	International diabetes federation
Ifng	Interferon gamma

IGF-Akt	Protein kinase B
IMS	Industrial methylated spirit
INS	Insulin
IPF1/PDX	Insulin promoter factor 1/ Pancreatic and duodenal homeobox 1
IRS-2	Insulin receptor substrate-2
IS1	Internal standards for polar fraction
IS2	Internal standards for non polar fraction
IS3	Internal standard
ITT	Insulin tolerance test
IVS	Interventricular septum
KEGG	Kyoto Encyclopedia of Genes and Genomes
KLF11	Kruppel-like factor 11
l12b	Interleukin 12B
LPL	Lipoprotein lipase
LPLs	Lysophospholipids
LV	Left ventricular
LV/TL ratio	Left ventricular/tibia length ratio
LVH	Left ventricular hypotrophy
lysoPCs	Lyso-glycerophosphocholines
MAP	Mitogen-activated protein
MeOH	Methanol
MI	Myocardial infraction
MMD	Manchester metabolomics database
mmHg	Millimeter of mercury
MODY	Maturity onset diabetes of the young
MRC	Medical research council
mRNA	Messenger RNA
MS	Mass spectrometry
MSTFA	(N-acetyl-N-(trimethylsilyl)-trifluoroacetamide)
mTOR	Mammalian target of rapamycin
MuRF-1	Muscle-specific ubiquitin ligases atrogin-1
NeuroD1	Neurogenic differentiation factor 1
ob/ob mice	Obese/obese mouse model
Parp1	Poly (ADP-ribose) polymerase family, member 1
PAX4	Paired box gene 4
PBS	Phosphate buffered saline
PCA	Principal components analysis
Pck1	Phosphoenolpyruvate carboxykinase
Pdk4	Pyruvate dehydrogenase kinase isozyme 4
Pdx1	Pancreatic and duodenal homeobox 1

PEP	Phosphoenol pyruvate
PEPCK	PEP Carboxykinase
PFK1	Phosphofructokinase-1
PI3K	Phosphatidyl inositol 3 kinase
Pik3cd	Phosphatidylinositol 3-kinase catalytic delta polypeptide,
Pik3r1	Phosphatidylinositol 3-kinase, regulatory subunit, polypeptide 1 (p85 alpha)
PK	Pyruvate kinase
PKC	Protein kinase C
PPAR- α	Peroxisome proliferator-activated receptor– α
Pparg	Peroxisome proliferator activated receptor gamma
Ptpn1	Protein tyrosine phosphatase, non-receptor type 1
PVDF	Polyvinylidene fluoride
PW	Posterior wall
Pygl	Liver glycogen phosphorylase
Q-PCR	Quantitative- polymerase chain reaction
QC	Quality control
QOF	Quality and outcomes framework
Rab4a	Member RAS oncogene family
RAS	Renin-angiotensin system
RBS	Random blood sugar
Retn	Resistin
RI	Retention index
RIPA Buffer	Radioimmunoprecitation buffer
RNA	Ribonucleic acid
ROS	Reactive oxygen species
RT	Reverse transcription
RT-PCR	Real time polymerase chain reaction
RWT	Relative wall thickness
SD	Standard deviation
SDS	Sodium dodecyl sulfate
SDS-PAGE	Sodium dodecyl sulfate-polyacrylamide gel electrophoresis
SEM	Standard error of mean
SERCA2a	Sarcoplasmic reticulium calcium ATPase
sIVS	Intraventricular septum in systole
sLVD	Left ventricle end systolic
SNP	Single nucleotide polymorphism
SNS	Sympathetic nervous system
SOLVD	Studies of Left Ventricular Dysfunction

SOP	Standard operating procedure
sPW	Posterior wall thickness in systole
STZ	Steptozotocin
Tau	Time constant for isovolumic relaxation
TBS	Tris-buffered saline
TBST	Tris buffered saline containing Tween-20
TGs	Triglycerides
Tnf	Tumor necrosis factor
Tnfrsf1b	Tumor necrosis factor receptor superfamily, member 1b
Ucp2	Uncoupling protein 2 (mitochondrial, proton carrier)
UPLC	Ultra performance liquid chromatography
Vamp2	Vesicle-associated membrane protein 2
VPR	Volume pressure recording sensor technology
WHO	World health organisation
WT	Wild type
ZDF rats	Zucker Diabetic Fatty

Abstract

A thesis submitted to The University of Manchester by Riyad Almaimani for the degree of Doctor of Philosophy entitled

''Investigation into the underlying mechanisms of diabetic cardiomyopathy using a mouse model of diabetes''
December 2015

Diabetes Mellitus (DM) is one of the most common metabolic disorders in the world with an estimated prevalence of over 415 million patients. Heart failure (HF) is the most common cardiovascular complication of diabetes. The prevalence of diabetes in patients with HF is reported at approximately 30%. However, the molecular mechanisms that contribute to the development of heart failure in diabetic patients remain uncertain.

To study this, a genetic mouse model of diabetes (GENA348) with a point mutation in the glucokinase gene was used. Glucokinase is a glucose sensor that controls insulin release. This mutation in the glucokinase is similar to that found in Maturity Onset Diabetes of the Young Type 2 (MODY2) in humans. Our group has previously shown that GENA348 mice exhibit a diabetic phenotype. At 6 months, the mice developed a diabetic cardiomyopathy analogous to that seen in clinical practice with the development of cardiac hypertrophy and diastolic dysfunction, which progressed to dilatation of the left ventricle and systolic dysfunction at 12 months.
The aim of the project was to examine the molecular and pathophysiological mechanisms that contribute to development of this cardiac phenotype in diabetic GENA348 mice in the setting of hypertension and at baseline.

To study the mice under hypertensive stress conditions, 6 month old-GENA348 HO and WT mice were infused with angiotensin II (ANG II) via minipump. After ANG II treatment, HO and WT GENA348 mice showed a significantly greater increase in systolic and diastolic blood pressure compared to untreated controls. It was evident that ANG II treatment resulted in cardiac hypertrophy with the same level observed in both HO and WT mice. The diastolic function was generally preserved in the WT and HO mice following the ANG II treatment. Our data indicates that the HO mice have had a blunted hypertrophic response to the hypertension induced by ANG II.
At baseline, two hypothesis-generating methods were used. Firstly, gas chromatography-mass spectrometry (GC-MS) and ultra performance liquid chromatography-mass spectrometry (UPLC-MS) were used on 12-month-old GENA348 mice heart and serum samples. Secondly, diabetes PCR array plates were used on 6- and 12-month-old GENA348 mice heart samples. For the GC-MS and UPLC-MS, there were 43 differences in metabolites from tissue samples and 93 from serum samples. The main altered metabolites from tissue samples were sugars and fatty acids. However, fatty acids, phospholipids and sphingolipids were the main altered metabolites from serum samples.
After the validation of the array plates the most apparent observation was that only two up-regulated genes, Phosphoenolpyruvate carboxykinase 1 (Pck1) and Glucose-6-Phosphatase, Catalytic Subunit (G6pc) showed a comparable pattern as the array results. Pck1 and G6pc are the main enzymes that play a key role in gluconeogenesis regulation. We also looked at the expression level

of one of the main transcriptional regulators of gluconeogenesis, Forkhead box protein O1 (FoxO1). It was found that the expression was altered at 12 months. In conclusion, it was clear that hyperglycaemia altered gene expression and the metabolites profiles in 12 month old HO mice, with evident alterations detected in genes involved in the metabolic regulation of the heart. In addition, this study may provide preliminary insight into pathophysiological alterations in the cardiac metabolism that may contribute to the development of diabetic cardiomyopathy.

Declaration

I declare that no portion of the work referred to in the thesis has been submitted in support of an application for another degree or qualification of this or any other university or other institute of learning.

Riyad Adnan Al-Maimani
School of Medicine
Faculty of Medical and Human Sciences

Copyright statement

Acknowledgements

First, praise is due to Allah, the Almighty for His blessings and mercy.
Immeasurable appreciation and deepest gratitude are extended to my supervisors Prof Mamas Mamas and Dr Elizabeth Cartwright for their full support and expert guidance throughout the years of my PhD and especially for their valuable advice during the review of this thesis. I would also like to thank my advisor Dr Delvac Oceandy for all of his valuable advice.

I am also deeply indebted to Dr Warwick Dunn, Dr Paul Begley and Dr Katherine Hollywood who were very cooperative during my metabolomics work at their lab, they also helped me with data processing and analysis. I would like to thank Dr Stephen Gibbons and Mr Sukhpal for their help in collecting samples for the metabolomics part of the project.

Special thanks are due to Prof Ludwig Neyses for his continuous commitment and provision. Many thanks to all the members and ex-members of our lab, especially to Mr Sukhpal and Dr Min for helping me during the in vivo work of my research. Also to Dr Tamer, Dr Zeinab, Dr Mohamed, Miss Florence, Dr Nick for their help during my early days in the lab.

Words cannot express how thankful and grateful I am for my parents to whom I owe all of my achievements and accomplishments. I dedicate this thesis to them and to all of my cherished family and friends who encouraged me and supported me during these challenging years.
Last but not least, I thank my university, the university of Umm Al Qura and the government of Saudi Arabia for their financial support.

Chapter one – General introduction

1 General introduction

1.1 Diabetes mellitus

1.1.1 Definition and epidemiology of diabetes

Diabetes Mellitus (DM) is the most common metabolic disorder in the western world and is considered as a major cause of morbidity and mortality (Roglic et al., 2005). It has been defined as “a syndrome - i.e. a collection of metabolic disorders - characterised by chronic hyperglycaemia with a defective regulation of multiple aspects of carbohydrate, lipid and protein metabolism resulting from a defect in insulin secretion, insulin action, or both.” DM may cause chronic cardiovascular complications, long-standing damage and dysfunction of many body organs (Alberti and Zimmet, 1998). According to World Health Organisation (WHO), significant hyperglycaemia is classified as random plasma glucose ≥ 200mg/dL (11.1mmol/L) or fasting plasma glucose levels ≥126 mg/dL (7mmol/L) (WHO, 2006).

Data from the International Diabetes Federation (IDF) shows prevalence of diabetes in the world is approximately 415 million people. Moreover, by 2040 this number is estimated to increase to 642 million (IDF, 2015). In the UK, the most up-to-date estimation by the Quality and Outcomes Framework (QOF) 2013 shows that there are approximately 3.3 million people who have been diagnosed with diabetes. Furthermore, by 2025, it is anticipated that 5 million people will have diabetes in the UK (Diabetes UK, 2014).

1.1.2 Economic impact of diabetes in the UK

The entire budget associated with diabetes in the UK currently stands at approximately £ 23.7 billion and by 2035, it is anticipated to increase to £ 39.8 billion (Diabetes UK, 2014). The numbers presented above are frightening and prove that diabetes should be considered as the biggest health challenge the

UK is currently facing. This presents a noticeably huge impact, both economically and socially, which must be addressed through increased awareness of the risks, changes in life style, improved prevention and treatment.

DM is associated with a number of complications including both macrovascular and microvascular complications affecting several organs leading to cardiovascular disease (CVD), nephropathy, retinopathy and neuropathy. These complications are life threatening and may cause severe damage which lead to heart failure, stroke, kidney failure, blindness and foot ulcers (IDF, 2009). Among these complications, CVD complications are one of the main causes of morbidity and mortality in diabetic patients (IDF, 2009)(More details in section 1.2).

Regulation of blood glucose is a key factor that contributes to the mechanism of homeostasis between hyperglycaemia and hypoglycaemia. Figure 1.1 shows the physiological regulation of blood glucose. Under hyperglycaemic conditions, beta cells in the pancreas release insulin, which acts at peripheral sites such as adipose tissues, skeletal muscles and the heart to recruit GLUT4 transporter to the membrane and stimulate glucose uptake. However, in hypoglycaemic conditions, pancreatic alpha cells release glucagon, which promotes glucose production in the liver (Marieb & Hoehn, 2005).

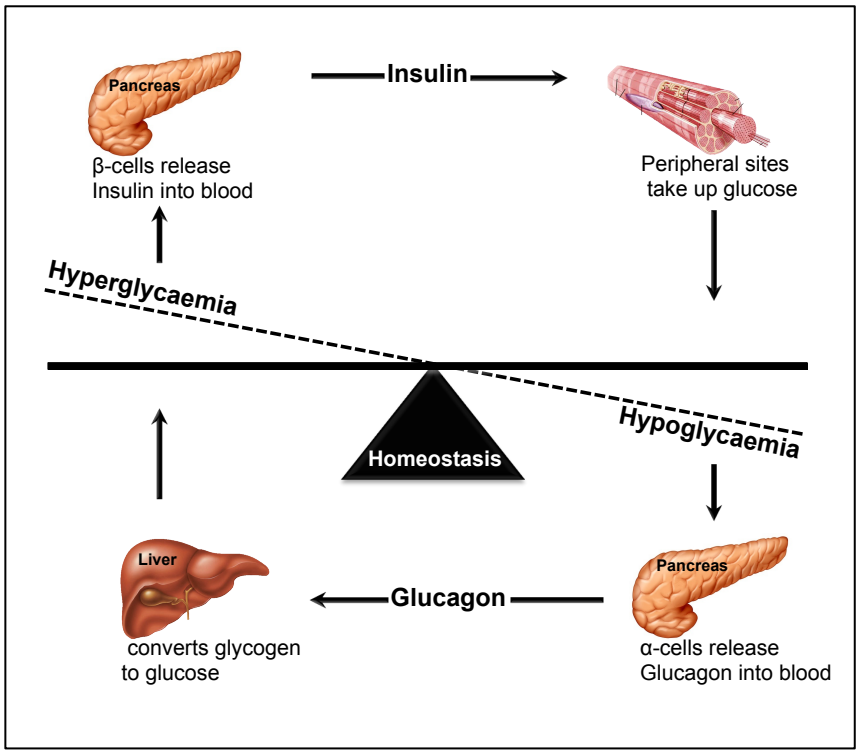

Figure 1.1 Homeostatic regulation of glucose

This figure shows the homeostatic regulation of glucose when blood glucose levels are elevated. Pancreatic beta cells produce insulin to recruit the catabolism of glucose. When blood glucose levels are reduced, pancreatic alpha cells release glucagon leading the liver to convert glycogen to glucose. The figure was adopted from (Marieb & Hoehn, 2005)

1.1.4 Classification of diabetes

Based on etiology, DM is classified as type 1 diabetes, type 2 diabetes and other specific types of diabetes (Williams and Pickup, 2004).

1.1.4.1 Type 1 diabetes mellitus

Type 1 diabetes occurs as a result of autoimmune destruction of insulin-producing cells (β-cells) in the pancreas, which results in an inability of the pancreas to produce sufficient insulin in response to a high level of glucose in the blood. Usually, it has an acute onset, developing over a short period of time. This type of diabetes appears mostly in childhood and in early adult life. It accounts for approximately 5-10% of all diabetic cases (Williams and Pickup, 2004).

1.1.4.2 Type 2 diabetes mellitus

Type 2 diabetes is characterised by impaired insulin secretion by the β-cells in addition to resistance to the action of insulin. This type of diabetes usually emerges in middle-aged individuals or the elderly, however it is increasingly seen in children and adolescents (IDF, 2015). It accounts for about 90% of all diabetic cases. It is highly associated with a family history of diabetes, ageing, obesity, lifestyle and lack of physical activity. Both hyperinsulinemia and insulin resistance result in impaired glucose tolerance. The development of type 2 diabetes is multifactorial and depends on both genetic and environmental components (Williams and Pickup, 2004).

1.1.4.3 Secondary diabetes mellitus

Other specific types of diabetes consist of a large group of diseases that include: genetic defects of β-cell function such as MODY 1-13 (which are discussed in more detail below), genetic defects in insulin action, diseases of

the exocrine pancreas, endocrinopathies and infection. It accounts for only 1-2 % of all cases of diabetes. (Williams and Pickup, 2004).

1.1.5 Maturity Onset Diabetes Of the Young (MODY)

MODY is a monogenic form of diabetes mellitus. It is a heterogeneous group of disorders accounting for less than 5% of all diabetic cases. It is characterised by specific features including an autosomal dominant trait penetrating through multiple generations, absence of ketosis and a slow onset of symptoms. Further, MODY normally appears before the age of 25 years without any evidence of β-cell autoimmunity as well as no sign of obesity (Stride and Hattersley, 2002). As a result of the developments and improvements in molecular genetics, it is currently known that there are about 13 subtypes of MODY. They are caused as a consequence of the mutations in different genes that are associated with β-cell function (Attiya & Sahar, 2012). These comprise mutations in the gene, which encodes the glycolytic enzyme glucokinase (MODY2). The most common of the other forms of MODY that encode transcription factors involved in insulin release are; hepatocyte nuclear factor (HNF) 4α (MODY1), HNF-1α (MODY3), insulin promoter factor 1 (MODY4) (Kanwal et al., 2011). The rest are considered very rare subtypes and the total list of genes are summarised in table1.1. The regulation of insulin and the contribution of these mutations are indicated in figure 1.2.

Type	Affected Gene	Gene name	Function
MODY1	HNF4A	Hepatocyte nuclear factor 4α	Transcription factor
MODY2	GCK	Glucokinase	Glycolytic enzymes
MODY3	HNF1A	Hepatocyte nuclear factor 1α	Transcription factor
MODY4	IPF1/PDX	Insulin promoter factor 1/ Pancreatic and duodenal homeobox 1	Transcription factor
MODY5	HNF1B	Hepatocyte nuclear factor 1β	Transcription factor
MODY6	NeuroD1	Neurogenic differentiation factor 1	Transcription factor
MODY7	KLF11	Kruppel-like factor 11	Transcription factor
MODY8	CEL	Carboxyl-ester lipase	Lipase
MODY9	PAX4	Paired box gene 4	Transcription factor
MODY10	INS	Insulin	Beta cells of the iselts of Langerhans
MODY11	BLK	Tyrosine kinase, B-lymphocyte specific	Tyrosine Kinase
MODY12	ABCC8	ATP-binding cassette, sub-family C, member 8	ATP-binding cassette
MODY13	KCNJ11	Potassium channel, inwardly rectifying subfamily J, member 11	Potassium channel

Table 1.1 Classification and clinical phenotypes of the MODY subtypes (Attiya & Sahar, 2012)

1.1.5.1 Clinical features of MODY

The clinical features of MODY vary from moderate fasting hyperglycaemia with limited complications, to severe and advanced hyperglycaemia with chronic vascular complications (Altshuler et al., 2000). Throughout childhood, MODY may not have any clinical signs, with only moderate rises in fasting hyperglycaemia (6-7mmol/L). In adults, MODY can persist clinically undiagnosed for a long time because of the absence of clinical signs and symptoms. Therefore, a large number of MODY patients are diagnosed coincidentally, through routine check-ups, for example during pregnancy (Velho et al., 1997). Nevertheless, in other cases, hyperglycaemia can be more evident and diabetic complications develop with age as a result of prolonged exposure to high glucose levels. At this stage, it becomes difficult to distinguish MODY from other forms of diabetes. It has been proposed that patients who have MODY are underestimated since large numbers of them have been wrongly diagnosed (Ehtisham et al., 2004). Furthermore, it is anticipated that 2-5% of type 2 diabetic people might in fact have MODY (Ledermann, 1995). As a consequence, the World Health Organisation established diagnostic criteria to help recognise MODY patients. These include: 1) Hyperglycaemia usually diagnosed before the age of 25 years in at least one and ideally two family members. 2) Autosomal-dominant pattern of inheritance. 3) Absence of insulin therapy at least 5 years after diagnosis or significant C-peptide levels even in a patient on insulin treatment. 4) Insulin levels in the normal range, although improperly low for the degree of hyperglycaemia, proposing a primary defect in beta-cell function and 5) low incidence of obesity (ADA, 2002).

1.1.5.2 Glucokinase mutation (MODY2)

Glucokinase mutation (MODY2) is considered to be one of the most common and well studied forms of MODY in comparison to other forms. It was the first MODY gene to be identified. MODY2 accounts for approximately 30-70% of all MODY cases (Thanabalasingham & Owen, 2011). The first mutation was reported in 1992, and now more than 600 mutations associated with the glucokinase gene have been reported in many populations, with the majority established in the UK, France and Spain (Osbak et al., 2009). In humans, mutations in the glucokinase gene result in three different syndromes; one is persistent hyperinsulinaemia hypoglycemia of infancy (PHHI), which is caused by heterozygous activating mutations that activate the enzyme. The second is MODY2, which is caused by heterozygous inactivating mutations that inactive the enzyme. The third is permanent neonatal diabetes mellitus (PNDM), which is caused by homozygous inactivating mutations that inactivate the enzyme (Fajans et al., 2001).

The precise prevalence of MODY2 has not been determined in large-scale population-based studies since mild hyperglycaemia and lack of symptoms means that patients are often not diagnosed (Osbak et al., 2009). Glucokinase is a member of the hexokinase family of enzymes. It functions as the glucose sensor for the beta cells in the pancreas. It plays a role in the ability of beta cells to assess blood glucose levels precisely. All hexokinases have the capability to mediate the phosphorylation of glucose to glucose-6-phosphate (Steck and Winter, 2011). However, glucokinase has a moderately low affinity for glucose and it is not inhibited by physiological concentrations of glucose-6-phosphate. This allows any increase in the level of blood glucose concentration to be sensed by glucokinase, simplifying the mechanism of phosphorylation of

glucose to glucose-6-phosphate, rising ATP production and eventually stimulating insulin secretion (Figure 1.2).

Although microvascular complications are considered as a substantial cause of mortality and morbidity in diabetes, it would be expected that complications in MODY2 patients are uncommon as a result of the relatively mild hyperglycaemia (7 mmol/L) and low prevalence of hypertension in patients with MODY2 (Velho et al., 1997). The majority of MODY2 patients are treated with diet alone. However, in rare cases, patients require pharmacological treatment (Steck and Winter, 2011). Approximately 2% of MODY2 patients need insulin treatment to maintain normoglycaemia and less than 50% develop overt diabetes which are usually patients who are old in age or obese (Fajans et al., 2001).

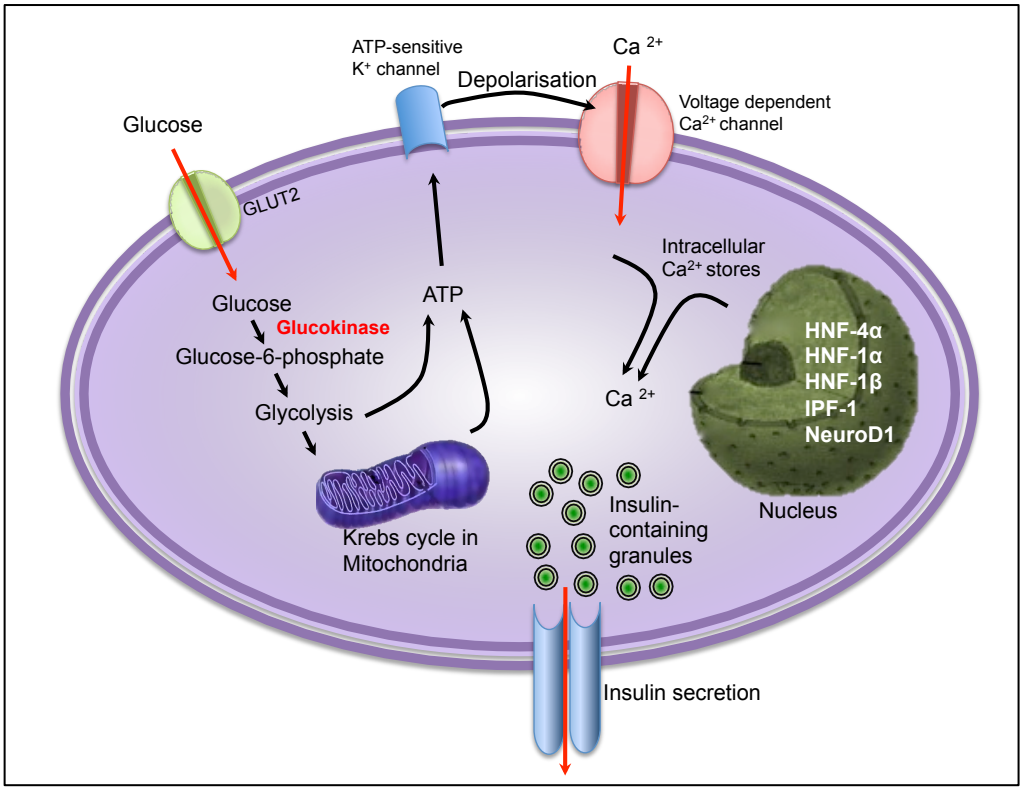

Figure 1.2 The Pancreatic Beta cell and its response to glucose.

GLUT-2 transports glucose through the cell surface into pancreatic beta cells where it catalyses the transfer of phosphate from ATP to glucose by the enzyme glucokinase to form glucose-6-phosphate. The ATP-sensitive potassium channels close when the ATP generated by glycolysis and the Krebs cycle increases as a result of high blood glucose levels and binds to the channel. This leads the voltage dependent calcium channels to open as the membrane is depolarised enabling calcium to enter the cell, which stimulates the release of calcium from intracellular Ca^{2+} stores. This triggers exocytosis of insulin and the fusion of insulin containing granules to the plasma membrane. The mutations in the transcription factors HNF-4α, HNF-1α, IPF-1, HNF-1β, NeuroD1 and the glucokinase enzyme impair this pathway. Mutations might result in the defect of insulin secretory responses to many factors, especially glucose, which exists before the onset of hyperglycaemia. The figure was adopted from (From Bell and Polonsky, 2001).

1.2 Cardiovascular disease and diabetes mellitus

Cardiovascular disease (CVD) including coronary artery diseases (CAD) and heart failure are the most common cause of morbidity and mortality in patients with diabetes. It accounts for 50-80% of diabetic mortality (WHO, 2004). Furthermore, CVD accounts for 52% of mortality in type 2 diabetes and 44% in type 1 (Morrish et al., 2001)(Diabetes UK, 2014). Diabetic patients are 2-4 times more likely to develop CVD than people without diabetes (WHO, 2004). When diabetic patients develop CVD, they sustain a worse prognosis for survival than CVD patients without diabetes (Wilson et al., 1998; Morrish et al., 2001).

1.3 Heart Failure and diabetes

Heart failure (HF) and myocardial infarction (MI) are amongst the most common types of CVD that causes death in diabetic patients. The prevalence of diabetes in HF patients is approximately 30% (Cohen-solal et al., 2008). Diabetic patients have approximately double the incidence of HF hospitalisation or death than non-diabetic patients (McMurray & Stewart, 2000).

HF is defined by the American Heart Association as “a complex clinical syndrome that may result from any structural or functional cardiac disorder that impairs the ability of the ventricle to fill with or eject blood” (Jessup et al., 2009). Furthermore, the Framingham Heart Study revealed an increased incidence of HF in diabetic men (2-fold) and women (5-fold). In younger diabetic patients (aged ≤ 65 years), the risk factor of increased HF incidence was higher in males (4-fold) and females (8-fold) than in non-diabetic patients (Kannel, 2000).

There are several potential mechanisms which associate diabetes to heart failure including, the presence of coronary artery disease and hypertension, the association with comorbidities which is the coexistence of two conditions or

disorders in the same patients, or through diabetic cardiomyopathy. On the other hand, many other mechanisms remain uncertain (Bauters et al., 2003).

1.4. Diabetic cardiomyopathy

Diabetic cardiomyopathy was originally described over forty years ago, based on autopsy data from four diabetic patients with heart failure in the absence of either coronary artery disease or hypertension (Rubler et al., 1972). Rubler et al. 1972 observed that LV hypertrophy was linked with myocardial fibrosis in those patients and introduced the concept of diabetic cardiomyopathy. Diabetic cardiomyopathy is defined as the existence of a primary myocardial disease found in a diabetic person with the absence of hypertension, valvular and other underlying coronary artery disease. The concept of diabetic cardiomyopathy is based on the idea that diabetes is a factor which causes alterations at the cellular level resulting in structural abnormalities (Hayat et al., 2004). This condition has been associated with type 1 and type 2 diabetes and is characterised by early-onset diastolic dysfunction and late-onset systolic dysfunction (Boudina and Abel, 2007). The prevalence of cardiomyopathy has been reported between 12-50% in patients with diabetes (Fuentes-Antrás et al., 2015).

1.4.1. Functional changes of the heart in diabetic cardiomyopathy

Brutsaert et al. have defined diastole as the period of time in the cardiac cycle where the myocardium fails to produce force and then returns to its normal state (Brutsaert and Housmans, 1980). Diastolic dysfunction occurs when the diastole process is prolonged and slowed down. It is characterised by passive filling of the left ventricle and the impairment of relaxation. Diastolic dysfunction has been described as an early feature of diabetic cardiomyopathy. Originally, scientists recognised diastolic dysfunction by using cardiac catheterisation where they noticed a reduction in the left ventricle end-diastolic volume and an elevation in end-diastolic pressure in diabetic patients without Coronary artery disease (CAD) (Regan et al., 1977).

While invasive cardiac catheterisation methods are considered the gold standard to assess diastolic dysfunction, standard echocardiography and tissue Doppler echocardiography are the most commonly used non-invasive methods to measure diastolic function (Schannwell et al., 2002). Systolic dysfunction is described as the later stage of diabetic cardiomyopathy, which develops after diastolic dysfunction. Systolic dysfunction occurs when the myocardial ability to eject blood is reduced. It is characterised by a depressed left ventricular ejection fraction (Hayat et al., 2004).

1.4.2. Structural changes occurring in the heart in diabetic cardiomyopathy

There are a number of studies that have revealed structural changes of the diabetic heart in animals and humans (Fang et al., 2004). The most common change that occurs in the diabetic heart is left ventricular hypertrophy, which is defined as an increase in the left ventricular mass (Hayat et al., 2004). There

are several postulated pathways for the development of hypertrophy, which include insulin signalling (Shulman et al., 2000), peroxisome proliferator-activated receptor– α (PPAR- α) (Finck et al., 2002), protein Kinase C (PKC) (Gurusamy et al., 2005) and angiotensin II (Ruggenenti and Iliev, 2008). Another essential change which occurs in the diabetic heart is fibrosis, which is the process of the formation of fibrous tissue in a reparative process (replacement) following myocytes loss (Fang et al., 2004).

1.4.3. Pathogenesis of diabetic cardiomyopathy

The pathogenesis of diabetic cardiomyopathy is thought to be multifactorial and incompletely characterised. There are several putative mechanisms that have been proposed, including metabolic disturbances, impaired calcium handling, activation of the renin-angiotensin system (RAS), increased oxidative stress and mitochondrial dysfunction (Zhang and Chen, 2012). These mechanisms trigger an alteration in downstream transcription factors that lead to changes in gene expression, myocardial substrate utilisation, myocyte growth, endothelial function and myocardial compliance. These processes may occur simultaneously to develop diabetic cardiomyopathy (Murarka and Movahed, 2010).

1.4.3.1. Metabolic disturbances

Alterations in cardiac metabolism and substrate utilisation have been continuously reported in the literature. In a normal heart, there are a number of substrates oxidised by the myocardium, comprising carbohydrates, fatty acids, amino acids, lactate and ketones (Avogaro et al., 1990). Amongst these substrates, carbohydrates and fatty acids provide the main energy resource. 30 % of ATP generation is through glucose and lactate oxidation, whereas fatty acids account for 70% of energy offered to the heart (Saito et al., 2003). In

diabetes mellitus, glucose uptake and glycolysis are reduced. In addition, disturbances in insulin function increase lipolysis and the release of fatty acid from adipose tissue. Under these conditions, the heart swiftly adjusts to using fatty acids for energy generation (An & Rodrigues, 2006). There are three significant characteristics involved in the metabolic disturbances that have emerged in diabetic cardiomyopathy: hyperlipidemia and hyperglycaemia.

1.4.3.1.1. Hyperlipidemia and lipotoxicity

Augmented lipolysis in adipocytes and enhanced lipogenesis in hepatocytes together, severely increase circulating fatty acids and triglycerides in diabetic patients. In addition, insulin triggers fatty acid transport into cardiac myocytes (Luiken et al., 2002). The elevated circulating lipids increase fatty acid transportation to cardiomyocytes. With the rise of intracellular fatty acid, heart tissue rapidly adapts through promoting fatty acid utilisation. However, in a condition where the fatty acid amount exceeds the oxidative capacity of the cardiomyocytes, the fatty acid is converted to lipids such as triglycerides, saturated fatty acid and ceramide, eventually lipotoxicity is the result. Accumulation of triglycerides and ceramide is stimulating oxidative stress and cardiomyocyte apoptosis which results in cardiac dysfunction and organ failure (Zhou et al., 2000). There are several studies which proposed that excessive fatty acid amount prompts lipotoxicity and contribute to the pathogenesis of cardiomyopathy (Zhou et al., 2000). A significant increase in fatty acid delivery with arising lipid storage, lipotoxic cardiomyopathy, and contractile impairment was observed in cardiac-specific overexpression of Lipoprotein lipase (LPL) (Yagyu et al., 2003). Furthermore, increased fatty acid utilisation by cardiac-specific overexpression of PPAR-alpha leads to cardiomyopathy and impaired

cardiac function (Finck et al., 2002). On the other hand, decreasing fatty acid supply or utilisation prevented the pathogenesis of cardiomyopathy in diabetic animals. It was found in obese ZDF rats, that using a PPAR-gamma agonist to decrease the plasma lipids leads to reduce cardiac triglycerides and ceramide and ultimately improve heart function (Zhou et al., 2000). Collectively, these studies suggested that increased fatty acid supply in the presence of diabetes alters cardiac lipid homeostasis and results in lipotoxicity.

1.4.3.1.2 Hyperglycaemia and glucotoxicity

Hyperglycaemia plays a key role in the development of diabetic cardiomyopathy. It occurs as a result of decreased glucose clearance and increased hepatic gluconeogenesis. In type 2 diabetic patients, endogenous glucose production is augmented. Chronic exposure to hyperglycaemia can result in cellular impairment, which may become irreversible over time, a process called glucotoxicity (Meyer et al., 1998). Brownlee and coworkers 2005 demonstrated the mechanism by which hyperglycaemia induces tissue injury through the generation of reactive oxygen species (ROS). There are a number of mechanisms that play a role in the development of DCM as a result of hyperglycaemia. These comprise: 1) the elevation of advanced glycation end products (AGEs); 2) the increase in hexosamine and polyol flux; and 3) the activation of protein kinase C (PKC). Table 1.2. summarises the mechanisms that contribute to the development of DCM in the case of hyperglycaemia (Poornima et al., 2006).

AGEs are a complex and heterogeneous group of compounds resulting from the non-enzymatic reaction between proteins and lipids in the presence of reducing sugars. Early glycation and oxidation processes lead to the formation of Schiff bases and Amadori products. Further glycation of proteins and lipids

produces molecular rearrangements, which result in the production of AGEs. AGEs can accumulate in tissues as part of the normal process of ageing but this accumulation occurs earlier and with an enhanced rate in diabetes and inflammation (Singh et al., 2001).

Excessive superoxide production in the mitochondria during hyperglycaemia leads to increased oxidative stress. The ratio NADPH/NAD+ declines as a result of the increased use of NADPH for the production of sorbitol by the reduction of glucose (increased polyol pathway flux). Subsequently, the NADPH available to maintain glutathione in the reduced form diminishes, which leads to oxidative stress (Wold et al., 2005). Furthermore, increased polyol pathway flux leads to inhibit glyceraldehyde-3-phosphate dehydrogenase (GAPDH) enzyme, which modifies the pathway through which glucose is oxidised, eventually leading to glucotoxicity (Du et al., 2003). This can result in the formation of AGEs and the activation of PKC. In hyperglycemia and oxidative stress, advanced glycation end products generation is enhanced and can then bind to their receptor RAGE, which lead to the formation of ROS and altered gene expression. PKC can also lead to activation of the main pathways that are involved in cardiac hypertrophy (p38 mitogen-activated protein kinase (MAPK) and c-Jun N-terminal kinase (JNK)) (Du et al., 2003).

Mediators	Mechanisms of action	Consequences
Increased AGE	Crosslink RyRs41; crosslink type III collagen 4	Decreased SR calcium release and myocyte contractility; increased ventricular stiffness; impaired ventricular filling
Increased hexosamine flux	Sp1-O-GluN acylation of transcription factors decreasing SERCA2a expression	Prolonged calcium transients; impaired relaxation
Increased polyol flux	Decreased regeneration of reduced glutathione leading to oxidative stress; increased DNA fragmentation; sorbitol-induced AGEs	Increased myocyte apoptosis; increased ventricular stiffness
Increased protein kinase C activation	Increased cardiac hypertrophy; increased extra cellular matrix; decreased SERCA 2a function	Impaired relaxation; increased ventricular stiffness

Table 1.2. Mechanisms contributing to the development of DCM in hyperglycaemia.

Although there are several pathophysiological mechanisms responsible for diabetic cardiomyopathy that have been suggested, the precise mechanisms underlying the disease remain incompletely understood.

Animal models of type 1 and type 2 diabetes have common traits with human diabetic cardiomyopathy and as a result, this has significantly advanced our knowledge of the underlying mechanisms of diabetic cardiomyopathy. Even though the mouse models share traits with human diabetic cardiomyopathy, they still do not exactly represent the human condition due to their limitations. For example, Streptozotocin (STZ) is one of the most commonly used models of type 1 diabetes. STZ injection may produce direct toxic effects on the myocardium independent of diabetes (Boudina & Abel, 2007). Another example of type 2 diabetes is the ob/ob and db/db mice, which are produced by leptin

and leptin receptor genes mutation, respectively. However, human leptin and leptin receptor genes mutation are associated with obesity and may not directly be associated with diabetes itself (Farooqi et al., 2007).

This brings into question the applicability of these models when one is investigating the complex mechanisms and signalling cascades involved in the pathogenesis of diabetic cardiomyopathy. It raises the question, are more appropriate and human relevant models needed to study the complex, multifactorial complications of diabetes on the heart?

1.5 GENA348; the mouse model used in this study

GENA348 has been described in the literature as a novel human relevant mouse genetic model of diabetes generated by the Medical Research Council (MRC). It was recognised through free-fed plasma glucose measurement in the N-ethyl-nitrosourea (ENU)-treated mice between the ages of 2 and 3 months. ENU is an alkylating agent, which particularly produces AT to TA transversion mutations at random sites through the genome in mice. These point mutations can generate different types of alleles, including loss or gain of function and hypomorphs or hypermorphs (Justice, 2000). In GENA348, the underlying gene was mapped to MODY2 homology region of mouse chromosome 11. Positional gene analyses revealed an A to T transversion mutation in exon 9 of the glucokinase gene, causing an isoleucine to phenylalanine change at amino acid 366 (Toye et al., 2004). Glucokinase has an important role in regulating the secretion of insulin in the pancreas. This mutation in glucokinase is analogous to that found in, MODY2, in humans, a monogenic form of diabetes (Nolan et al., 2000). GENA348 HO mice are viable and more glucose intolerant than HT or WT animals, unlike HO global and β-cell glucokinase knockout mice which die prenatally. In addition, when the activity levels of glucokinase were assessed, it was found that HO mice had 14% activity of WT littermates and HT had 67%. Furthermore, glucokinase protein levels were measured, it was found that HO mice showed a large 54-66% reduction in the glucokinase protein compared to WT mice. However, HT mice showed a small insignificant increase in the glucokinase protein level (Toye et al., 2004). This model replicates a human form of diabetes, MODY 2, where patients have a mutation in the glucokinase gene. These patients develop a mild hyperglycaemia, which can be managed through diet alone. Nevertheless, the rarer homozygous form results

in permanent neonatal diabetes which requires insulin in the first few days of life (Fajans et al., 2001). The question of why the homozygous GENA348 mice are more hyperglycemic and do not need insulin for survival is probably because these mice have higher basal blood glucose levels than humans, as WT mice often have blood glucose levels that reach up to 9 mmol/L.

Our group has used this mouse model and revealed the following; by the age of 3 months, notable hyperglycaemia had developed in the HO mice compared to their WT controls. From 3 to 6 months, there was a significant increase in the blood glucose in the HO mice to a level of 20.6±0.8mmol/L after which blood glucose levels stayed constant. There was also a significant increase in the levels of FFAs and free glycerol in the serum of 6-month-old GENA348 HO mice compared to their WT littermates (FFAs: WT: 1.5±0.17mmol/L, HO: 2.1±0.14mmol/L, p=0.025) (free glycerol WT: 0.67±0.06mmol/L, HO: 1.0±0.07mmol/L, p=0.01). However, there was no significant change in insulin concentration in the HO mice (1.29±0.31µg/l) compared to WT controls (1.66±0.56µg/l) (p=0.65)(Gibbons, 2011). The method used to assess insulin levels was not sensitive enough to detect the differences between HO and WT GENA348 mice. A method that is more sensitive should be used in future to assess the level of insulin such as the insulin tolerance test (ITT).

The direct effects of elevated blood glucose on the heart was examined and revealed that at 3 months there were no significant changes in cardiac structure or function. By 6 months, the diabetic mice developed significant cardiac hypertrophy and diastolic dysfunction, which progressed to dilatation of the left ventricle and systolic dysfunction, at 12 months. This is similar to the clinical manifestations of diabetic cardiomyopathy and is equivalent to that seen in

clinical practice with the development of cardiac hypertrophy and diastolic dysfunction (Gibbons, 2011).

While there are various pathophysiological mechanisms responsible for diabetic cardiomyopathy that have been proposed, the exact mechanisms underlying the disease are still far from elucidated. Therefore, using a relevant mouse model of diabetes to human will help us to characterise the molecular and pathophysiological mechanisms that may contribute to development of diabetic cardiomyopathy and may also provide insight into potential therapeutic targets. The general aim of the project was to examine the molecular and pathophysiological mechanisms that contribute to development of cardiac phenotype in diabetic GENA348 mice in the setting of hypertension and at baseline.

Chapter 2 General method

2.1 Methods

2.1.1 Animals

All Animal procedures were carried out according to the guidelines and protocols approved by the University of Manchester Ethics Committee and fulfilled with the United Kingdom Animals (Scientific Procedures) Act 1986. Mice were kept in a specific pathogen-free environment in the designated Medical and Scientific Establishments of the University of Manchester. They were provided with food and water *ad-libitum.* In this study, all mice used were (C3H X BALB/c) male. They were maintained through a combination of breeding (HT X HT) initially and later (HO X HO) and (WT X WT) to produce sufficient mice for experiments.

2.1.2 Molecular analysis

2.1.2.1 PCR

2.1.2.1.1 DNA extraction

In order to examine the genotype of the animal, genomic DNA was extracted from ear tissue of mice. Ear snips were collected from the relevant mice and stored at -20 °C until use. The snips were digested by adding 200µl of lysis buffer (50mM Tris, 100nM EDTA, 0.5% SDS) and 10µl of proteinase K (10mg/ml). Samples were incubated overnight at 56 °C. The next day, the supernatant was transferred to a new tube after the digested samples were centrifuged at 15493 xg for 10 minutes. To precipitate the DNA, 300µl of propan-2-ol was added and the tube was inverted (30x). The samples were centrifuged again at 15493 xg for 5 minutes and the supernatant was removed. The DNA pellet was washed in 100µl of 70% ethanol and centrifuged quickly.

The pellet was air dried and resuspended in 50-85µl TE buffer (10mM Tris-HCl pH 7.5, 1mM EDTA pH 8) depending on the pellet size. To quantify the amount of DNA, a Nanodrop spectrophotometer was used.

2.1.2.1.2 Genotyping

To genotype the GENA348 mice; a single nucleotide polymorphism (SNP) assay (Applied Biosystems Technology) was used. This method uses the TaqMan® SNP Genotyping Assay 5' nuclease technology which enables two allele-specific TaqMan® MGB probes (allele1=VIC-MGB and allele2=FAM-MGB) and a PCR primer pair to identify the particular SNP target. The primers and probes distinctively align with the genome which allows the technology of TaqMan® genotyping to provide unique genotype specificity (Figure 2.1).

2.1.2.1.3 Reaction mix and PCR amplification

To prepare the reaction mix, 12.50µl of TaqMan Universal Master Mix was added to 1.25µl SNP assay. Then, in a 96 well PCR plate, 11.25µl of DNA (20ng) and 13.75µl of the reaction mix was added before starting the PCR as illustrated in table 2.1. The results of the assay can be automatically determined by a genotyping software provided with real-time thermal cyclers through using autoscaling for generating the allele discriminating plot (HO (allele 2/ allele 2), HT (allele 1/ allele 2), WT (allele 1/ allele 1).

Steps	Cycles	Duration	Temperature
Hold	1	10 minutes	95°C
Denaturation	40	15 seconds	92°C
Annealing/ extension		1 minute	60°C

Table 2.1 PCR conditions for SNP assay

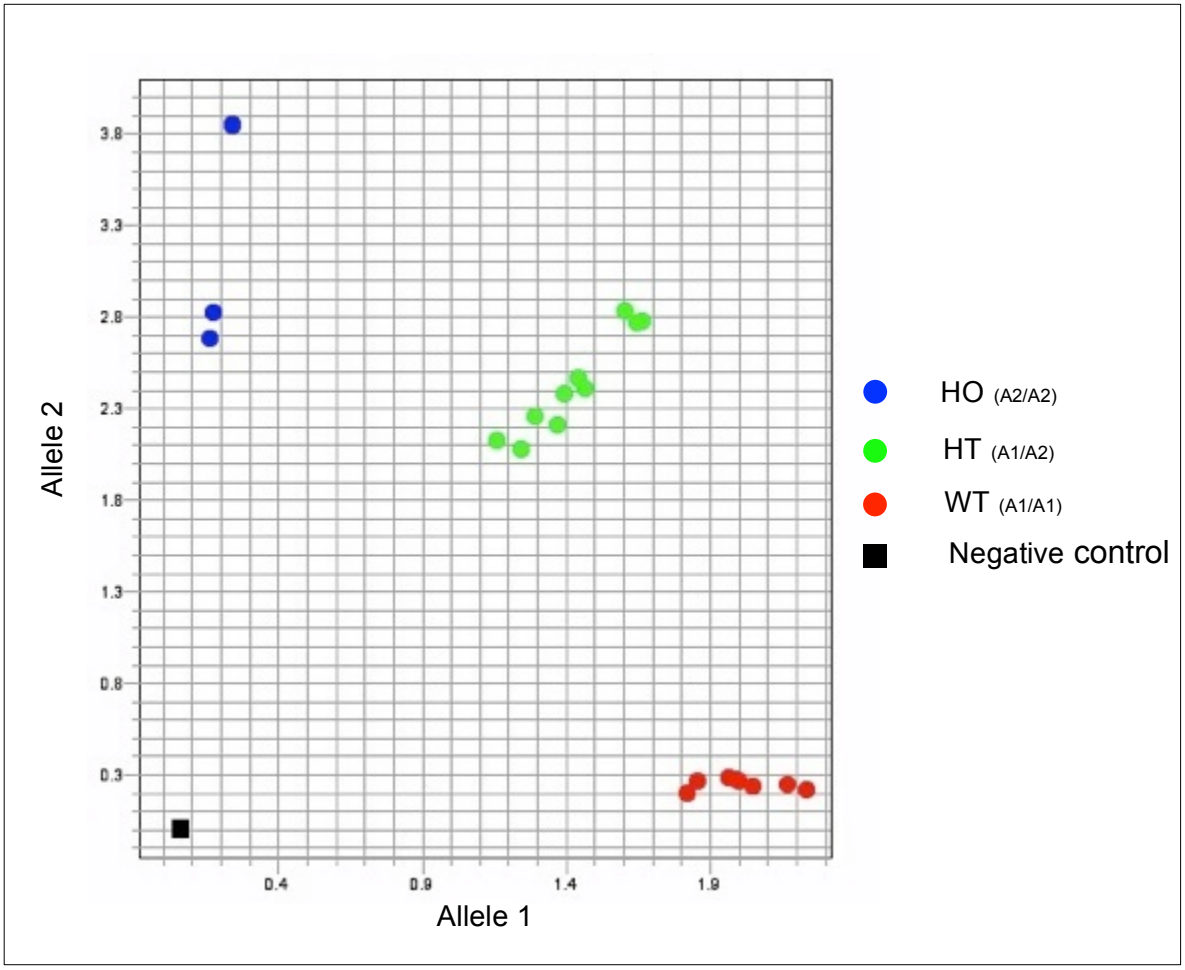

Figure 2.1 Allelic discrimination plot of genotyping in the GENA348 mice.

DNA was used after it was extracted from ear snips and quantified in a single RT-PCR assay with a specific primer designed around the SNP. From the figure, it is clearly observed that this technique is able to differentiate between the three genotypes.

2.1.2.2 Real Time Polymerase Chain Reaction (RT-PCR)

This method was used to measure the expression of mRNA of a target gene after its conversion to single stranded complimentary DNA (cDNA) through reverse transcription (RT).

2.1.2.2.1 RNA isolation and quantification

In order to extract total RNA from heart tissue, 1 ml of TRIZOL (Invitrogen Ltd) was added to a dounce beaker homogeniser with the heart tissue and homogenised till all lumps were removed. The homogenate was left at room temperature for 15 minutes. Then, 200µl of chloroform was added before the microfuge tube was shaken vigorously for 15 seconds and spun down (15493 xg for 15 minutes at 4°C). The upper aqueous phase (containing the RNA) was transferred to a new microfuge tube. To precipitate the RNA, 700µl of ice-cold propan-2-ol was added. After that, the samples were incubated for 10 minutes at room temperature and spun down (15493 xg for 10 minutes at 4°C). The supernatant was discarded and the pellet was washed in 100µl of 70% ethanol and centrifuged (15493 xg for 5 minutes at 4°C).

The RNA pellet was resuspended in 20-30µl of diethylpyrocarbonate (DEPC)-treated water after the ethanol was removed and air-dried the pellet. To quantify the concentration of RNA, a nanodrop spectrophotometer ND-1000 (Thermo Scientific)(absorbance 260nm) was used. A good RNA quality should have an OD260/280 ratio greater than 1.8. To prevent degradation of the RNA, all RNA work was performed on ice and under RNAse free conditions. Finally, the RNA was stored at -80 °C.

2.1.2.2.2 Quantitative-PCR (Q-PCR)

In order to determine the level of mRNA expression of the target gene, a two-step Q-PCR technique was used. The first stage was to convert 2µg/µl of total RNA to cDNA using a high-capacity cDNA reverse transcription kit (Applied Biosystems) according to the manufacturer's instructions. The produced cDNA was diluted 20 times in RNase -free water and kept at -20 °C until use. The second stage was the amplification of the cDNA using q-PCR reaction mixture

consisting of: 5µl SYBR Green (Agilent Technologies), 1µl specific primer assay (Qiagen), 1µl cDNA and 3µl DEPC water.

All samples were loaded in triplicate using a 96 well plate (Starlab), each containing the following controls; lacking cDNA, lacking primers, lacking reverse transcriptase enzyme and RNase-free water only. No amplification was seen in the samples in the absence of reverse transcriptase. The plate was run on a 7500 Fast Real Time PCR instrument (Applied Biosystems) using the Q-PCR reaction conditions outlined in table 2.2. To ensure that only one PCR product was present, a melt curve step was included. mRNA gene expression was then calculated using the delta-delta CT method of relative quantification (Livak & Schmittgen, 2001) in which the CT value for the gene of interest was normalised to the mean of two different endogenous controls (GAPDH and β-actin). The primers used in this study are listed in table 2.3.

Steps	Cycles	Duration	Temperature
Enzyme initiation	1	3 minutes	95°C
Denaturation	40	30 seconds	95°C
Annealing		30 seconds	60°C
Elongation		30 seconds	95°C
Melt curve	1	15 seconds	95°C
		1 minute	60°C
		15 seconds	95°C
		15 seconds	60°C

Table 2.2 SYBR Green Q-PCR cycling conditions.

Primer	Cat. Number	Primer	Cat. Number
Mm_ BNP	QT00107541	Mm_Rab4a	QT00103369
Mm_Pck1	QT00153013	Mm_Tnfrsf1b	QT01077636
Mm_Pdx1	QT00102235	Mm_Parp1	QT00157584
Mm_Cebpa	QT00311731	Mm_Pygl	QT00146846
Mm_Adrb3	QT01195901	Mm_Tnf	QT00104006
Mm_Il12b	QT00153643	Mm_Ucp2	QT00138943
Mm_Gpd1	QT00154777	Mm_Ctla4	QT00103929
Mm_Aqp2	QT00113610	Mm_G6pc	QT00114625
Mm_Gcgr	QT00112560	Mm_Retn	QT00093450
Mm_Hnf4a	QT00144739	Mm_Pparg	QT00100296
Mm_Ifng	QT01038821	Mm_Pik3cd	QT00149962

Table 2.3 Primers used in this study

The catalogue number was used as the primer sequences are not provided by the company

2.1.2.3 Protein analysis by western blot

To measure protein expression in the tissue extract, western blotting was used. Gel electrophoresis was used to separate protein according to size followed by immunological analysis using antibody-based detection of a target protein.

2.1.2.3.1 Whole cell protein extraction

Heart tissues were collected from sacrificed mice using a schedule 1 method either used directly or snap frozen in liquid nitrogen for storage at -80 °C. Hearts were washed in PBS to remove blood clots and cut into small sections. Sections were then homogenised in a Potter-Elvehjem glass homogeniser in 1000µl (whole heart) of ice-cold RIPA buffer (1x PBS, 1% IGEPAL CA-630, 0.5% Sodium deoxycholate, 0.1% Sodium dodecyl sulfate (SDS), 20µM PMSF,

500ng/ml Leupeptin, 1µg/ml Aprotium, 500ng/ml Pepstatin A, pH 7.5). The homogenised heart sections were centrifuged at 825 xg for ten minutes at 4°C. The supernatant containing the proteins was kept and stored at -80°C for future use. 20µl was kept separately for protein concentration determination.

2.1.2.3.2 Determination of total protein concentration

Protein determination was made using a standard bicinchoninic acid (BCA) protein assay kit (Thermo Scientific), following the manufacturer's instructions. The principle of the assay is relying on the formation of copper sulphate complex under alkaline conditions, followed by the reduction of copper sulphate ions to Cu^{1+}, which then bind to BCA forming a product of measurable absorbance at 562 nm. The concentration of unknown proteins can therefore be measured using a range of known BSA protein standards (0-2 mg/ml). Protein standards and samples were then loaded onto a 96 well plate in triplicate. Following the addition of the BCA reagent, the plate was incubated at 37°C for 30 minutes and mean absorbance was detected on an optical plate reader at 562 nm (Thermo Labsystems).

2.1.2.3.3 Western blot

To quantify the abundance of the protein of interest, western blot analysis was used. 5-30 µg of total protein per sample (dependent on the size of a target protein) was mixed with 2X Laemmli solution (β-mercaptoethanol, 0.05 % bromophenol blue, 20% (v/v) glycerol, 10% (w/v) SDS) (Sigma Aldrich) at a ratio of 2:1. Samples were then boiled for five minutes at 95 °C and loaded onto an SDS-PAGE, which was made of a resolving gel (4-16%) and staking gel (Table 2.4) along with a ladder (Bio-Rad). Gels were then run in Tris glycine buffer (25mM Tris base, 0.25M glycine, 0.1% SDS) at 127V for 90 minutes. To transfer the protein to a polyvinylidene fluoride (PVDF) membrane (Millipore),

the semi-dry transfer apparatus (Invitrogen) and transfer buffer (25mM Tris base, 0.25M glycine, 20% methanol) were used at 200mA per gel for 90 minutes.

Resolving gel	Stacking gel
4-16% acrylamide/bis-acrylamide (37.5:1)	5% acrylamide/bis-acrylamide (37.5:1)
0.375 M Tris-base (pH 8.8)	0.375 M Tris-base (pH 6.8)
0.1% SDS	0.1% SDS
0.1% ammonium persulphate	0.1% ammonium persulphate
0.04% TEMED	0.04% TEMED

Table 2.4 Buffers used in preparation of SDS-PAGE gels

The membrane was blocked for one hour in 3% bovine serum albumin (BSA-Sigma Aldrich) in Tris-buffered saline (TBS) (150mM NaCl, 10 mM Tris base) to prevent non-specific binding when probed with antibody. The membrane was washed three times in TBST (TBS containing 0.05% Tween-20) to remove the blocking agent. Then, the membrane was incubated with a primary antibody overnight in the cold room. To remove excess unbound antibody, the membrane was washed using TBST three times for five minutes each. After that, the membrane was incubated with the relevant horseradish peroxidise (HRP)-conjugated secondary antibody for two hours. Lists of the antibodies used in this study are listed in table 2.5. The membrane was washed three times in TBST. To detect targeted protein bands, enhanced chemiluminescence (ECL) western blotting reagents containing 1µl/ml H_2O_2 (GE healthcare) was used onto Bio-Rad molecular imager (ChemiDoc ^{TM} XRS+ imaging system).

The membrane was stripped using a stripping buffer (0.1M glycine, pH 2.5) for 30 minutes at room temperature and then in TBST three times before probing with antibody to detect a housekeeping gene to normalise the level of the

protein of interest. Band intensities, which reflect the protein abundance, were calculated using Image Lab™ software (Bio-Rad).

	Antibody	Supplier	Cat. Nr	Dilution
1	Angiotensin II type 1 R	abcam	ab124734	1:1000
2	FOXO1	abcam	ab52857	1:1000
3	P-FoxO1 (Thr24)/FoxO3a (Thr32)	Cell sig	9464s	1:1000
4	β-actin	abcam	ab20272	1:5000

Table 2.5 Antibodies used in this study.

2.1.3 Angiotensin II infusion in GENA348 mice

To determine whether hypertension would increase the stress in the heart and lead to the accelerated appearance of the cardiac phenotype in GENA348 mice, the following was performed. 6-month-old male GENA348 Ho mice and WT control mice received angiotensin II (ANG II, Sigma-Aldrich) or vehicle (ddH_2O) through a subcutaneously implanted osmotic minipump (Alzet, model 1002) for a period of two weeks. ANG II was selected as a model to induce hypertension, as firstly, it is one of the most commonly used mouse models in the literature (Monassier et al., 2006; Bilsen et al., 2014) as well as in our lab. Secondly, ANG II can rapidly induce an increase in blood pressure of approximately +45-60 mmHg.

Initially the concentration of ANG II used was 1 mg/kg/day as previous studies in our lab showed a significant increase in blood pressure when this dose was used. However, in GENA348 mice, no response was observed. To determine the dose that produces raised blood pressure, a dose response experiment was

performed. A range of doses was examined and blood pressure was recorded by using a non-invasive tail cuff method. It was found that 2mg/kg/day was the appropriate dose to use with GENA348 mice.

For the implantation of osmotic mini-pumps, the mice were first anaesthetised using 3-4% isoflurane with 1 litre/minute oxygen flow rate and maintained with 1-3% isoflurane. Then, the upper back region was shaved, and the osmotic mini-pump was inserted through a 1 cm incision and the skin was closed. Mice were given 0.1 mg/kg Buprenorphine as a pain relief and allowed to recover in a 37°C incubator. After the experiment was completed, cardiac structure and function was assessed by echocardiography and haemodynamic. Thereafter, the mice were sacrificed and their hearts harvested for further analysis. The surgery was performed by Dr Min Zi.

2.1.4 Blood pressure measurement

Systolic and diastolic blood pressure in conscious mice was measured at baseline (before implanting the mini-pump) and during the treatment as illustrated in figure 2.2. Measurements were taken by the tail-cuff method using a Volume Pressure Recording (VPR) sensor technology (CODA, KENT Scientific Corporation, CA, USA), which is clinically validated and provides a very high degree of correlation with the radiotelemetry method and the other blood pressure measurements (Feng et al., 2008). This method offers a unique chance to concurrently measure the systolic, diastolic and mean blood pressure, the heart rate, tail blood volume and blood flow (Feng et al., 2008). Mice were trained to the system for three days before data was obtained (15 minutes each day). For each mouse, the first set of ten measurements was eliminated and the reported blood pressure was the average of the next ten measurements. Accepted cycles were used for data analysis.

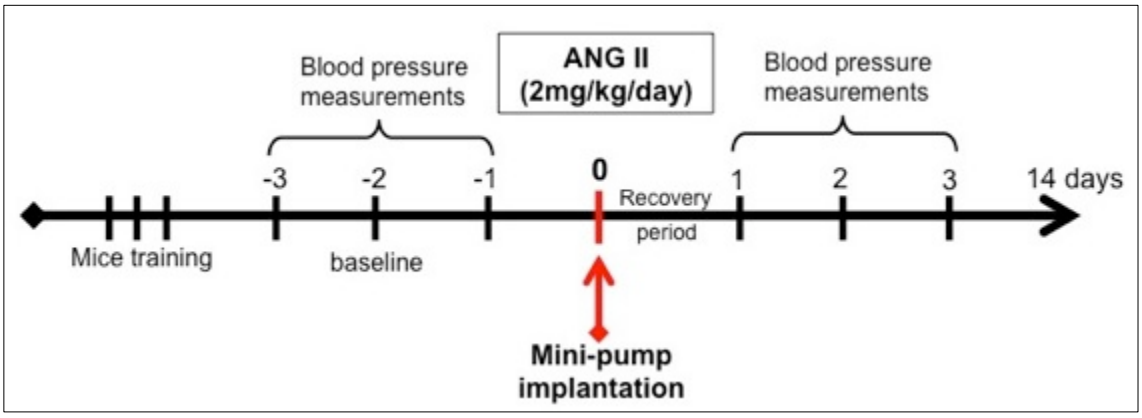

Figure 2.2 Schematic diagram of the blood pressure measurements

Mice were acclimatised to the CODA system for three days before data was acquired. Three independent measurements were taken at baseline on three different days. After osmotic mini-pumps implantation, mice were kept for three days to recover. After that, another three independent measurements were taken.

2.1.5 *In vivo* analysis of cardiac structure and function

The *in vivo* cardiac phenotype of GENA348 mice was characterised using transthoracic echocardiography and haemodynamic analysis. Mice were anesthetized using isoflurane inhalation (3-4% with oxygen at flow rate of 1 litre/ minute) in all experiments. These techniques were performed by Dr Min Zi.

2.1.5.1 Transthoracic echocardiography

Echocardiography (Echo) is a non-invasive technique, which uses standard two- dimensional and Doppler ultrasound to allow visualization of the heart. It was used to examine the function and structure of the left ventricle in GENA348 mice. Two-dimensional images of the heart were taken by using an Acuson Sequoia C256 ultrasound instrument fitted with a 14 MHz transducer (Siemens) applied parasternally to the shaved area. The transducer was covered with a warmed transmission gel to improve ultrasound transduction. M-mode images were taken from the short axis provided measurements of diameter of the left ventricle end-diastolic (dLVD) and end-systolic (sLVD), interventricular septum (IVS) and posterior wall (PW) thicknesses; representative images of which are shown in figure 2.3. From these data, other parameters to assess the cardiac function and structure listed in table 2.6 were calculated.

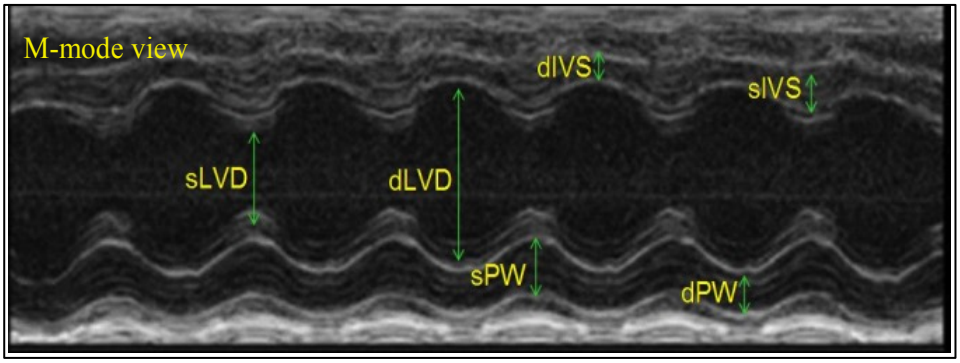

Figure 2.3 Echocardiography image on M-mode view

Representative M-mode view from which the shown parameters were acquired. **sLVD:** left ventricle diameter in systole, **dLVD:** left ventricle diameter in diastole, **sIVS:** intraventricular septum in systole, **dIVS:** intraventricular septum in diastole, **sPW:** posterior wall thickness in systole, **dPW:** posterior wall thickness in diastole.

N	Parameter	Formula
1	**Fractional shortening (FS%)**	[(dLVD - sLVD)/dLVD] x100
2	**Ejection fraction (EF%)**	[(dVol - sVol)/dVol] x100
3	**Relative wall thickness (RWT)**	(dIVS+dPW)/dLVD
4	**Left ventricular mass (LVM)**	$1.055X[(dLVD+dPW+dIVS)^3-dLVD^3]$

Table 2.6 Formula derived from echocardiography data for the measurement of cardiac morphology and function. 1.055 is the specific gravity of the myocardium (g/ml).

2.1.5.2 Haemodynamic measurements

Haemodynamic measurements are the most common invasive technique used to evaluate cardiac function. This technique was carried out following a protocol described previously (Liu et al., 2009). A 1.4-Fr high-fidelity micromanometer catheter (SPR-839, Millar Instruments) was inserted into the left ventricle through the right carotid artery under the Olympus stereomicroscope. Pressure signals were measured and analysed with a PowerLab system (Millar Instruments). Cardiac diastolic and systolic functions were analysed using the pressure volume data. The heart rate and left ventricular systolic and end-diastolic pressures were measured and the maximal change of left ventricular systolic pressure (dP/dt_{max}) and diastolic pressure (dP/dt_{min}), and indices of contractility and relaxation were analysed using Millar's PVAN^{TM} software. After the haemodynamic measurements were taken, mice were sacrificed. Figure 2.4 illustrates the protocol used for haemodynamic measurements.

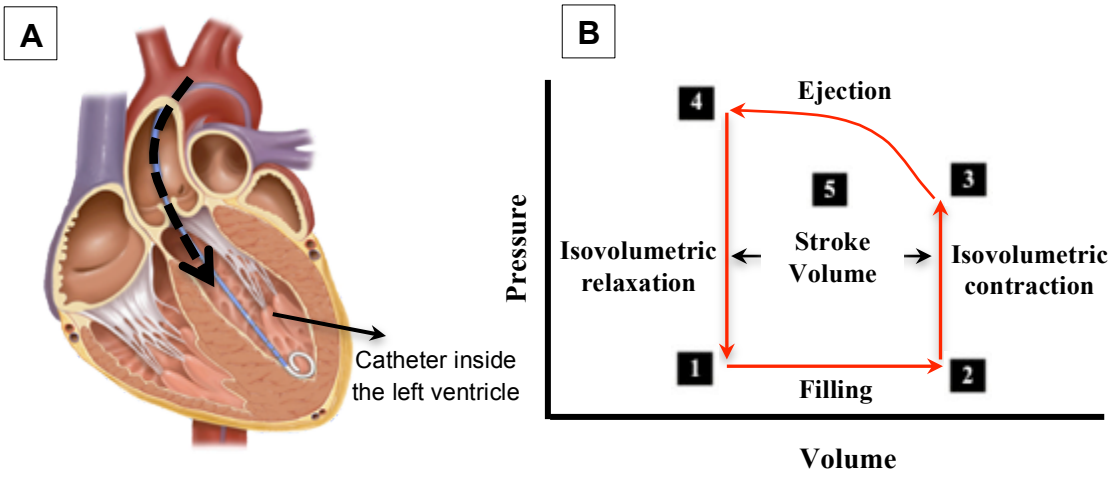

Figure 2.4 Graphic illustration of pressure-volume loop catheter

A- The position of insertion the pressure-volume loop catheter in the left ventricle through aorta. **B**- Pressure-volume loop elucidating the phases of the cardiac cycle which include; 1) mitral valve opening, 2) mitral valve closure, 3) aortic valve opening, 4) aortic valve closure and 5) stroke volume. Figure was adopted from http://www.ddah.org.uk/phenotyping-pressure-volume-loops.htm.

2.1.5.3 Heart weight normalised to body weight

In order to measure the extent of cardiac hypertrophy *in vivo*, the heart weight/ body weight (HW/BW) ratio was calculated. Before mice were killed by cervical dislocation, body weight (g) was measured using a top pan balance. Hearts were removed from sacrificed mice, drained of blood and weighed on a fine balance.

2.1.6 Histological analysis

2.1.6.1 Preparation of hearts

After mice were euthanized by cervical dislocation, the whole heart was dissected into three pieces following removal of blood. Two parts were snap frozen in liquid nitrogen and stored at -80°C for further analysis, the third (middle) part was fixed in 4% paraformaldehyde for three days at 4°C. The samples were dehydrated overnight using an automated tissue processor (Shandon Citadel 2000) before being embedded in paraffin wax. 5 µm thick sections were obtained using a microtome and mounted onto poly-L-lysine coated glass slides. The slides were kept in a 37°C oven for two days. The heart sections were deparaffinised by firstly heating the slides on a heat block, then by placing them in xylene for five minutes. Slides were rehydrated by immersion in decreasing concentrations (100%, 80%, 75%) of industrial methylated spirit (IMS) three times for five minutes. Finally, the slides were washed for five minutes under running tap water prior to staining.

2.1.6.2 Haematoxylin and eosin staining for cell size measurements

In order to measure cardiomyocyte size, the most common staining protocol was used; haematoxylin and eosin (H&E). Slides with heart sections were placed in haematoxylin for five minutes to stain the nuclei and then rinsed under running tap water for two minutes. They were subsequently immersed in acidic alcohol (1% hydrochloric acid in 70% ethanol) for about five seconds and washed in running tap water for five minutes. The slides were then counterstained with eosin for two minutes and rinsed in tap water for one minute. The slides were then dehydrated in ascending concentrations of IMS (75%, 80%, 100%) three times for five minutes. Finally, slides were placed in xylene to remove all traces of alcohol and then mounted under coverslips with

DPX (Distyrene, plasticizer and xylene). Slides were left to dry overnight before imaging on a pannoramic slide scanner (3DHISTECH). The measurement of cell cross sectional area was determined on approximately 100 cells per heart using Pannoramic Viewer software to obtain a mean values for each heart. All measurements were performed in a blinded manner.

2.1.6.3 Masson's trichrome staining for fibrosis

To stain interstitial and perivascular fibrosis, Masson's trichrome staining was used. The rehydrated slides were placed in Bouin's fixative for two hours to improve stain quality. The slides were rinsed in running tap water for ten minutes. After staining with haematoxylin for five minutes, slides were washed in running tap water for five minutes and then differentiated in acidic alcohol solution for ten seconds and after that rinsed for five minutes in running warm water. To stain cardiomyocyte red, slides were placed in a red solution (0.9% biebrich scarlet, 0.1% ponceau fuchsin in 1% acetic acid) for five minutes and washed with distilled water. The slides were differentiated in 5% phosphomolybdic acid (GCC diagnostics) for fifteen minutes to remove the red solution from the fibrosis area. The slides were rinsed in running tap water, stained for ten minutes with aniline blue (GCC diagnostics) to stain collage fibers. After rinsing slides were treated for one minute with, 1% acetic acid, dehydrated, mounted and imaged as described for H&E staining. The percentage of fibrosis was quantified using Pannoramic Viewer software in a blinded manner.

2.1.7 Statistical analysis

Data in the figures and tables were expressed as mean ± standard error of mean (SEM). Statistical analysis was performed using GraphPad Prism (version 6.00 for Mac, GraphPad Software, La Jolla California USA, www.graphpad.com). For comparisons between two groups, a student's unpaired t-test was used. However, A two-way analysis of variance (ANOVA) followed by a Bonferroni post hoc was used to determine the statistical difference between four groups considering $P<0.05$ as statistically significant in all experiments.

Chapter 3

Response of GENA348 mice to hypertension induced by angiotensin II infusions.

3.1 Introduction

3.1.1 Hypertension and diabetic heart disease

High blood pressure (hypertension) is one of the most common chronic conditions in the world. It affects approximately 40% of adults aged 25 and over globally. In 2008, hypertension affected approximately one billion people in the world (WHO, 2013) and it is expected that by 2025, more than 1.56 billion people will be hypertensive worldwide (WHO, 2012).

Cardiovascular disease (CVD) accounts for about 17 million deaths worldwide per year. Of those deaths, hypertension complications account for approximately 9.4 million deaths annually (WHO, 2013). Hypertension itself is considered as a significant risk factor for cardiovascular morbidity and mortality (Grossman & Messerli, 2008). Furthermore, it is well known that hypertension is more prevalent in patients with diabetes than in those without diabetes (Grossman & Messerli, 2008). The incidence of hypertension is approximately two-fold greater in diabetic patients than in patients without diabetes. However, the incidence of diabetes is about 2-3 times higher in hypertensive patients than in patients with normal blood pressure (Grossman & Messerli, 2008).

Much work has focused on the interaction between hypertension and diabetes and their influence on cardiac phenotypes. In isolation, diabetic patients with heart failure have a worse prognosis than non-diabetic patients with heart failure. The Framingham data exposed a 4-fold higher incidence of congestive heart failure in diabetic men and a 8-fold increase in diabetic women, compared with non-diabetic patients (Grossman, 2009).

Hypertension also has an influence on the incidence and development of cardiovascular events and microvascular complications. It was established by a meta-analysis done by the Prospective Studies Collaboration that cardiovascular mortality is two times higher with each 20/10 mmHg rise in blood pressure (Kannel, 2009). The Framingham data revealed a high population-attributable risk of hypertension for the pathogenesis of heart failure in women, (accounting for 59% of cases) compared to men (39%) (Grossman & Messerli, 2008).

Hypertension and diabetes are important risk factors resulting in elevated cardiovascular mortality and morbidity (Sowers and Epstein, 1995). Hypertension exaggerates the cardiovascular complications accompanying diabetes and vice versa. Coexistence of the two conditions leads to marked cardiac structural and functional changes than with either condition alone (Wold et al., 2001). Factor and coworkers explained the pathologic features established on post-mortem outcomes in diabetic patients with hypertension and compared those features to all participants in all the study groups. Among the four groups, patients with both diabetes and hypertension had more pronounced left ventricular wall thickness and cardiac hypertrophy. In addition, a high degree of fibrosis was observed in the hypertensive diabetic hearts compared to the other groups. (Factor et al., 1980). The distribution of dense interstitial connective tissue through the myocardium is the most outstanding microscopic finding in the hearts of hypertensive diabetic patients (van Hoeven & Factor, 1990).

Echocardiographic assessments have also revealed an increase in the left ventricular mass and a high rate of left ventricular hypertrophy in hypertensive diabetic patients. It has also been illustrated that the inter-ventricular septum is

thickened in diabetic patients with hypertension compared to other groups (Venco et al., 1987). Collectively, in these findings, structural and functional abnormalities are more severe in hypertensive diabetic patients compared with patients with either condition alone.

Similar myopathological features have been observed in animal models. Factor and coworkers studied a large group of rats with streptozotocin (STZ) -induced diabetes and renovascular HTN. They observed a greater degree of fibrosis in diabetic rats with hypertension when compared to controls.

Black et al. studied the pathology of the heart in a well-described model of combined diabetes and hypertension; spontaneously hypertensive rats with STZ-induced diabetes. They found that there was a marked increase in the level of interstitial fibrosis in the hearts of the diabetic hypertensive group. It was anticipated that the increase in interstitial fibrosis in the heart when hypertension is combined with diabetes results in increased cardiac muscle stiffness and leads to impaired cardiac function (Black et al., 2010).

In another combined model of diabetes and hypertension, db/db mice were infused with a low dose of angiotensin II (ANG II) (1mg/kg/day) to induce a relatively mild hypertension for 4 weeks. Bilsen and colleagues found that there was a pronounced cardiac hypertrophy in the diabetic mice after ANG II treatment compared to the other groups. Echocardiographic analysis revealed that diastolic wall thickness was significantly augmented in ANG II treated diabetic mice after the initiation of ANG II treatment (Bilsen et al., 2014). Collectively, data from animal studies showed that the combination of diabetes and hypertension could result in marked adverse alteration to the cardiac structure and function.

In both humans and experimental animals, studies suggest that the presence of hypertension and diabetes at the same time results in a more severe cardiomyopathy than would be expected with either of the conditions alone. A greater understanding of how the cardiomyopathy seen in diabetes is influenced by hypertension and the underlying mechanisms of action is needed.

3.2 Hypothesis

Hypertension will exaggerate the cardiac phenotype in 6 months old GENA348 mice and will lead the cardiac phenotype to develop quickly and at an early age compared to WT controls.

3.3 Aims

To induce hypertension in GENA348 mice and determine whether hypertension would increase the stress on the heart and exaggerate the cardiac phenotype in HO GENA348 mice compared to WT controls.

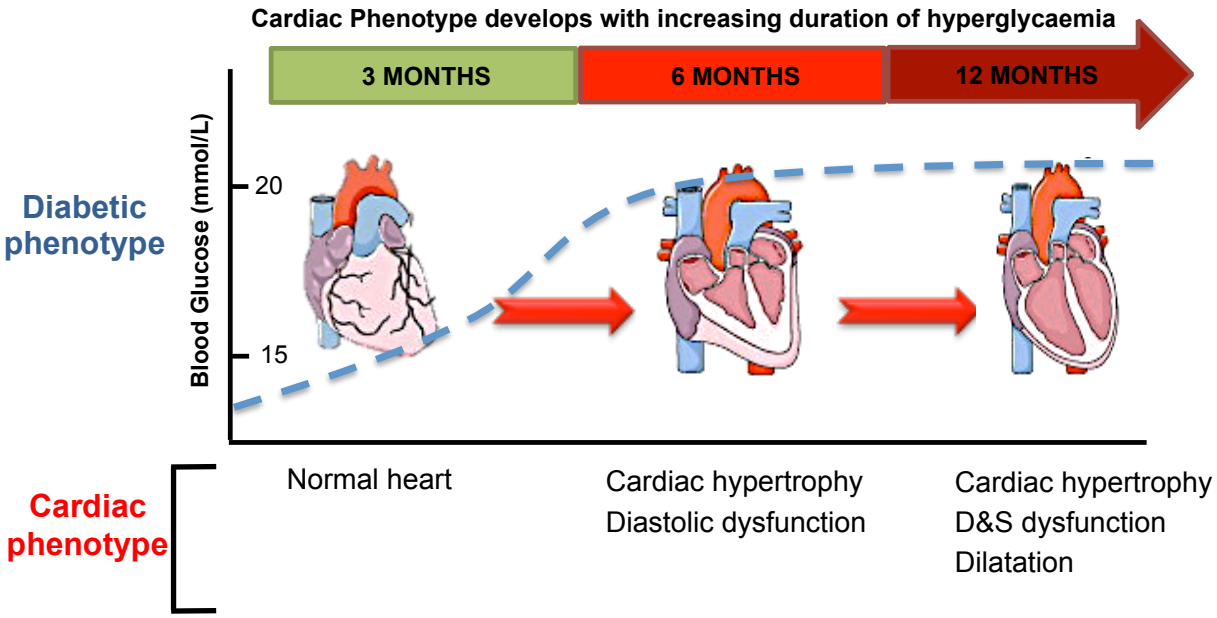

Figure 3.1 schematic diagram shows the diabetic and cardiac phenotype that developed in the HO GENA348 mice compared to WT controls.

3.4 Results

3.4.1 Determination of the dose of ANG II to induce raised blood pressure in GENA348 mice

It has been shown that a dose of 1 mg/kg/day has successfully induced a significant increase in blood pressure in different strains of mice (Monassier et al., 2006; Bilsen et al., 2014). However, in GENA348 mice, no clear response was observed. A dose response curve was performed. A range of doses was examined in WT GENA348 mice and blood pressure was recorded by using a non-invasive tail cuff method. It was found that both systolic and diastolic blood pressure remained unchanged with 1 and 1.5 mg/kg dose (Figure 3.2). On the other hand, the dose of 2mg/kg/day showed an increase in systolic and diastolic blood pressure in the GENA348 mice.

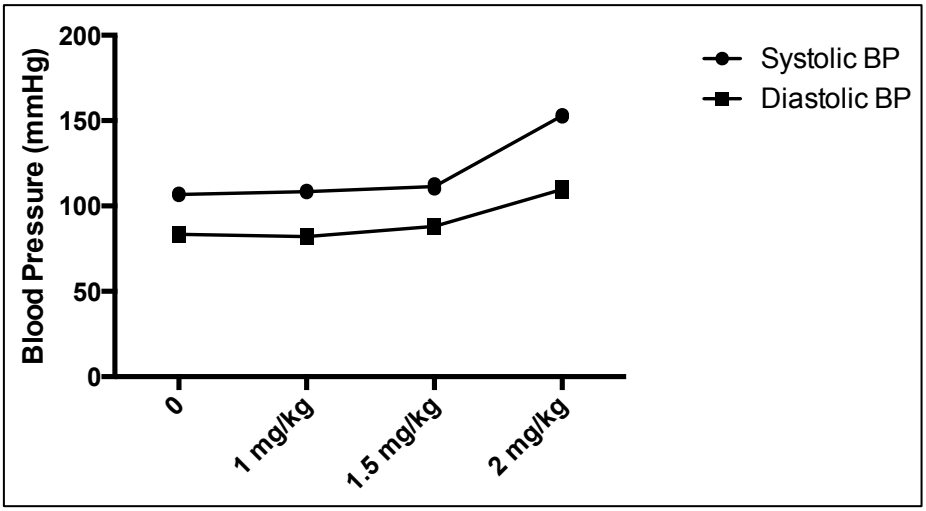

Figure 3.2 A dose response curve was performed to determine the proper dose of ANG II to induce hypertension to the GENA348 mice.

6-month-old WT GENA348 mice were given a range of ANG II doses from (1 to 2 mg/kg/day). Systolic and diastolic blood pressure was measured by using the tail-cuff method. It was found that 2 mg/kg/day of ANG II treatment led to an increase in both systolic BP (152.48 mmHg) and diastolic BP (109.74 mmHg). Data are presented as mean. N=2.

Small numbers of mice were used as a preliminary experiment to determine whether the GENA348 HO mice would have a differential response compared to WT mice. HO mice and WT control mice received ANGII (2mg/kg/day) or vehicle (ddH_2O) through a subcutaneously implanted osmotic minipump for two weeks. Blood pressure was measured using the tail-cuff method at baseline (before implanting the mini-pump) and after the treatment. It was found that in water-treated GENA348 HO and WT mice, blood pressure remained unchanged after pump administration. However, ANG II-treated GENA348 HO and WT mice showed an increase in both systolic and diastolic blood pressure. ANG II treatment led to a similar increase in blood pressure in both WT and HO GENA348 mice (Figure 3.3 A&B).

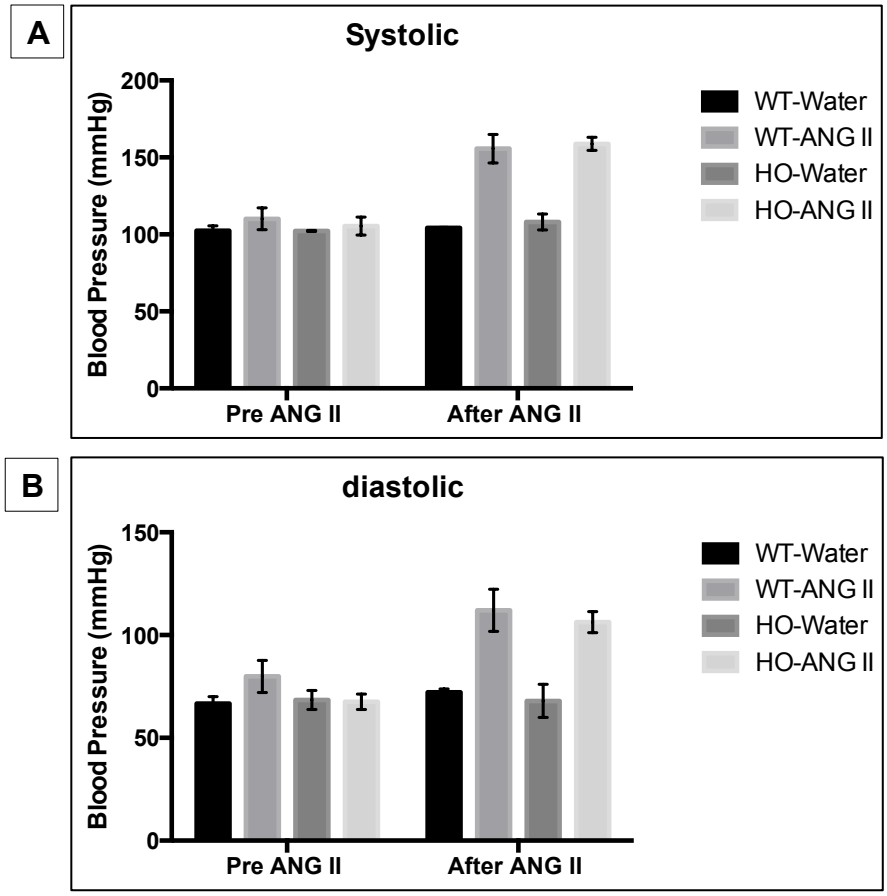

Figure 3.3 Blood pressure measurement pre and after the ANG II treatment in the GENA348 mice.

WT and HO GENA348 mice were given ANG II (2 mg/kg/day) or water via osmotic mini-pumps for two weeks. A-Systolic and B-diastolic blood pressure was measured at baseline and after implanting the mini-pumps using tail-cuff method. Whereas in water-treated GENA348 HO and WT mice, both systolic and diastolic blood pressure remained unchanged, ANG II-treated mice showed an increase in blood pressure to the same extent in both mice. Data are expressed as mean. N= 2-3

3.4.2 Effect of 2mg/kg/day ANG II treatment on blood pressure in the GENA348 WT and HO mice.

In this project, ANG II (2 mg/kg/day) was used to induce hypertension in 6-month-old GENA348 mice for a period of two weeks to establish if an increase in blood pressure associated with diabetes would result in the exaggeration of the cardiac phenotype observed in GENA348 mice. Prior to the ANG II treatment, blood pressure was normal in both WT and HO GENA348 mice. Figure 3.4 demonstrates that ANG II treatment led to a significant increase in both systolic and diastolic blood pressure to the same extent in both WT and HO mice (Systolic BP; WT-water vs. WT-ANG II (112.72±3.8 vs. 152.86±5.3mmHg, HO-water vs. HO-ANG II (105.3±4.2 vs. 153±5.9 mmHg, ***p<0.001) Diastolic BP; WT-water vs. WT-ANG II (84.28±5.2 vs. 108.54±6.2mmHg, *p<0.05; HO-water vs. HO-ANG II (67.4±5.1 vs. 111.55±5.7mmHg, **p<0.01).

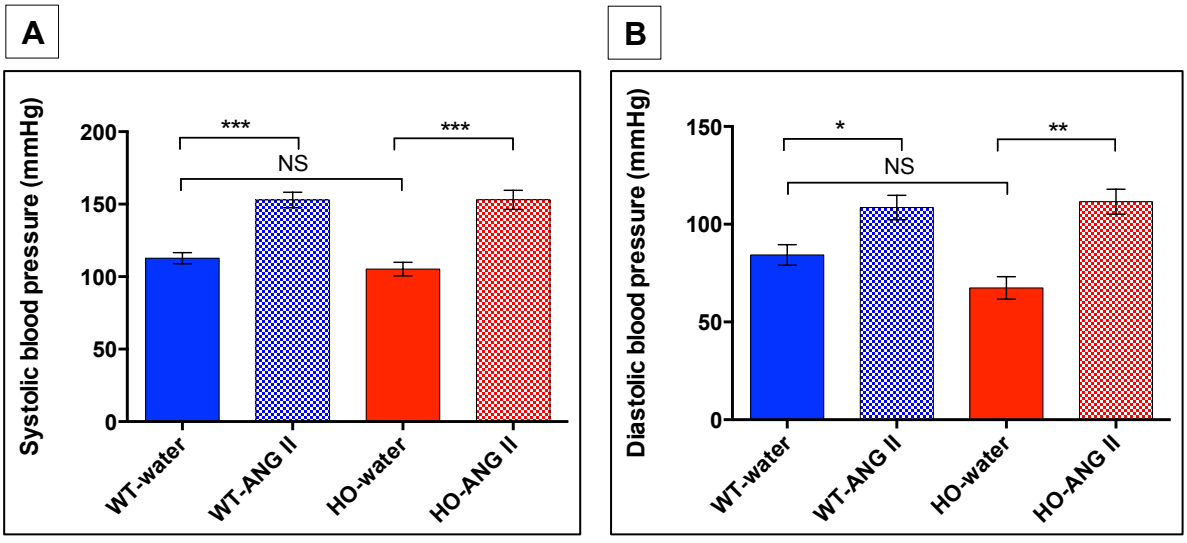

Figure 3.4 Systolic and diastolic blood pressure of GENA348 mice following treatment with ANG II for two weeks.

Six-month-old GENA348 mice were given ANG II (2 mg/kg/day) or water via osmotic mini-pumps for two weeks. A-Systolic and B-diastolic blood pressure was measured at baseline and after implanting the mini-pumps as described using the tail-cuff method. *P<0.05 **P<0.01, ***P<0.001 for ANG II treated mice when compared to water-treated mice. ANG II treatment led to a significant increase in both systolic BP (WT: 40.2 mmHg, HO: 47.7 mmHg) and diastolic BP (WT: 24.2 mmHg, HO: 44.2 mmHg) to the same extent in both mice. Data are expressed as mean±SEM. N= 4-5.

3.4.3 Cardiac structure and function in 6-month-old GENA348 mice after ANG II treatment.

Cardiac structure and function was assessed in GENA 348 mice following ANG II treatment. Increased heart weight is associated with cardiac hypertrophy; therefore, the heart weight to body weight ratio was determined.

Before ANG II infusion, there was a significant increase in the HW/BW ratio (WT: 3.46±0.06, HO: 3.81±0.06, p=0.02) in the HO mice compared to WT controls (Figure 3.5). This was expected as the cardiac phenotype developed at this age. After ANG II treatment, both HO and WT mice showed an increase of 26% and 37% respectively, in heart weight normalised to body weight ratio compared to untreated controls mice (WT-water vs. WT-ANG II and HO-water vs. HO-ANG II). (WT-ANG: 4.83±0.37, HO-ANG: 4.96±0.25, p=0.81). The increase in the normalised heart weight was similar after ANG II infusion in both WT and HO, which indicates that there is no change in the heart weight to body weight ratio with this model of hypertension.

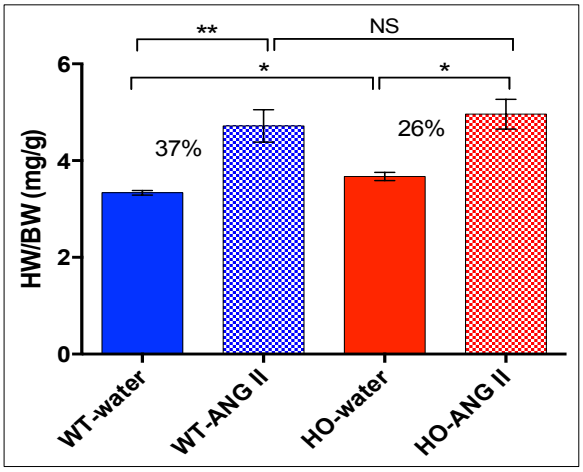

Figure 3.5 The hypertrophic response in GENA348 mice following two weeks of ANG II treatment.

Heart weight normalised to body weight rose similarly in both HO and WT control mice following ANG II treatment (WT-water vs. WT-ANG II (3.31±0.03 vs. 4.83±0.4 mg/g, **p<0.01; HO-water vs. HO-ANG II (3.82±0.06 vs. 4.96±0.3mg/g, **p<0.01)). Data are expressed as mean±SEM. N= 4-5.

3.4.3.1 In *vivo* analysis of cardiac structure

Transthoracic echocardiography was performed on ANG II treated GENA348 HO mice and WT controls to determine if induction of hypertension by using ANG II led to changes in the cardiac structure and function. Prior to ANG II treatment, there was a significant increase in the internal dimensions of the left ventricle as well as the left ventricle mass in the HO mice compared to WT controls (Table 3.1). After ANG II infusion, there were no significant differences in most of the echocardiographic parameters in the HO mice compared to WT controls (Table 3.1). Relative wall thickness showed a comparable pattern to the HW/BW ratio with a significant increase in both HO and WT mice following ANG II treatment compared to untreated controls (WT-water vs. WT-ANG II and HO-water vs. HO-ANG II) (Figure 3.6).

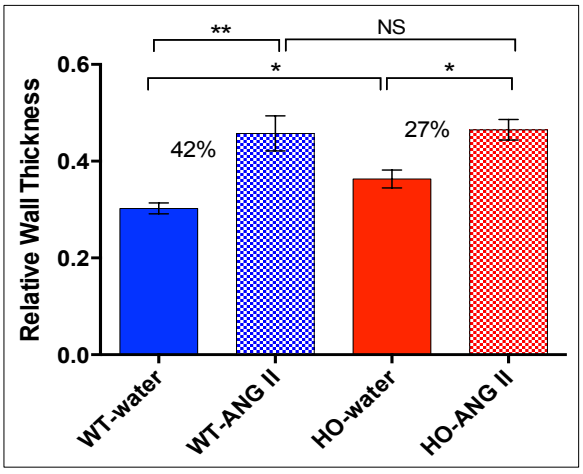

Figure 3.6 Relative wall thickness in GENA348 mice following two weeks ANG II treatment.

Relative wall thickness also found the hypertrophic response to ANG II treatment to be comparable amongst WT and HO mice (WT-water vs. WT-ANG II (0.30±0.007 vs. 0.46±0.03, **p<0.01; HO-water vs. HO-ANG II (0.37±0.02 vs. 0.47±0.02, *P<0.05)). The hearts do not increase in size by the same percentage change. Data are expressed as mean±SEM. N= 4-5.

Parameters	WT			HO				
	Water (N=4)	ANG II (N=5)	*P* WT-W VS WT-ANG	Water (N=4)	*P* WT-W VS HO-W	ANG II (N=5)	*P* HO-W VS HO-ANG	*P* WT-ANG VS HO-ANG
Chamber size								
dLVD (mm)	4.34 ± 0.1	4.24 ± 0.2	0.66	4.79 ± 0.05	0.04*	4.19 ± 0.2	0.14	0.72
sLVD (mm)	2.91 ± 0.1	2.61 ± 0.2	0.27	3.61 ± 0.05	0.02*	2.82 ± 0.2	0.02*	0.23
Wall thickness								
dIVS (mm)	0.81 ± 0.05	0.98 ± 0.03	0.03*	0.92 ± 0.07	0.29	0.98 ± 0.04	0.55	0.23
sIVS (mm)	1.45 ± 0.07	1.68 ± 0.05	0.05*	1.48 ± 0.05	0.85	1.54 ± 0.09	0.67	0.05
dPW (mm)	0.73 ± 0.03	0.83 ± 0.07	0.31	0.81 ± 0.07	0.39	0.86 ± 0.04	0.56	0.68
sPW (mm)	1.21 ± 0.02	1.36 ± 0.09	0.23	1.11 ± 0.08	0.26	1.20 ± 0.05	0.38	0.26
LV mass (mg)	127.4 ± 6.4	145.01 ± 9.4	0.24	167.82 ± 9.3	0.03*	147.6 ± 13.5	0.38	0.69

Table 3.1 Echocardiographic parameters of left ventricular dimensions of GENA348 mice following ANG II treatment

Transthoracic echocardiography was performed on ANG II treated GENA348 HO mice and WT controls. Values are presented as mean ± SEM, $p<0.05$ was considered significant.

sLVD: left ventricle diameter in systole, **dLVD:** left ventricle diameter in diastole, **sIVS:** intraventricular septum in systole, **dIVS:** intraventricular septum in diastole, **sPW:** posterior wall thickness in systole, **dPW:** posterior wall thickness in diastole. **LV mass:** left ventricular mass.

3.4.3.2 In *vivo* analysis of cardiac function

To provide a more comprehensive insight into the cardiac function of the 6-month-old GENA348 mice following ANG II treatment, a pressure-volume loop catheter was used. Before ANG II infusion, there was a significant decrease in both ejection fraction and fractional shortening in the HO mice compared to WT controls (Table 3.2). After ANG II treatment, diastolic function appeared to be preserved, as there were no significant changes in diastolic function parameters in the HO mice compared to WT controls (WT-ANG II vs HO-ANG II)(Table 3.2). However, there was a significant increase in both ejection fraction and fractional shortening in the ANG II HO mice compared to HO controls.

Parameters	WT			HO				
	Water (N=4)	ANG II (N=5)	*P* WT-W VS WT-ANG	Water (N=4)	*P* WT-W VS HO-W	ANG II (N=5)	*P* HO-W VS HO-ANG	*P* WT-ANG VS HO-ANG
Systolic Function								
EF %	69.89 ± 2.4	76.19 ± 3.1	0.22	56.68 ± 3.7	0.04*	68.95 ± 2.5	0.04*	0.15
FS %	33.19 ± 1.7	38.55 ± 2.6	0.19	24.49 ± 2.1	0.04*	32.52 ± 1.8	0.04*	0.15
dP/dt max (mmHg/s)	6811.5 ± 435.9	8018 ± 1265.4	0.5	5792.67 ± 1338.7	0.5	6727.25 ± 793.4	0.6	0.5
Diastolic Function								
dP/dt min (mmHg/s)	-5869.7 ± 544.4	-6914.5 ± 1169.7	0.5	-5382 ± 1204.4	0.7	-4949.25 ± 503.9	0.7	0.3
Tau (msec)	6.71 ± 0.4	7.20 ± 0.6	0.6	6.35 ± 1.3	0.8	7.47 ± 0.6	0.5	0.6

Table 3.2 Cardiac function in GENA348 mice following ANG II treatment for two weeks

3.4.3.3. Histological analysis of 6 month-old GENA 348 mice after ANG II treatment.

To determine whether there was cellular hypertrophy in the 6-month-old GENA348 mice after ANG II treatment, the cardiomyocyte cross sectional area was calculated. Heart sections were stained with haematoxylin and eosin and then the cell size was measured by drawing around the perimeter of the cells to assess the cross sectional area. Prior to ANG II treatment, individual cardiomyocytes were significantly larger in the HO mice compared to their WT controls displaying cellular hypertrophy had developed at 6 months (WT: 231±12, HO: 300±14, p=0.02, 26%). After ANG II infusion, there was a significant increase in the cardiomyocyte cross sectional area in both WT and HO to the same extent (Figure 3.7A). Quantification of mean cardiomyocyte cross sectional area of approximately 100 cells per heart indicated a comparable degree of hypertrophy in both WT and HO GENA348 mice after ANG II treatment (WT-ANG II: 355±43, HO-ANG II: 380±27, p=0.62)(Figure 3.7B).

To determine if there was an interstitial fibrosis in the 6-month-old GENA348 mice after ANG II treatment, Masson's trichrome staining was used. There was no evidence of increased fibrosis in the HO GENA348 mice before ANG II treatment. However, ANG II infusion induced approximately a similar degree of fibrosis in both WT and HO GENA348 mice compared to controls (Figure 3.8B). These findings were confirmed later by looking at the mRNA expression of collagen 1 alpha 1(COL1A1) and collagen III alpha 1(COL3A1) using the Q-PCR (Figure 3.8C).

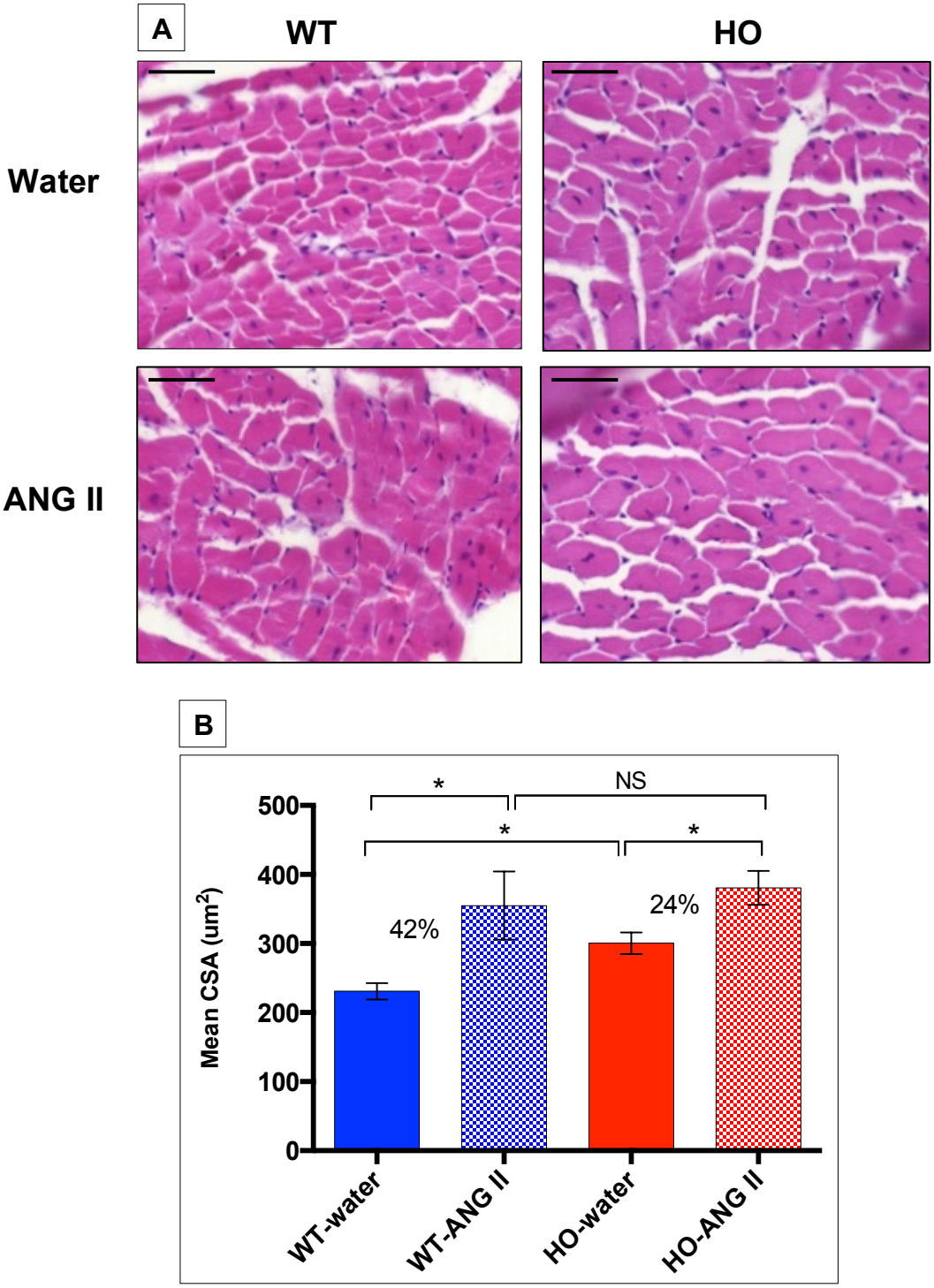

Figure 3.7 Cardiomyocyte cross sectional area in GENA348 mice following two weeks of ANG II treatment

A- Representative H&E stained heart sections from which mean cardiomyocyte cross sectional area was calculated. Scale bars = 50µm. B- Quantification of mean CSA of approximately 100 cells per heart using Pannoramic Viewer software as described. ANG II treatment induced a similar degree of growth in WT and HO myocytes compared to controls ($p<0.05$ was considered significant). Data are expressed as mean±SEM. N= 4-5.

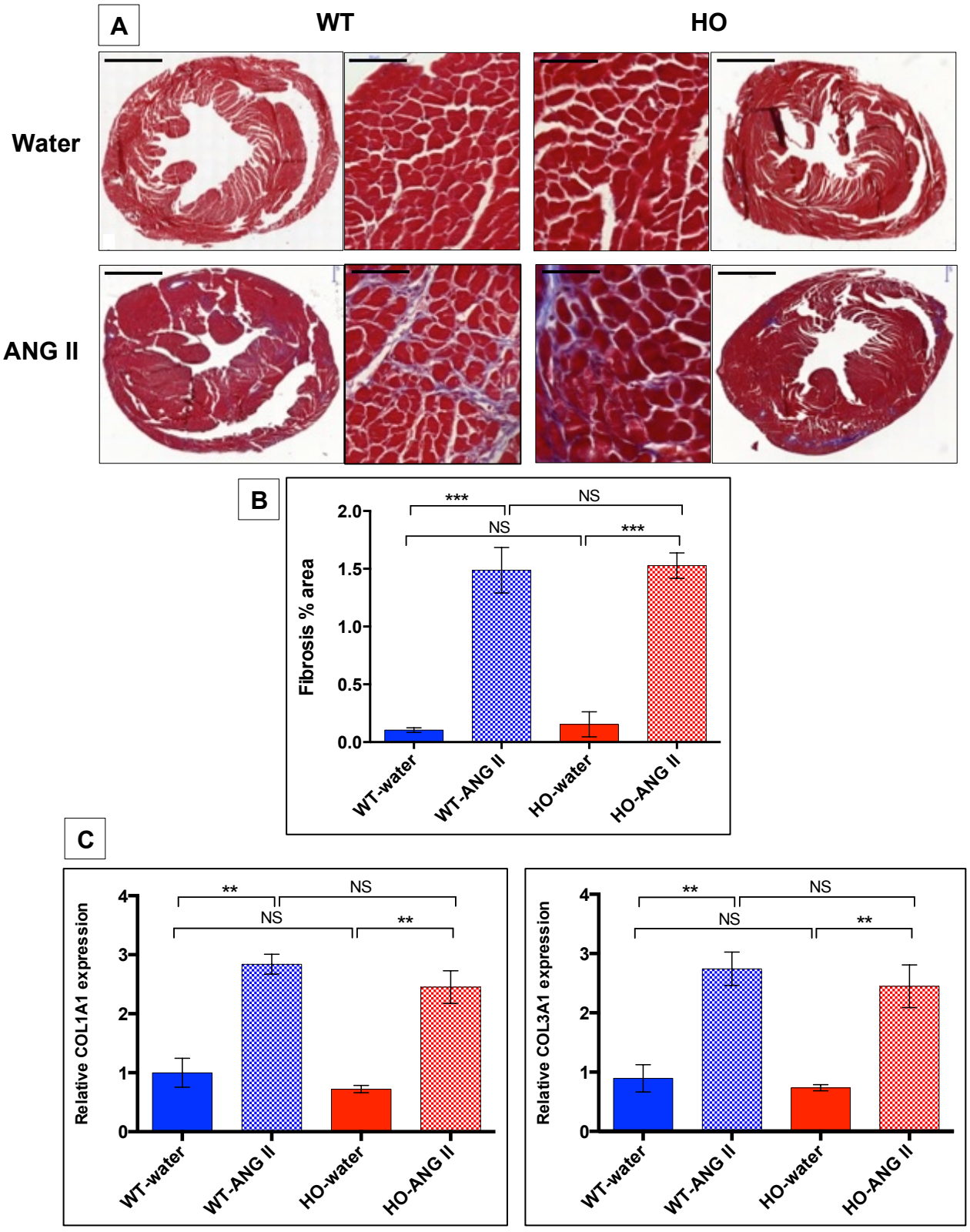

Figure 3.8 Histological and molecular analysis of the fibrotic response in GENA348 mice following two weeks of ANG II treatment

A- Representative Masson's trichrome stained heart sections from which the percentage of interstitial fibrosis was calculated. Scale bars; higher magnification= 50µm, low magnification=1000µm. Collagen fibres (blue), muscle fibres (red). B- Quantification of the percentage of fibrosis using Pannoramic Viewer software as described. ANG II treatment induced a similar degree of fibrosis in WT and HO GENA348 mice compared to controls ($p<0.05$ was considered significant). C-COL1A1 and COL3A1 mRNA expressions increased after ANG II treatment in WT mice, and to a lesser extent in HO mice, $^{**}p<0.01$. Data are expressed as mean±SEM. N= 4-5.

3.4.3.4. Molecular analysis of 6 month-old GENA 348 mice after ANG II treatment.

Q-PCR was employed to measure the mRNA expression of the hypertrophy marker brain natriuretic peptide (BNP) in 6-month-old GENA348 mice following ANG II treatment. Prior to ANG II infusion, there was a significant 1.4 fold increase in the expression of BNP in the HO mice, compared to WT controls. This was in line with HW/BW ratio, RWT and CSA previous data. After ANG II treatment, there was a 2.9 and 2.5 fold increase in the expression of BNP in the WT and HO mice compared to their controls (WT-water vs. WT-ANG II and HO-water vs. HO-ANG II) (Figure 3.9). The increase in the expression of BNP was roughly similar after ANG II infusion in WT and HO mice, indicating that although the hypertensive stress did quite dramatically affect the cardiac phenotype, there was no difference in the resulting phenotype in the HO and WT mice.

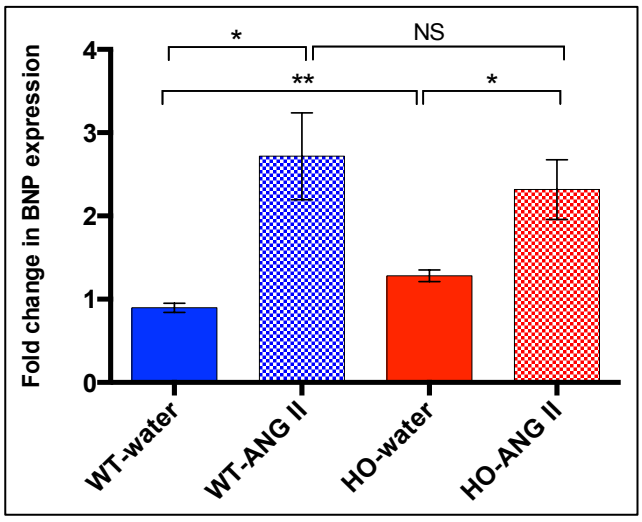

Figure 3.9 Q-PCR quantification of BNP expression in GENA348 mice after ANG II infusion

Using RT-PCR quantification, BNP expression was measured in heart tissue of six-month-old GENA348 mice following ANG II treatment. There was a similar increase in the BNP expression in the WT and HO mice compared to their controls. Data are presented as mean ±SEM. *P<0.05 **P<0.01. Data are expressed as mean±SEM. N= 4-5.

3.4.4 Expression of angiotensin II, type 1 receptor in GENA348 mice following ANG II treatment.

The expression level of the AT1R was examined to investigate why there was no difference in the resulting cardiac phenotype in the HO and WT mice following ANG II treatment even though the 6 months HO mice have had cardiac hypertrophy before the ANG II treatment.

The biological effects of ANG II are produced through two G protein-coupled receptors, the angiotensin type 1 (AT1R) and type 2 (AT2R) receptors. ANG II play a fundamental role in the development of hypertension as well as in the pathophysiology of myocardial hypertrophy, fibrosis and remodelling. In cardiovascular diseases, the cellular and molecular actions of ANG II are mediated by AT1R (Chen & Coffman, 2015).

Immunoblot analysis was employed to look at the expression level of the AT1R. There was a significant 0.5 fold reduction in the expression of AT1R in HO mice, following ANG II treatment, compared to their WT controls (Figure 3.10). Our data suggest that ANG II signaling is blocked or interrupted at receptor level.

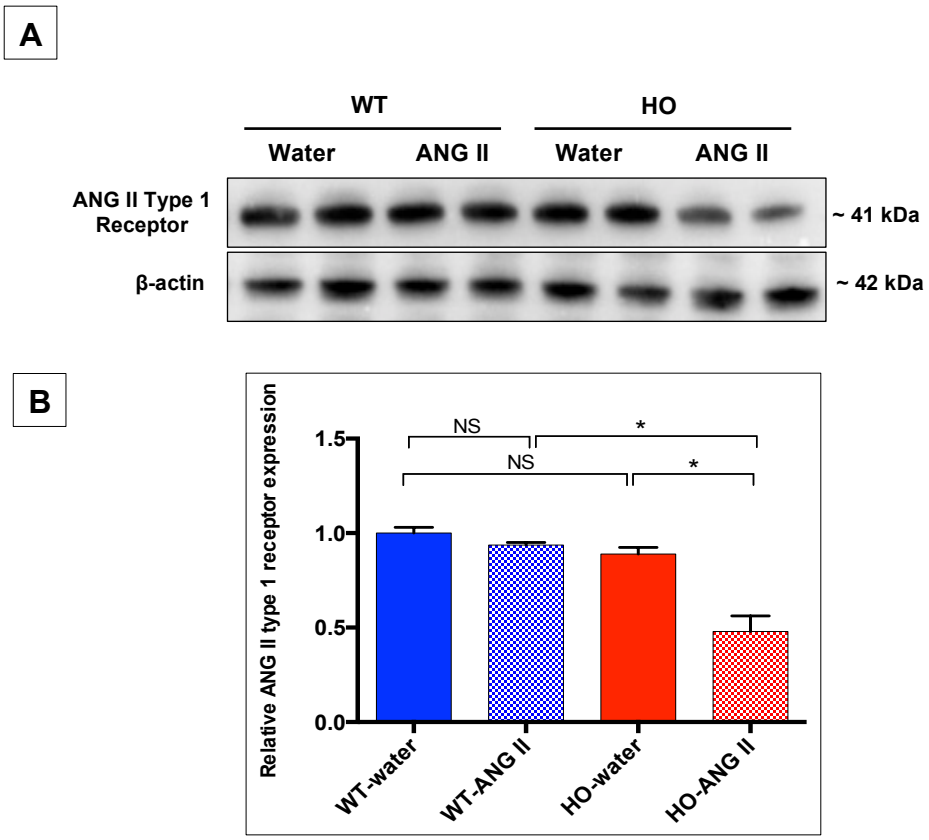

Figure 3.10 Expression of angiotensin type 1 receptor 1a in GENA348 mice following ANG II treatment.

A- Western blot analysis of the angiotensin type 1 receptor 1a from six-month-old GENA348 WT mice and HO mice, which have been treated with or without ANG II. B- Densitometric analysis of the immunoblot A showed a significant decrease in the expression of the angiotensin type 1 receptor 1a in HO mice following ANG II treatment compared to WT-ANG II. Data are presented as mean ±SEM. *P<0.05. N= 4.

3.5 Discussion

Hypertension and diabetes are important risk factors leading to increased cardiovascular mortality and morbidity. The combination of these disorders can result in noticeable adverse changes to the structure and function of the heart, which contributes to elevate the risk of heart failure. It is still unknown how diabetes and hypertension interact to promote heart failure development and the underlying mechanisms are not fully understood. The aim of this study was to induce hypertension in GENA348 mice and determine whether the increased stress on the heart would lead to an accelerated cardiac phenotype in HO GENA348 mice.

3.5.1 Pronounced hypertensive response to ANG II infusions in 6-month-old GENA348 mice

In this project, hypertension was induced by continuous infusion of ANG II (2 mg/kg/day) using a minipump for a period of two weeks, resulting in a 40-50 mmHg increase in blood pressure. Notably, the rise in blood pressure induced by ANG II was the same in both WT and HO mice.

The degree of blood pressure increase in our study is comparable to that observed in previous studies using different mice models (Jung et al., 2005; Ong et al., 2012). Bilsen and colleagues found a 30-40 mmHg rise in blood pressure in a combined model of diabetes and hypertension in which db/db mice where infused with a low dose of ANG II (1 mg/kg/day) to induce a relatively mild hypertension for 4 weeks (Bilsen et al., 2014). Collectively, ANG II infusion increased blood pressure to the same extent in both WT and HO mice.

3.5.2 Cardiac structure and function in 6-month-old GENA348 mice before ANG II treatment, at the basal level.

In our study and prior to ANG II infusion, GENA348 HO mice at 6-month-old developed a cardiac hypertrophy characterised by a significant increase in the dPW, cross sectional area, BNP expression and a significant diastolic dysfunction (Gibbons, 2011). This is in contrast to the study, which was undertaken by Bilsen and colleagues (2014), using diabetic (db/db) mice where they showed that type 2 diabetes per se is not associated with adverse cardiac structural and functional changes before ANG II treatment. However, combined with hypertension, diabetes seems to promote hypertrophic remodelling (Bilsen et al., 2014). In line with the study by Bilsen, Daniels and colleagues found that there was no evidence of marked cardiac dysfunction and structural remodelling in Zucker Diabetic Fatty (ZDF) rats (Daniels et al., 2012). Collectively, while the 6 month-old GENA 348 mice developed a cardiac phenotype at baseline, other studies with different diabetic models reported normal cardiac structure and function at baseline.

3.5.3 Cardiac structure in 6-month-old GENA348 mice after ANG II treatment.

It was clear that ANG II treatment resulted in cardiac hypertrophy but there was no difference based on the genotype of mice, as indicated from the echocardiographic parameters. This is in line with the HW/BW ratio, relative wall thickness, cross sectional area and BNP expression. In contrast to our data, Bilsen and colleagues found that there was a significant change in the cardiac structure of the db/db mice after ANG II infusion compared to WT controls. The left ventricular/tibia length (LV/TL) ratio has significantly increased in ANG II treated mice, and LV/TL is significantly greater in ANG II treated diabetic mice

compared to controls. In their study, echocardiographic analysis revealed that diastolic wall thickness was significantly augmented in ANG II treated diabetic mice after the induction of ANG II treatment. Additionally, at the level of the cardiomyocyte, ANG II mediated the increase in the cardiomyocyte cross sectional area and it was more noticeable in mice with diabetes than non-diabetic mice (Bilsen et al., 2014).

3.5.4 Cardiac function of 6-month-old GENA348 mice after ANG II treatment.

The hypertension induced by ANG II infusion did not significantly alter diastolic function in the WT and HO mice. However, there was a significant increase in both ejection fraction and fractional shortening in the ANG II-HO mice compared to HO controls which indicates that ANG II improves the systolic function in HO mice. In contrast to our results, Bilsen and colleagues reported that the cardiac function of ANG II treated db/db mice was largely preserved. However, there were signs of mild systolic dysfunction illustrated by lower FS% and a reduced response of the +dp/dt max (Bilsen et al., 2014).

In our study, we observed a similar degree of fibrosis in both WT and HO GENA348 mice after ANG II treatment. In addition, mRNA expression of collagens I and II confirmed the fibrosis results. This is consistent with the cardiac function data from GENA348 mice after the ANG II infusion. However, in contrast to our data, Black et al., used spontaneously hypertensive rats and streptozotocin (STZ) to induce type 1 diabetes, they found a marked increase in the level of interstitial fibrosis in the heart of the diabetic hypertensive rats after 6 months duration of diabetes (Black et al., 2010).

These evident differences in the results could be due to the differences in the animal models and the dose of ANG II and the duration of treatment. Bilsen et al., used db/db mice and the dose of ANG II was 1mg/kg/day for a period of 4 weeks. Two weeks of ANG II treatment might not be long enough to alter the cardiac function of the GENA348 HO mice. An alternative model of hypertension will be of great interest. Non-pharmacological models would be a future consideration such as the DOCA-Salt model and the two-kidney one-clip renovascular hypertension model.

3.5.5 Expression of angiotensin II, type 1 receptor in the HO GENA348 mice following ANG II treatment

Although 6 months GENA348 mice developed cardiac hypertrophy, when they were treated with ANG II both HO and WT had the same level of hypertrophy. This indicates that the HO mice have had a blunted response to the stimulus. This experiment investigates why this happens.

In cardiovascular diseases, the cellular and molecular actions of ANG II are entirely mediated by angiotensin type 1 receptors (AT1Rs) (Chen & Coffman, 2015). Western blot was used to examine the expression level of the angiotensin type 1 receptor 1a (AT1R) in the heart of 6 month-old GENA348 HO and WT mice. There was a significant 0.5 fold decrease in the expression of AT1R1a in HO mice, after ANG II treatment, compared to the ANG II treated WT controls. The data suggest that ANG II signalling might be blocked or interrupted at the receptor level. In the literature, it was found that chronic exposure to ANG II may downregulate its own receptors (Lassegue et al., 1995; Touyz et al., 1999), which may underlie why ANG II does not augment the cardiac phenotype in GENA348 mice. This alteration was only observed in HO mice not WT and the potential mechanism behind that is the hyperglycemia in

HO mice induced more ANG II production as it was reported in the literature (Lavrentyev et al., 2007). Through using streptozotocin (STZ)-induced diabetic cardiomyopathy rats, Yan et al. found that the level of ANG II in the blood and the myocardium was significantly higher in the diabetic cardiomyopathy group than in controls (Yan et al., 2016). Circulating ANG II levels need to be measured in GENA348 mice to check whether there is a difference in the level of ANG II between HO and WT mice.

3.6 Limitations of the study

ANG II has several functions and influences in affecting cardiovascular physiology directly or indirectly. In addition, acute or chronic stimulation of ANG II and short-term or long-term exposure to ANG II give different responses in cardiac hypertrophy, remodelling and fibrosis. It is quite difficult to discern whether these changes in cardiac hypertrophy and fibrosis reflect an augmented sensitivity to hypertension or ANG II itself.

In absolute terms, long-term exposure of the cardiac muscle to hypertensive conditions in different diabetic mice is still short when compared to the duration of hypertension in hypertensive patients (weeks vs. months and years). As a consequence, we did not observe a change in the cardiac phenotype with the ANG II model of hypertension. Prolonging the experimental period would be a future consideration.

Circulating angiotensin II levels need to be assessed either by ANG II enzyme immunoassay kit or radioimmunoassay in order to confirm difference in the level of ANG II between HO and WT GENA348 mice.

It is very important to take into consideration the limitations of using animal models. Many of the diabetic animal models described in literature share comparable characteristic features of diabetes and have allowed investigation that would be impossible in humans. None of the known single models are exactly equivalent to human diabetes. However, each model acts as an important tool for investigating genetic, metabolic and pathophysiological mechanisms that could also operate during the development of diabetes in humans. Therefore, caution must be taken during the interpretation of the results obtained from these diabetic models. In addition, there are no studies in the literature regarding cardiac function changes in MODY2 in humans.

3.7 Conclusion

Hypertension and diabetes have long been recognised as one of the most important risk factors for cardiovascular disease. The combination of these disorders can lead to evident alterations in the cardiac structure and function, which participates in increase the risk of heart failure. The underlying mechanisms of interaction between diabetes and hypertension to promote heart failure development are not fully understood.

The aim of this study was to induce hypertension in GENA348 mice and determine whether the increased stress on the heart would lead to an accelerated cardiac phenotype in HO GENA348 mice.

To study this, hypertension was induced by infusion of 2mg/kg/day of ANG II using a minipump for two weeks. It was found that ANG II treatment led to a significant increase in both systolic and diastolic blood pressure to the same extent in both WT and HO mice. Furthermore, cardiac structure and function was assessed in GENA348 mice following ANG II treatment, It was clear that

ANG II treatment resulted in cardiac hypertrophy but there was no difference in the level of hypertrophy between the mice. The diastolic function was generally maintained in the WT and HO mice following the ANG II treatment and the systolic function was slightly improved after ANG II infusion. Our data indicates that the HO mice have had an attenuated hypertrophic response to the hypertension induced by ANG II. This perhaps is in part due to a reduction in the ANG II receptor type 1 as a consequence of chronic ANG II infusion although other mechanisms cannot be excluded.

In addition, an alternative model of hypertension will be of great interest to study the effect of hypertension and diabetes on the heart. Non-pharmacological model would be a future consideration.

Chapter 4 Metabolomics

4.1 Introduction

4.1.1 Introduction to metabolomics.

Metabolomics is defined as the comprehensive characterisation of the small endogenous molecule metabolites in a biological system. It provides an overview of the global metabolic status and biochemical events associated with the biological system (Dunn et al., 2011a). Metabolomics plays a fundamental role in the study of sophisticated mammalian systems. It is also has a role in obtaining greater pathophysiological understanding of the onset and progression of diseases such as cardiovascular diseases and diabetes mellitus and associated complications (Dunn et al., 2011c).

Two experimental approaches are currently applied in metabolomics. Firstly: targeted studies of a small number of metabolites, which rely on quantitative measurements. These kinds of studies involve the application of biochemical and analytical platforms for the quantification of known metabolites of biological interest (Suhre et al., 2010). Secondly: untargeted metabolic profiling which performs a holistic study of large numbers of metabolites. No prior knowledge is required in these types of studies and can therefore be applied to detect novel metabolic biomarkers of disease and drug effectiveness in addition to analysing the global metabolic profile of the entire system as well (Dunn et al., 2011a). The second experimental approach was applied to our study in this chapter.

Metabolomics is routinely used as a hypothesis-generation technique or a discovery technique where biological experiments are planned to obtain robust data from which biological hypotheses can be produced. Validation of these discoveries can be carried out to test the hypotheses (Kell & Oliver, 2004).

Since no specific analytical method can accommodate the chemical variety and sensitivity of the whole metabolome, consequently, a multiplatform methodology might offer a more comprehensive understanding of metabolic changes. Mass spectrometry (MS) is one of the most common, sensitive and efficient used methods in metabolomics studies, and frequently combined with other appropriate methods for the analytical separation of compounds such as chromatography (gas or liquid) (Dunn et al., 2011a). The mass spectrometer works on the principle that it ionises and fragments the components as they come from different types of chromatography. It then separates them according to their specific mass-to-charge ratio (m/z), and then records the relative abundance of each ion type (Finehout & Lee, 2004).

Since the 12-month-old HO GENA348 mice developed significant cardiac hypertrophy with diastolic and systolic dysfunction and dilatation, it was interesting to evaluate whether there are changes observed in cardiac metabolites in association with the development of the cardiomyopathy observed in 12-month-old GENA348 mice.

4.2 Hypothesis

Hyperglycaemia as a result of genetic mutation in the glucokinase gene results in altered cardiac metabolism, which could contribute to the development of diabetic cardiomyopathy.

4.3 Aim

- To investigate whether metabolic profiling of serum and heart tissue can provide valid and useful information on metabolic changes during the development of cardiomyopathy in the 12-month-old GENA348 mice.
- To gain insight into the pathophysiological mechanism that could participate in the pathogenesis of diabetic cardiomyopathy.

4.4 Methods

4.4.1 Hypothesis generating techniques

Broadly speaking, there are two categories of research methodologies; hypothesis testing and hypothesis generating. The most common and more traditional is the hypothesis testing as it allows experiments to be designed on the grounds of previous knowledge. On the other hand, hypothesis generating methods do not depend on any particular prior knowledge and these methods provide new insights into prospective pathways which otherwise might be overlooked (Chang & Talamini, 2011). Metabolomics and microarray technology studies have developed as an important hypothesis generating methods and allow simultaneous analysis of an enormous number of gene targets and metabolites. To examine these methodologies, firstly: Gas chromatography-mass spectrometry (GC-MS) and Ultra performance liquid chromatography-mass spectrometry (UPLC-MS) were used on 12-month-old GENA348 mice heart and serum samples. Secondly: diabetes PCR array plates were used on 6- and 12-month-old GENA348 mice heart samples (data presented in chapter 5).

4.4.2 Sample preparation

Two types of samples were used; serum was chosen as a suitable biological fluid as it may offer a metabolic footprint of biological function and it was used previously in literature to examine the metabolites profiles (Ugarte et al., 2012; Dunn et al., 2014). Heart tissue was chosen as well since the 12-month-old HO GENA348 mice developed cardiac phenotype, characterised by a significant cardiac hypertrophy, diastolic dysfunction, systolic dysfunction and dilatation of the left ventricle.

4.4.2.1 Serum

Venous blood was collected from the jugular vein by venipuncture under general anesthesia and allowed to clot for up to two hours at room temperature and then left at 4°C overnight. The clotted material was removed the next day by centrifugation for 15 min at 825 xg and the supernatant serum was then transferred to a new microfuge tube and stored at - 80°C until required.

All samples were prepared according to a standard operating procedure (SOP) as described (Dunn et al., 2011b). Briefly, 200 µl of serum was used and mixed with 100 µl of internal standard solution (0.167 mg ml^{-1} malonic acid d_2, succinic acid d_4, glycine d_5, citric acid d_4, D-fructose $^{13}C_6$, L-tryptophan d_5, L-alanine d_7, stearic acid d_{35}, benzoic acid d_5 and octanoic acid d_{15}) followed by the addition of 600 µl of methanol. The mixture was vortexed and centrifuged for 15 min at 15493 xg. The supernatant was separated into four 370µl aliquots. A centrifugal vacuum evaporator (Savant SPDD331DDA; Thermo Scientific) was used to dry the samples overnight. Quality control (QC) samples were prepared by pooling aliquots of all the serum samples collected, and extracting 200 µl fractions of the pool as described above. Dried samples were stored at 4°C until required.

4.4.2.2. Tissues

Hearts were excised and washed in cold phosphate buffered saline (PBS-Invitrogen) to remove blood clots and were immediately snap frozen in liquid nitrogen and stored at -80°C until required. Tissue collection was done by Stephen Gibbons and Sukhpal Prehar.

The heart weight was determined by being placed in a cooled and pre-weighted Eppendorf tube. 50mg of frozen heart was allowed to thaw on ice, extracted in a two step procedure, and homogenised for ten minutes by using a Tissuelyser II at 25 Hz after adding 400µl of methanol (MeOH). 400µl of previously cooled

chloroform (CHCl3) was added to the mixture. 50µl of an internal standard (IS3) and a single 3mm tungsten carbide bead were added to each tissue sample. After extraction, 400µl of H_2O was added to each tube, followed by brief vortex mixing. Tubes were then kept at room temperature for 10 minutes prior to centrifugation for 5 minutes at 2292 xg. After that, 400µl of the (top) polar layer (water/methanol) and 270µl of the (bottom) non-polar layer (chloroform) were transferred to separate 2 ml microcentrifuge tubes containing 50µl of appropriate internal standards (IS1 for polar fraction, IS2 for non-polar) and were lyophilised (HETO VR MAXI vacuum centrifuge attached to a HETO CT/DW 60E cooling trap; Thermo Life Sciences). Pooled quality control (QC) samples were prepared by combining 100 µl aliquots of each extraction solution as described above. Aliquots were finally transferred to Eppendorf tubes and lyophilised.

4.4.3. GC-MS analysis

The Gas Chromatography (GC) works on the principle that a sample mixture will separate into individual components by their volatility. Volatile components pass through the capillary column and arrive in the mass spectrometer. The mass spectrometer ionises and fragments the components. The fragments produced by any given metabolite reflect the strength of the bonds between its atoms, therefore a typical mass spectrum is recorded which provides information about the chemical structure of the metabolite (Guo & Lankmayr, 2012).

Two-stage chemical derivatisation procedure was performed in order to increase metabolic volatility and thermal stability (Halket et al., 2005 and Koek et al., 2006). 60 µl of O-methyl-hydroxylamine solution (20 $mg.ml^{-1}$ in pyridine) was added to the lyophilised samples and heated at 80°C for 20 minutes

followed by addition of 60 µl MSTFA (N-acetyl-N-(trimethylsilyl)-trifluoroacetamide) and heating at 80 °C for further 20 minutes. To allow normalisation of retention times, 20 µl of a retention index (RI) solution (3 $mg.ml^{-1}$ C_{10}, C_{12}, C_{15}, C_{19}, C_{22}, C_{26}, C_{28}, C_{30} and C_{32} *n*-alkanes) was added and followed by centrifugation for 15 minutes at 15493 xg. After that, the supernatant was transferred to 300 µl glass inserts placed in 2 ml chromatography vials. Samples were analysed in random order using an Agilent 6890 N gas chromatograph (Agilent Technologies, Stockport, UK) and a MPS2L autosampler (Gerstel, Baltimore, MD) coupled to a LECO Pegasus III electron impact mass spectrometer (LECO UK, Stockport, UK). The GC and MS operating parameters were as previously described (Begley et al., 2009). Five QC samples were injected at the start of each analytical batch, followed by a QC sample every fifth injection and two QC samples at the end of the analytical batch.

4.4.4. UPLC-MS analysis

The Ultra Performance Liquid Chromatography (UPLC) is a special version of HPLC (High Performance Liquid Chromatography) which is a type of chromatography which relies on pumps to pass a high pressure liquid solvent containing the sample mixture across a column filled with solid adsorbent particles leading to the separation of the sample components (Tautenhahn et al., 2008). The main difference between UPLC and HPLC is the pump pressure which is 40MPa in the HPLC. However, in the UPLC the pressure can reach up to 100MPa, which allows for better separation of smaller particle size which is less than 2µm while it is normally 5µm in HPLC (Novakova et al., 2006).

Lyophilised tissue extracts and QC samples derived from the non-polar chloroform extract were reconstituted in 100 µl 50:50 methanol:water, vortex for

15 second and centrifuged for 15 minutes at 15493 xg. The supernatant was transferred to a 2 ml low-volume chromatography vial, sealed and stored in an autosampler at 4°C. Samples were randomly analysed using an Acquity UPLC system (Waters, Corporation, Elstree, UK) coupled to an electrospray LTQ-Orbitrap XL hybrid mass spectrometer (ThermoFisher, Bremen, Germany). Chromatographic separation was done using a Hypersil GOLD column (100 x 2.1 mm, 1.9 µm; ThermoFisher Scientific, Runcorn, UK) operating at a column temperature of 50°C. Two solvents were applied; solvent A containing 0.1% formic acid in water and solvent B comprising 0.1% formic acid in MeOH at a flow rate of 0.40 ml min^{-1}. Five QC samples were injected at the start of each analytical batch, followed by a QC sample every fifth injection and two QC samples at the end of the analytical batch.

4.4.5. Data pre-processing and data analysis

- GC-MS: Raw data files (.peg format) obtained from the GC-MS platform were processed using the ChromaTof software (Leco Corp. v3.25) as previously described to construct a data matrix (metabolite peak vs. sample no.) (Dunn et al., 2011a). GC-MS data pre-processing and data analysis was performed by Dr Paul Begley.

- UPLC-MS: Raw data files (.raw format) obtained from the UPLC-MS platform were converted to the NetCDF format employing the File convertor program in the XCalibur software (ThermoFisher Scientific, Bremen, Germany). An open-source deconvolution program (XCMS), running on R version 2.6.0, was used to deconvolute the UPLC-MS data (Dunn et al., 2011a). UPLC-MS data-pre-processing and data analysis was performed by Dr Katherine Hollywood.

Quality assurance (QA) was later used in both GC-MS and UPLC-MS analysis and only metabolic features that were identified as greater than 60% of all QC

samples and with a relative standard deviation (SD) for measured peak areas of below than 20% were kept for data analysis. All other metabolic features that did not pass the QA criteria were eliminated from the dataset and overlooked in following data analysis.

For all tests in this discovery phase experiment, features were considered significant when the P-value is <0.05. A non-conservative P-value was used since the experiment purpose was to carry out discovery studies to elucidate changes related to molecular pathophysiological changes. Additional screening was carried out by the grouping of metabolites to their similar metabolite pathway, similar metabolic class or comparable chemical structure. Here we only discussed groups of metabolites, instead of single metabolites, from a biological point of view.

4.4.6. Metabolite identification

- The GC-MS platform: Metabolite features detected on this platform were identified using freely available mass spectral libraries, which includes Golm metabolome database (Kopka et al., 2005) or present in the Manchester Metabolomics Database (MMD) in-house library (Brown et al., 2009). The identification becomes definitive when the mass spectrum is combined with the retention time or retention index measured from authentic chemical standard. The identification becomes putative only when a match to a mass spectrum was observed, but where the retention indexes data for authentic standard was not available (Dunn et al., 2011a).

- The UPLC-MS platform: Metabolite features detected on this platform were performed by applying the PUTMEDID–LCMS set of workflows operating in Taverna. For putative identification of metabolic features, the accurate mass for each peak was allocated a single or multiple molecular formula matching in

mass to the experimentally determined mass with a mass error of < ± 5 ppm. The molecular formula can subsequently be searched for in different databases including: the Human Metabolome Database (HMDB), Kyoto Encyclopedia of Genes and Genomes (KEGG) and ChemSider (Dunn et al., 2011a).

4.4.7 Principal components analysis (PCA)

It is a widely used statistical procedure that uses a linear transformation to convert a set of observations into a set of new variables called principal components (PCs) which simplifies the visualisation of complex data for exploratory analysis (Ivosev et al., 2008). The contribution that every variable makes to a PC is entitled the loading, and the amount of the PC present in a specific sample is recognised as the score. The final results of PCA are visualised as projections of multidimensional scores and loadings in 2 or 3 dimensional plots. Understanding the sample information (scores) can be very difficult if an unanticipated cluster is identified, but is easier if there are few samples and where any expected separation is detected (Abdi & Williams, 2010).

4.5 Results

4.5.1 Metabolic phenotyping of heart tissue samples acquired from 12-month-old GENA348 mice WT and HO mice.

This study was aimed to investigate whether there are changes observed in cardiac metabolites in association with the development of the cardiomyopathy observed in 12-month-old GENA348 mice. Heart tissue (WT n=13 and HO n=13) samples were collected, applying the same standard operating procedure (SOP). GC-MS and UPLC-MS in positive and negative ion modes were applied as previously described. After quality assurance procedures, 50 metabolic peaks exhibited a significant difference between WT and HO GENA348 mice were detected by GC-MS. In addition, 70 metabolic features of statistical significance between WT and HO GENA348 mice were identified by UPLC-MS. These metabolic features were taken forward for additional data analysis.

Principal components analysis (PCA) was carried out using all detected metabolic features to evaluate the variability in the data and find if any outliers existed.

Figure 4.1 displays the PCA score plots (PC1 versus PC2) for heart tissue samples. One potential outlier was identified in heart tissue samples and was removed prior to univariate data analysis. A clear separation was observed in heart tissue samples from data acquired from GC-MS platform indicate a large difference in the heart tissue metabolome related to the differences between WT and HO GENA348 mice.

Figure 4.2 displays the PCA score plots (PC1 versus PC2) for data acquired from (A) UPLC-MS (+) and (B) UPLC-MS (-) platforms from heart tissue samples. No clear separation was observed for heart tissue samples and this is due to differences between individual samples rather than HO vs. WT.

Table 4.1 describes the 27 metabolic features that were statistically significant (P< 0.05) when comparing WT control versus HO diabetic 12-month-old GENA348 mice from data acquired from GC-MS platform from heart tissue samples. Specific metabolic classes were over-represented in the results comprise of sugars (6 metabolites), lipids (1 metabolite), fatty acids and related metabolites (4 metabolites), amino acids and related metabolites (8 metabolites) and other metabolites (8 metabolites).

Table 4.2 shows the 16 metabolic features that were statistically significant (P< 0.05) when comparing WT control versus HO diabetic 12-month-old GENA348 mice from data acquired from UPLC-MS platform from heart tissue samples. Specific metabolic classes were over-represented in the results comprise of amino acids and related metabolites (4 metabolites), fatty acids and related metabolites (4 metabolites), lysophospholipids (4 metabolites) and monoacylglycerophosphoinositols (4 metabolites).

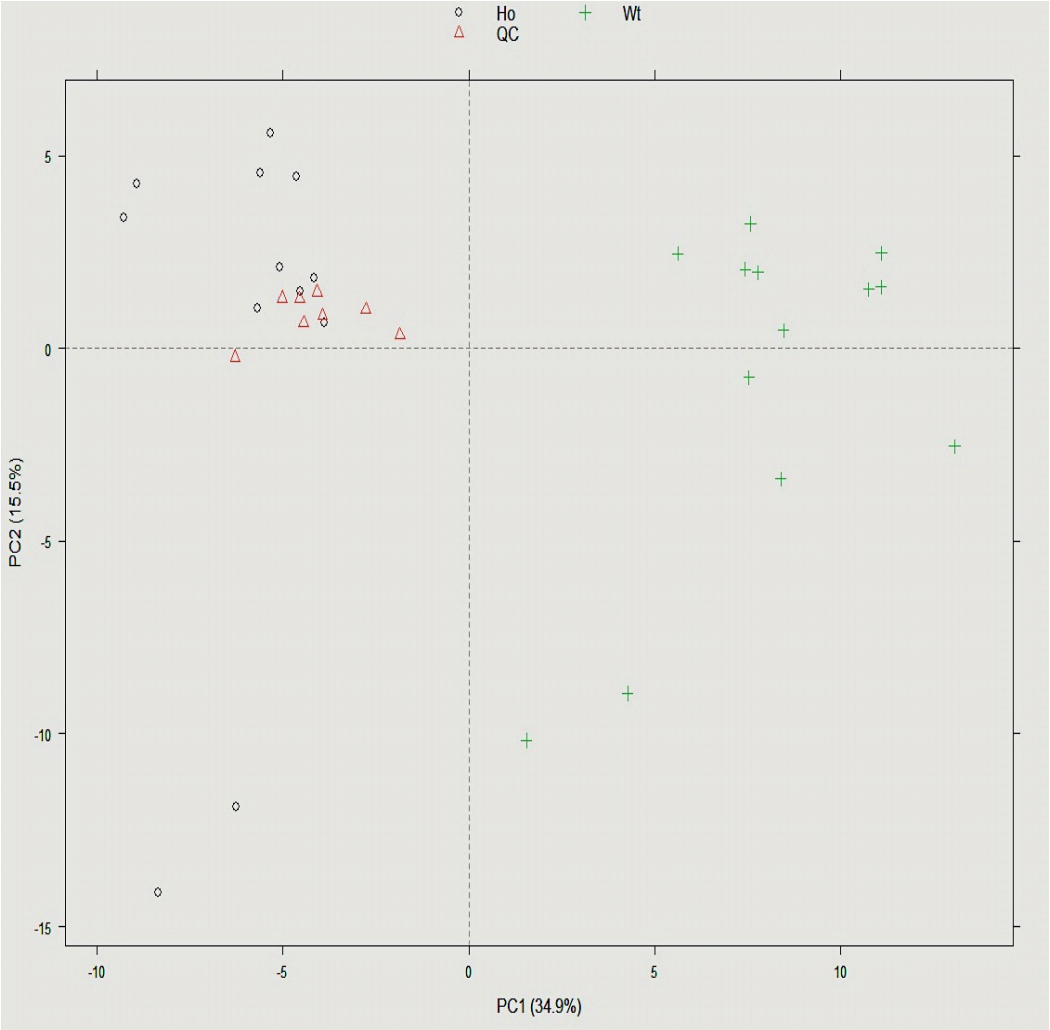

Figure 4.1 Principle components analysis (PCA) score plots

Data acquired on GC-MS platform from heart tissue samples from 12 month old GENA348 mice. One potential outlier was excluded prior to univariate data analysis. A clear separation was observed from heart tissue samples from data acquired from GC-MS platform. Black circle (HO samples), green cross (WT samples) and red triangle (QC samples).

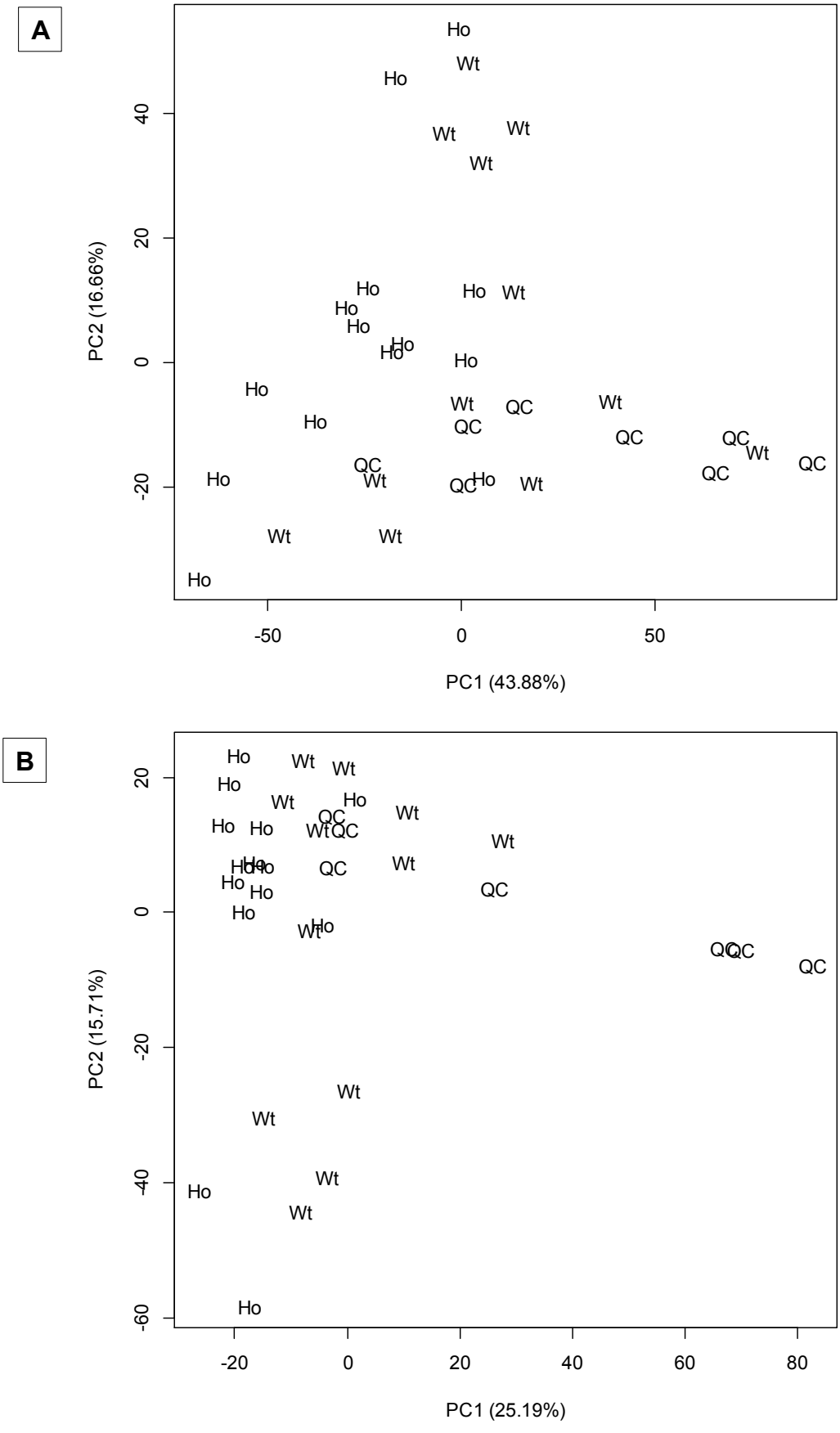

Figure 4.2 Principle components analysis (PCA) score plots (A, B)

Data acquired in positive (A) and negative (B) platforms for non-polar chloroform extracts of heart tissue samples from GENA348 mice. No clear separation was observed for tissue samples and subject ID, not class, dominates the separation

N	Metabolite - (Tissue-GC-MS)	P-value	Fold change
	Sugars		
1	Glucose	0.001	5.882
2	Glycerol-3-phosphate	0.002	2.564
3	Fructose-6-phosphate	0.003	2.941
4	Threonic acid	0.002	2.564
5	Glucose-6-phosphate	0.004	3.571
6	Glyceric acid-3-phosphate	0.000	4.545
	Lipids		
1	Glycerol	0.024	2.174
	Fatty Acids		
1	Linoleic acid	0.021	1.852
2	Propanoic acid 2-methyl-3	0.006	1.515
3	Hexadecanoic acid	0.020	1.176
4	Myristic acid	0.009	1.149
	Amino Acids		
1	Alanine	0.001	2.326
2	Tyrosine	0.001	3.125
3	Lysine	0.052	1.348
4	Serine	0.000	2.564
	Amino Acids Derivatives		
1	Creatinine	0.024	1.667
2	Pyroglutamic acid	0.000	2.041
3	L_Methionine	0.002	2.941
4	Citrulline	0.005	1.125
	Others		
1	myo-inositol	0.001	2.381
2	Scyllo-inositol	0.001	2.326
3	Nicotinamide	0.032	3.125
4	Pantothenic acid	0.001	2.778
5	Maleic acid	0.000	1.961
6	Phosphate	0.049	1.282
7	Lactic acid	0.028	2.564
8	Urea	0.032	2.500

Table 4.1 Metabolites shown as statistically significant (P < 0.05) when comparing WT and HO 12-month-old GENA348 mice from data acquired on GC-MS platform from heart tissue samples.

N	Metabolite - (Tissue-UPLC-MS)	P-value	Fold change
	Amino Acids and related metabolites		
1	N-Ribosylhistidine	0.001	1.580
2	L-[(N-Hydroxyamino)Carbonyl]Phenylalanine	0.001	1.569
3	5-Carboxy-2-oxohept-3-enedioate AND/OR Argininic acid	0.003	1.271
4	N(omega)-(L-Arginino)succinate	0.003	1.493
	Fatty acids and related metabolites		
1	3beta,21-Dihydroxy-pregna-5,7,9(11)-trien-20-one diacetate AND/OR 9,10-Dihydroxy-12,13-epoxyoctadecanoate	0.001	1.464
2	methyl 9-butylperoxy-10,12-octadecadienoate AND/OR methyl 13-butylperoxy-9,11-octadecadienoate	0.002	0.537
3	5-hydroperoxy-7-[3,5-epidioxy-2-(2-octenyl)-cyclopentyl]-6-heptenoic acid	0.003	1.442
4	2-Tridecanoyloxy-Pentadecanoic Acid AND/OR (+)-C27-Phthienoic acid AND/OR 2,4-dimethyl-2-pentacosenoic acid	0.005	1.507
	Lysophospholipids		
1	LysoPE(18:2)	0.000	1.419
2	LysoPC(22:2)	0.001	1.320
3	LysoPE(22:6)	0.001	1.235
4	LysoPE(20:3)	0.002	1.233
	Monoacylglycerophosphoinositols		
1	PI(20:1)	0.001	1.322
2	PE(20:4) AND/OR PE(18:1)	0.001	1.190
3	PI(14:1)	0.003	1.235
4	PI(20:2) AND/OR DG(28:2)	0.003	1.151

Table 4.2 Metabolites shown as statistically significant (P < 0.05) when comparing WT and HO 12-month-old GENA348 mice from data acquired on UPLC-MS platform from heart tissue samples.

4.5.2 Metabolic phenotyping of serum samples acquired from 12- month-old GENA348 WT and HO mice.

The present study was designed to investigate whether there are changes observed in serum metabolites in 12-month-old GENA348 HO mice compared to WT controls.

Serum (WT n=14 and HO n=13) samples were collected, applying the same standard operating procedure (SOP). GC-MS and UPLC-MS in positive and negative ion modes were applied as complementary analytical platforms to profile a range of metabolites existent in the serum of GENA348 mice. Following quality assurance procedures, 20 metabolic peaks showed a significant difference between WT and HO GENA348 mice were detected by GC-MS. In addition, 500 metabolic features of statistical significance between WT and HO GENA348 mice were detected by UPLC-MS. These metabolic features were taken forward for additional data analysis.

Principal components analysis (PCA) was carried out as previously described (in section 4.5.1). Figure 4.3.A displays the PCA score plots (PC1 versus PC2) for data acquired from GC-MS platform from serum samples. Two potential outliers were identified in serum samples and were removed prior to univariate data analysis. The quality control (QC) samples were firmly clustered in comparison to the other samples, exhibiting that the reproducibly of data obtained in a single GC-MS experiment is high. No clear separation was observed for serum samples and the separation was due to differences between individual samples rather than HO vs. WT (Figure 4.3.B).

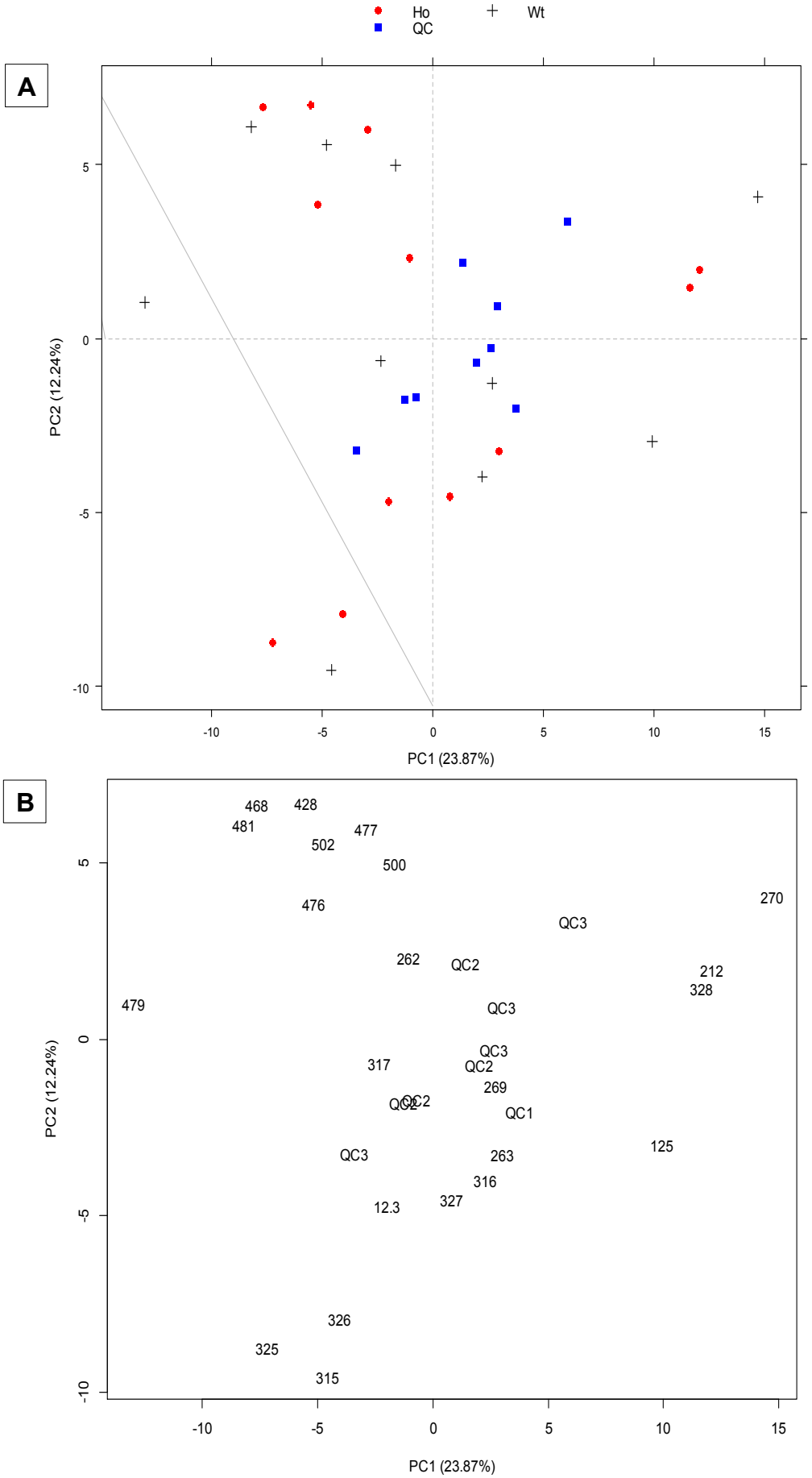

Figure 4.3 Principle components analysis (PCA) score plots

A-Data acquired on GC-MS platform for serum samples from 12 month old GENA348mice. Two potential outliers were excluded prior to univariate data analysis. In addition, four low volume samples were excluded as well. No clear separation was detected for serum samples and subject ID, not class, dominates the separation. Red circle (HO samples), black cross (WT samples) and blue square (QC samples). B- this plot shows the subject ID of the samples for plot A.

Figure 4.4 shows the PCA score plots (PC1 versus PC2) for data acquired from (A) UPLC-MS (+) and (B) UPLC-MS (-) platforms from serum samples. One potential outlier was identified in serum samples and was removed prior to univariate data analysis. No clear separation was observed for serum samples and subject ID, not class, dominates the separation.

Table 4.3 describes the 5 metabolic features that were statistically significant ($P < 0.05$) when comparing WT control versus HO diabetic 12-month-old GENA348 mice from data acquired from GC-MS platform from serum samples. Only creatinine and less common sugars are statistically significant.

Table 4.4 reveals the 88 metabolic features that were statistically significant ($P < 0.05$) when comparing WT control versus HO diabetic 12-month-old GENA348 mice from data acquired from UPLC-MS platform from serum samples. Specific metabolic classes, which were over-represented in the results, include fatty acids and related metabolites (20 metabolites), amino acids and related metabolites (10 metabolites), phospholipids (34 metabolites), sphingolipids (12 metabolites), triglycerides (8 metabolites) and acyl glycerides (4 metabolites).

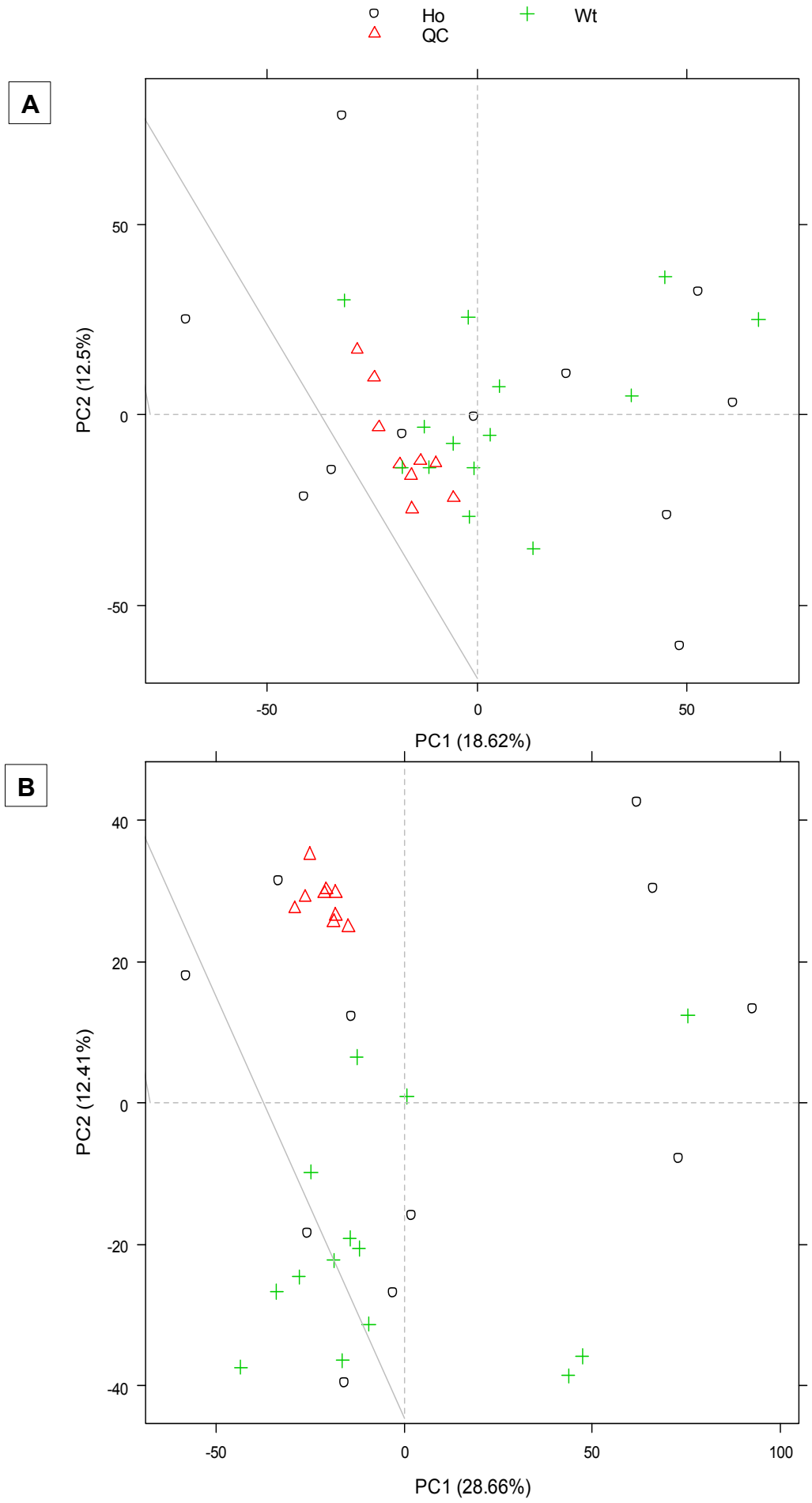

Figure 4.4 Principle components analysis (PCA) score plots (A, B)

Data acquired in positive (A) and negative (B) platforms for non-polar chloroform extracts of serum samples from GENA348 mice. No clear separation was observed for serum samples and subject ID, not class, dominates the separation. Black circle (HO samples), green cross (WT samples) and red triangle (QC samples).

N	Metabolite -(serum-GC-MS)	P-value	Fold change
	Sugars		
1	Arabinose	0.002	1.756
2	Fucose	0.010	2.174
3	Sorbose	0.046	0.307
	Amino Acids		
1	Cysteine	0.053	0.595
	Other metabolites		
1	Creatinine	0.039	0.501

Table 4.3 Metabolites shown as statistically significant (P < 0.05) when comparing WT and HO 12-month-old GENA348 mice from data acquired on GC-MS platform for serum samples.

N	Metabolite -(serum-ULPC-MS)	P-value	Fold change
	Fatty acids and related metabolites		
1	10,16-Dihydroxyhexadecanoic acid AND/OR Ustilic acid A AND/OR 9,16-dihydroxy-palmitic acid AND/OR Heptadecatrienoic acid AND/OR Pentadecanoic acid AND/OR (+)-12-methyl myristic acid	0.025	2.190
2	Methyl 8-[3,5-epidioxy-2-(3-hydroperoxy-1-pentenyl)-cyclopentyl]-octanoate	0.018	2.073
3	2-Methoxy-5Z-hexadecenoic acid AND/OR 9-Keto heptadecylic acid AND/OR 16-oxo-heptadecanoic acid	0.034	2.055
4	Oxo-nonadecanoic acid	0.047	1.920
5	Hydroxydecanoic acid AND/OR hydroxy capric acid	0.025	1.760
6	Nonadecanoic acid AND/OR Tuberculostearic acid AND/OR 16-methyl-octadecanoic acid AND/OR 4,14-dimethyl-heptadecanoic acid	0.039	1.759
7	12,13-dihydroxy-11-methoxy-9-octadecenoic acid AND/OR 2-Oxooctadecanoic acid AND/OR 9-hydroxy-10Z-octadecenoic acid AND/OR 16-methyl-10-oxo-heptadecanoic acid	0.013	1.758
8	Methyl 8-[2-(2-formyl-vinyl)-3-hydroxy-5-oxo-cyclopentyl]-octanoate	0.028	1.688
9	Pentadecanal AND/OR 4-hydroxy palmitic acid AND/OR 15-hydroxy-hexadecanoic acid	0.045	1.684
10	Hexacosanedioic acid AND/OR 16Z-pentacosenoic acid	0.046	1.664
11	11-bromo-dodecanoic acid	0.007	1.654
12	Hexadecanedioic acid AND/OR 9-hydroxy-16-oxo-hexadecanoic acid AND/OR 5,8-heptadecadiynoic acid AND/OR 2,5-dimethyl-2E-tridecenoic acid AND/OR 2-pentadecenoic acid	0.007	1.567
13	Dodecatetraenoic acid AND/OR 5,11-dodecadiynoic acid	0.034	1.558
14	(6Z,9Z,12Z)-Octadecatrienoic acid AND/OR Punicic acid AND/OR 16-methyl-6Z,9Z,12Z-heptadecatrienoic acid	0.010	1.541
15	Arabinonic acid AND/OR Apionic acid AND/OR Ribonic acid	0.010	1.513
16	3-Oxo-hexadecanoic acid AND/OR Ambrettolic acid AND/OR 16-hydroxy-9E-hexadecenoic acid AND/OR 2-keto palmitic acid AND/OR 10-oxo-14-methyl-pentadecanoic acid	0.028	1.513
17	Hydroxynervonic acid AND/OR 24-hydroxy-10Z-tetracosenoic acid AND/OR 3-oxo-tetracosanoic acid	0.010	1.359
18	(9Z)-(7S,8S)-Dihydroxyoctadecenoic acid AND/OR Octadecanedioic acid AND/OR 7-methyl-6E-hexadecenoic acid AND/OR 10E-heptadecenoic acid	0.034	1.347
19	6,7-dihydroxy-4-oxo-2-heptenoic acid AND/OR (4E)-2-Oxohexenoic acid AND/OR 2-Hydroxy-cis-hex-2,4-dienoate AND/OR 6-hydroxy-2-hexynoic acid	0.027	1.340
20	15-methyl palmitic acid AND/OR 2,6-dimethyl-pentadecanoic acid AND/OR 2-methyl-hexadecanoic acid	0.007	1.332

Table 4.4 Metabolites shown as statistically significant (P < 0.05) when comparing WT and HO 12-month-old GENA348 mice from data acquired on UPLC-MS platform for serum samples.

N	Metabolite -(serum-ULPC-MS)	P-value	Fold change
	Amino Acids and related metabolites		
1	Deoxyhypusine	0.034	1.574
2	N-Acetyl-L-citrulline	0.025	1.417
3	3-Nitrotyrosine	0.018	1.325
4	L-Phenylalanine	0.010	1.295
5	Argininosuccinic acid	0.028	1.178
6	3,5-Diiodothyronine	0.025	0.826
7	Taurine	0.034	0.693
8	O-(4-Hydroxy-3,5-diidophenyl)-3,5-diiodo-L-tyrosine	0.020	0.659
9	L-alpha-aspartyl-L-hydroxyproline	0.011	0.465
10	Homocysteinesulfinic acid	0.019	0.289
	Phospholipids		
1	PS(O-16:0/14:1) AND/OR PS(P-16:0/14:0) AND/OR PS(P-18:0/12:0)	0.023	4.175
2	PS(25:0)	0.028	4.147
3	PS(42:6) AND/OR PG(42:8) AND/OR PS(38:0) AND/OR PC(37:4) AND/OR PE(40:4) AND/OR PC(35:1) AND/OR PE(38:1) AND/OR PC(35:1)	0.046	3.381
4	PS(O-16:0/17:2) AND/OR PS(P-16:0/17:1) AND/OR PS(P-18:0/15:1) AND/OR PA(O-16:0/21:0) AND/OR PA(O-18:0/19:0) AND/OR PA(O-20:0/17:0)	0.020	3.220
5	PC(O-16:0/3:0) AND/OR PC(O-17:0/2:0) AND/OR PC(O-18:0/1:0) AND/OR PC(3:0/O-16:0) AND/OR PC(19:0/0:0)	0.010	2.630
6	PC(39:1) AND/OR PE(42:1) AND/OR PE(33:1)	0.002	2.397
7	PC(15:0/16:0) AND/OR PC(16:0/15:0) AND/OR PE(14:0/20:0) AND/OR PE(16:0/18:0) AND/OR PE(18:0/16:0) AND/OR PE(20:0/14:0) AND/OR PC(10:0/21:0) AND/OR PC(11:0/20:0)	0.034	2.171
8	PS(38:0) AND/OR PG(40:5) AND/OR PC(35:1) AND/OR PE(38:1) AND/OR PC(35:1) AND/OR PC(37:4) AND/OR PE(40:4)	0.018	1.908
9	PC(32:3) AND/OR PE(35:3) AND/OR PC(30:0) AND/OR PE(33:0) AND/OR PE(33:0) AND/OR PA(37:4)	0.046	1.839
10	PC(40:3) AND/OR SM(d18:0/22:0) AND/OR SM(d18:2/24:1)	0.018	1.705
11	PE(42:4) AND/OR PC(37:1) AND/OR PE(40:1) AND/OR PA(44:5) AND/OR PC(O-16:0/O-18:0)	0.003	1.696
12	PE(42:2) AND/OR SM(d17:1/24:1) AND/OR SM(d18:2/23:0)	0.034	1.696
13	PS(P-20:0/22:4)	0.034	1.652
14	PE(18:3/dm18:1) AND/OR PE(18:4/dm18:0) AND/OR PE(20:4/dm16:0) AND/OR PE(16:0/dm18:1) AND/OR PE(16:1/dm18:0) AND/OR PE(18:1/dm16:0)	0.034	1.645
15	PC(20:1)	0.012	1.632
16	PS(39:7)	0.014	1.615
17	PC(32:0) AND/OR PE(35:0)	0.005	1.590
18	PC(35:4) AND/OR PE(38:4) AND/OR PC(33:1) AND/OR PE(36:1) AND/OR PA(40:5) AND/OR PC(O-14:0/O-16:0)	0.032	1.556
19	PS(36:1) AND/OR PG(36:3) AND/OR PC(33:2) AND/OR PE(36:2)	0.025	1.550
20	PE(16:0/dm18:1) AND/OR PE(16:1/dm18:0) AND/OR PnE(16:0/18:1)	0.004	1.546
21	PC(35:4) AND/OR PE(38:4) AND/OR PE(36:4) AND/OR PC(33:1) AND/OR PE(36:1) AND/OR PA(40:5) AND/OR PC(O-14:0/O-16:0)	0.045	1.545
22	PS(36:1) AND/OR PG(36:3) AND/OR PC(33:2) AND/OR PE(36:2)	0.045	1.545
23	PS(40:0) AND/OR PG(42:5) AND/OR PC(37:1) AND/OR PE(40:1) AND/OR PE(42:4)	0.007	1.542
24	PC(30:2) AND/OR PE(33:2) AND/OR AND/OR SM(d18:0/12:0) AND/OR SM(d18:2/14:0)	0.017	1.515

Table 4.4 Metabolites shown as statistically significant (P < 0.05) when comparing WT and HO 12-month-old GENA348 mice from data acquired on UPLC-MS platform for serum samples *(continued)*

N	Metabolite -(serum-ULPC-MS)	P-value	Fold change
	Phospholipids		
25	PE(42:4) AND/OR PC(37:1) AND/OR PE(40:1) AND/OR PA(44:5) AND/OR PC(O-16:0/O-18:0)	0.020	1.507
26	PA(O-16:0/18:4) AND/OR PA(P-16:0/18:3) AND/OR PA(P-16:0/18:3) AND/OR PA(O-16:0/16:1) AND/OR PA(O-18:0/14:1)	0.009	1.472
27	PA(P-16:0/12:0)	0.034	1.472
28	PE(36:5) AND/OR PE(34:2) AND/OR PA(38:6)	0.017	1.414
29	PC(33:2)AND/OR PE(36:2) AND/OR PA(38:3)	0.034	1.397
30	PC(O-16:0/19:0) AND/OR PE(O-18:0/20:0) AND/OR PE(O-16:0/22:0)	0.045	1.366
31	PC(31:0) AND/OR PE(34:0)	0.034	1.359
32	PC(37:6) AND/OR PE(40:6) AND/OR PC(38:3) AND/OR PE(38:3) AND/OR PC(35:3) AND/OR PA(42:7) AND/OR PC(33:0)	0.021	1.358
33	PI(38:4)	0.034	1.345
34	PA(O-16:0/16:1) AND/OR PA(O-18:0/14:1) AND/OR PA(P-16:0/16:0)	0.039	1.341
	Sphingolipids		
1	SM(d18:1/23:0)	0.003	2.650
2	SM(d16:1/22:1) AND/OR SM(d18:1/20:1) AND/OR SM(d18:2/20:0)	0.020	2.442
3	SM(d16:1/23:0) AND/OR SM(d17:1/22:0) AND/OR SM(d18:1/21:0) AND/OR SM(d19:1/20:0) AND/OR SM(d20:1/19:0)	0.050	2.321
4	Ceramide (d18:1/22:0)	0.008	2.260
5	N-Lignoceroylsphingosine AND/OR Ceramide (d18:1/24:0)	0.002	2.204
6	Tricosanamide	0.006	2.199
7	SM(d17:1/24:1) AND/OR SM(d18:2/23:0)	0.013	1.839
8	SM(d18:2/24:1) AND/OR SM(d18:0/22:0)	0.025	1.705
9	SM(d18:2/14:0) AND/OR SM(d18:0/12:0)	0.025	1.354
10	N-Stearoylsphingosine AND/OR Ceramide (d18:1/18:0)	0.014	1.931
11	Ceramide (d18:1/24:1)	0.001	1.796
12	Cer(d18:1/22:1)	0.004	1.453
	Triglycerides		
1	TG(51:6) AND/OR TG(49:3)	0.037	1.813
2	TG(42:0)	0.050	1.659
3	TG(34:2)	0.027	1.646
4	TG(52:4) AND/OR TG(50:1)	0.006	1.407
5	TG(52:3) AND/OR TG(50:0)	0.007	1.389
6	TG(52:2)	0.002	1.162
7	TG(54:3) AND/OR TG(52:0)	0.045	1.149
8	TG(36:2)	0.045	1.067
	Acyl glycerides		
1	DG(35:5)	0.016	1.939
2	DG(36:3) AND/OR DG(34:0)	0.016	1.925
3	DG(40:3)	0.022	1.531
4	MG(16:1)	0.034	1.433

Table 4.4 Metabolites shown as statistically significant (P < 0.05) when comparing WT and HO 12-month-old GENA348 mice from data acquired on UPLC-MS platform for serum samples *(continued)*

4.6 Discussion

Diabetes is a multifactorial metabolic disorder and the majority of patients with diabetes are at greater risk of cardiovascular diseases. In order to study the metabolic changes in an experimental model of diabetic cardiomyopathy, GENA348 mice, GC-MS and UPLC-MS based metabolic profiling was applied.

Investigation of serum and heart tissue from 12-month-old HO GENA348 mice with comparison to WT controls was performed. This age was chosen as the 12-month-old HO GENA348 mice developed cardiac hypertrophy with diastolic and systolic dysfunction at this age.

The identification of alterations in relative metabolite concentrations exposed alterations of particular metabolic pathways or areas of metabolism in response to diabetic cardiomyopathy. Our results showed that there were 43 differences in metabolites from heart tissue and 93 from serum from data acquired from both GC-MS and UPLC-MS platforms.

Using a combination of GC-MS and UPLC-MS provides a complementary platform, since each of them offers detection of different sets of metabolites. GC-MS method provides limited coverage as only non-polar volatile and low molecular weight compounds are detected by this method. Metabolites identified include amino acids and carbohydrates. It also provides a great confidence regarding the identities of the metabolites being detected. However, sample preparation for GC-MS is complex compared with UPLC-MS, as sample derivatisation is required.

On the other hand, UPLC-MS method provides greater coverage as higher molecular weight metabolites such as many classes of lipids can be detected by this method. However, more follow-up work is required to verify the

identifications observed as there are no spectral libraries for UPLC-MS identifications as seen for GC-MS.

4.6.1 Alterations in the serum and heart tissue metabolome in the 12 month old GENA348 mice.

In our study, it was found that the main altered classes of metabolites from heart tissue samples were sugars and fatty acids which were observed in GENA348 HO mice compared to WT controls. However, fatty acids, phospholipids and sphingolipids were the main altered metabolites classes from serum samples from data acquired from both GC-MS and UPLC-MS platforms.

4.6.1.1 Alterations in glycolysis metabolism in the heart.

In our data set, high sugar concentrations were observed in the GENA348 mice when compared with the WT controls. In addition, the glycolysis metabolism might be altered as there were increases in the concentration of the following metabolites; 5.9 fold increase in the glucose, 2.6 fold increase glycerol-3-phosphate, 2.9 fold increase in fructose-6-phospahte, 4.5 fold increase in glyceric acid-3-phosphate and 3.6 fold increase in glucose-6-phosphate.

It has been shown in Type 1 diabetic patients that their cardiac glucose uptake is considerably reduced as a result of the absence of insulin production (Avogaro et al., 1990; Doria et al., 1991). Insulin triggers glucose uptake by prompting the transcription of the GLUT4 glucose transporter in metabolically active tissues such as the heart, liver and skeletal muscle. Furthermore, the triggering of insulin signalling stimulates the translocation of GLUT4 comprising cytoplasmic vesicles to the plasma membrane, which is its site of action (Tremblay et al., 2003 ; Karnieli & Armoni, 2008).

There was also a significant decrease in the levels of GLUT4 in the cardiac

muscle in the STZ-induced type 1 diabetes in rats. This was as a result of the reduction in the rates of the cardiac glucose oxidation, which influence cardiomyocytes to rely heavily on fatty acids as a source of energy due to the lack of insulin production (Camps et al., 1992 ; Munoz et al., 1996). Notably, large amounts of fat are available to the heart in type 1 diabetes as a result of increased lipolysis in adipose tissue, which is usually repressed by insulin (Nishino et al., 2007).

While there was a reduction in the GLUT4 expression in the heart of type 2 diabetic patients, functional study of the heart of type 2 diabetic patients showed that the cardiac glucose uptake was normal in response to insulin and insulin sensitivity was preserved (Utriainen et al., 1998; Jagasia et al., 2001; Armoni et al., 2005). Furthermore, in type 2 diabetic mice, there was a reduction in glucose oxidation in the heart as a result of reduced GLUT4 protein expression and impaired insulin signalling (Carroll et al., 2005). Buchanan and colleagues reported that there was a reduction in the cardiac glucose uptake in the db/db mouse model of type 2 diabetes and that was related to increased fatty acid oxidation (Buchanan et al., 2005).

Glucose uptake in the heart is tightly regulated by insulin action and the presence of GLUT4 on the plasma membrane. Unlike fatty acids, whose entry into cardiomyocytes is not controlled by hormones and is mainly determined by the availability of lipids in the blood (An & Rodrigues, 2006). As a consequence of high lipid content in the bloodstream, the heart takes in considerably more fatty acids and suppresses glucose uptake (Peterson et al., 2004). It was proposed that there are some mechanisms, by which the cardiac glucose utilization is reduced. Elevated fatty acid oxidation is known to increase citrate, which then inhibits phosphofructokinase (PFK), which is the rate-limiting step in

glycolysis. Another proposed mechanism is when higher fatty acid oxidation enhances acetyl-CoA which then phosphorylates and inhibits the pyruvate dehydrogenase (PDH) through the stimulation of pyruvate dehydrogenase kinase, isozyme 4(PDK4) (Wu et al., 1998). Collectively, in both types of diabetes and in human and animal model studies, the heart is forced to utilise fatty acids as an alternative substrate to keep normal ATP levels and at the same time to reduce glucose oxidation.

4.6.1.2 Alterations in fatty acids metabolism in the heart and serum

Alterations in multiple fatty acids and other lipid species were revealed in our study. There were significant increases in the fold changes of fatty acids in both the heart (7 fatty acids) and serum (20 fatty acids). Phospholipids were increased as well in the serum samples (34 phospholipids).

It was reported that in diabetic hearts, there was a shift from glucose oxidation towards fatty acids as the energy source (Nishino et al., 2007) as previously discussed in section 4.6.1.1.

These changes imply either an alteration in adipose tissue storage of circulating fatty acids and impairment of hepatic fatty acids esterification or a change to the utilisation of fatty acids through β-oxidation of fatty acids in the mitochondria (Liu et al., 2011).

All tissues, including the heart, need essential fatty acids and lipids. With diabetes, hearts are expected to have metabolic imbalance and lipid accumulation. The accumulation of fatty acids and lipid species in or across the myocardium were detected in human and animal models with diabetes and heart failure (Borradaile & Schaffer, 2005) and it was suggested that excess

fatty acids and lipids are associated with the pathogenesis of cardiac dysfunction (Summers, 2006 and Park et al., 2007).

The defined mechanism by which the myocardial lipid accumulation leads to cardiomyopathy is uncertain. However, it was proposed that fatty acids could generate direct toxic effects on myocytes and can lead to impaired myofibrillar function (Dyntar et al., 2001). In addition, fatty acids can induce apoptosis (Zhou et al., 1999) as a result of the accumulation of the reactive oxygen species (ROS) produced by the triggering of protein kinase C signalling pathway and as a toxic by-product of lipid oxidation (Dyntar et al., 2001). Impairment of the balance between fatty acid uptake and oxidation leads the excess fatty acids to produce complex lipids such as phospholipids and triglycerides (Park & Goldberg, 2012). The previously stated data indicates that myocardial fatty acid levels are associated with impaired cardiac function of which is found in diabetic hearts.

In order to support the role of a change in metabolism in aggravating cardiac dysfunction, several studies have treated some animal models of diabetes with either PPAR-α or PPAR-γ agonists for three to six weeks. Zhou and colleagues reported that when they treated ZDF rats with PPAR-γ agonists at 6 weeks of age, they observed that the cardiac metabolism and heart function were improved (Zhou et al., 2000). In another study, altering cardiac metabolism by treating ZDF rats with PPAR-γ agonists also enhanced cardiac function (Golfman et al., 2005). Enhanced contractile function and normalised cardiac metabolism occur as a result of overexpression of GLUT4 in db/db mice (Semeniuk et al., 2002). These studies indicate that acute alterations in metabolism can possibly induce damage to the cardiac tissue which can be reversible. While these initial changes are insufficient to produce cardiac

functional alterations, early interventions would be favored in order to propose protection against the development of cardiomyopathy in the more advanced stages of the disease.

4.6.1.3 Alterations in sphingolipid and ceramide metabolism in the serum

Impairment of sphingolipid metabolism has been proposed to contribute to metabolic stress in diabetes and leads to the development of diabetic cardiomyopathy (Park & Goldberg, 2012). In addition, accumulation of ceramide in the cardiomyocytes might alter the balance of glucose and fatty acid oxidation and lead to impaired myocardial glucose utilization and eventually leads to cardiac dysfunction (Park & Goldberg, 2012).

Sphingolipids have increased in this study and this has been observed previously in different animal models of diabetic cardiomyopathy (Basu et al., 2009 ;Park & Goldberg, 2012). Fatty acids also stimulate the production of ceramides, which facilitate various toxic processes (Park et al., 2008). Though it is still uncertain, which lipid metabolites directly cause cardiomyopathy. In various animal models, ceramide accumulation in the heart associates with impaired heart function. Basu and colleagues illustrated that elevated myocardial ceramide levels are correlated with impaired diastolic function in two different diabetic animal models; Akita Ins2 (WT/C96Y) mice and Zucker diabetic fatty (ZDF) rats (Basu et al., 2009). Some of the most compelling data supporting the role of ceramide toxicity and the improvement in impaired heart function was achieved by the reduction of heart ceramide through pharmacologic and genetic intervention in ZDF rats and Akita Ins2 (WT/C96Y) mice (Park & Goldberg, 2012). These results suggest that ceramide-independent mechanisms contribute to the development of heart dysfunction resulting from lipotoxicity.

4.7 Limitations and future work:

Sample collection is a very important part in any large-scale metabolomics study. Failure to collect the samples correctly at the start of the study may invalidate the whole rationale of the study.

No clear separation was observed in serum data and this is due to differences between individual samples rather than HO vs. WT as stated previously in the results section. In our study, mice were killed by cervical dislocation. However, anesthesia was used on some of the mice in order to collect blood samples from them. The best way is not to use any anesthetics, as anesthetics will affect blood biochemical parameters. A study which is done by Gil and colleagues investigated the effects of 4 types of anesthetics on several plasma biochemical parameters in rabbits. They concluded that anesthetic administration has significantly increased or decreased the levels of some of biochemical parameters in the plasma (Gil et al., 2004). In addition, sample collection was not standardised as samples have been collected at different times, mice may have been hungry or just fed, differences in their feeding state can have an impact on the metabolome.

There has been a lot of discussion in the metabolomics community about serum versus plasma, but there is no firm conclusion. Serum has an issue with clotting time, but plasma also has issues. It was found that heparin in some tubes had degraded, leading to the appearance of high levels of sugars in the plasma (Dr P Begley, personal communication).

What needs to be remembered is that metabolomics compares metabolite abundances in matched populations of disease cases and healthy controls, but does not provide absolute quantitation for metabolites in a given sample. Part of the case-control matching process is to ensure that any sample handling

artifacts such as metabolite degradation during serum clotting affects both cases and controls to a similar degree.

This study is considered as an initial study to define large alterations in the metabolic profile from serum and heart samples. The next step will be to perform a metabolomics targeted study for a particular metabolic group of interest such as sugars and fatty acids to validate the results after defining the limitations. In addition, if both results are similar, pathways upstream and downstream of the targets could be examined.

4.8 Conclusion

In summary, GENA348 HO mice have shown certain metabolic alterations that have been previously reported and some changes that require further investigation. For the GC-MS and UPLC-MS, there were 43 differences in metabolites from the heart tissue samples and 93 from serum samples. The main altered metabolites from tissue samples were sugars and fatty acids. However, fatty acids, phospholipids and sphingolipids were the main altered metabolites from serum samples. This study is considered as a preliminary study to define large changes and develop further targeted studies to be performed while defining the limitations.

Chapter 5 Gene expression

Hypothesis generating technique in the GENA348 mice-Part 2

5.1 Introduction

Gene expression is defined as the process where information from a gene is used in the synthesis of a biologically active protein. Alteration of gene expression can impair the ability of the cell to function (Rockman & Kruglyak, 2006). mRNA expression is associated with the transcriptional activity of several genes in mammalian tissues and offers an overview of most of the various developmental and pathophysiological states. In that process, many genes are altered to either up-regulated or down-regulated depending on a specific disease (Wada et al., 2001).

Alterations in gene expression play an important role in the pathophysiological changes, which arise in response to diabetes (Reece et al., 2006). Although, real-time RT-PCR is one of the most sensitive and reliable methods for gene expression analysis, it is anticipated that microarray technology will be widely employed (Murphy, 2002). Microarray is a powerful tool for a range of applications including, detecting underlying mechanisms of disease, developing new diagnostic tools and determining the expression levels of huge numbers of genes simultaneously (Slonim & Yanai, 2009). However, the data interpretation is challenging and it requires extensive post-experimental analysis. Unlike real-time RT-PCR the post-experimental analysis is much quicker (Murphy, 2002).

5.2 Hypothesis

Hyperglycaemia as a result of genetic mutation in the glucokinase gene results in altered gene expression in the heart.

5.3 Aims

- To investigate the changes in diabetic gene expression profiles in the heart of GENA348 mice.
- To identify molecular and cellular signalling that may contribute to the change of the cardiac metabolism in GENA348 mice.

5.4 Methods

5.4.1 Diabetes PCR array plates

The Mouse Diabetes RT² *Profiler*™ PCR Array takes advantage of the combination of real-time PCR performance and the ability of microarrays to detect the expression of many genes simultaneously and in relatively little time. These plates allow the examination of the expression of a focused panel of genes associated with the onset and progression of diabetes and its complications. These genes are classified into six functional groups, including: transcription factors, receptors, transporters and channels, nuclear receptors, metabolic enzymes and secreted factors, signal transduction proteins and transcription factors. This array can be used as a rapid and reliable method to establish how diabetes in GENA348 mice changes gene expression in the heart. Then, the outcome will help in studying changes in cardiac metabolism. A short synopsis of the method is elucidated in figure 5.1. Samples were taken from the heart of 6 and 12 months old HO & WT GENA348 mice. Three mice were used per group.

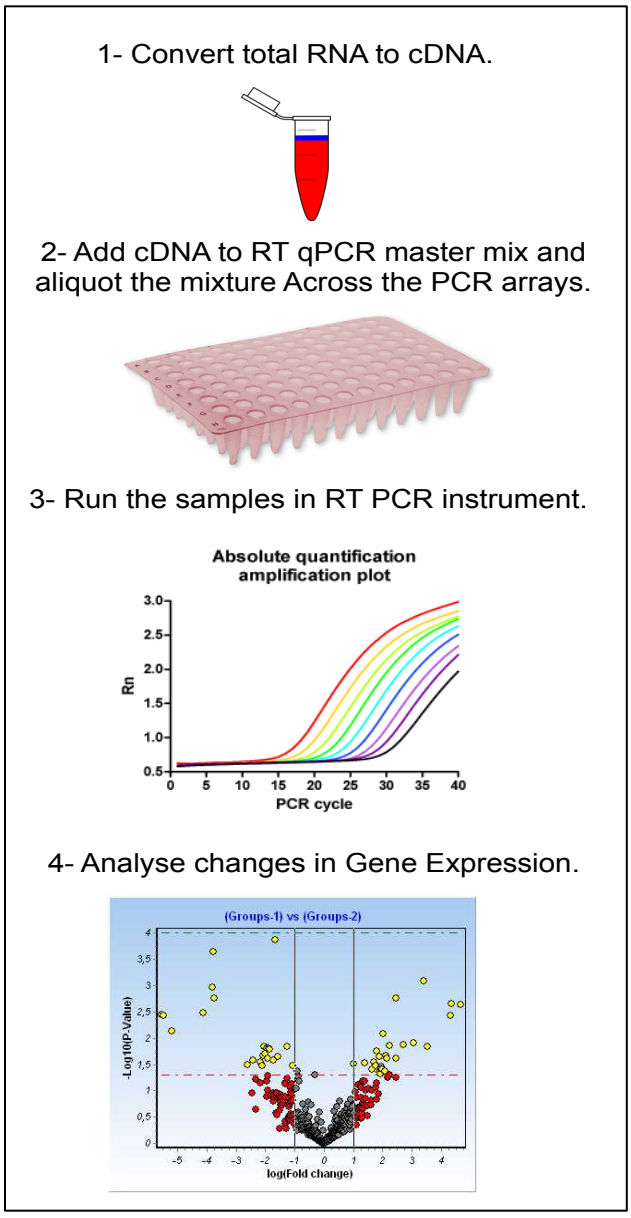

Figure 5.1 Overview of the PCR array procedure.

Experimental RNA samples were converted to first strand cDNA before being mixed with RT qPCR Master Mix. The mixture was aliquoted into each well of the same plate and then the plate was run on the real-time PCR instrument. Data analysis was performed using Free PCR Array data analysis software (version 3.5). The figure is adopted from http://www.sabiosciences.com.

The RT^2 First strand Kit was used to remove any residual genomic DNA contamination and to convert RNA to cDNA according to manufacturer's instruction (QIAGEN). RNA was extracted as described in section 2.1.2.2.1 Briefly, for each RNA sample, the combination of the following was used in a sterile PCR tube; 2µg of total RNA with 2µl of GE (5X gDNA Elimination Buffer). Lastly, H_2O was added to make the final volume of 10µl. Then, samples were mixed, briefly centrifuged and incubated at 42 °C for 5 minutes. Immediately after that, samples were chilled on ice for at least one minute. The reverse transcription cocktail was prepared according to manufacturer's instructions and 10µl of it was added to 10µl of the Genomic DNA Elimination mixture. To allow reverse transcription, the samples were incubated at 42°C for exactly 15 minutes. Then, to stop the reaction, samples were heated at 95°C for 5 minutes. Finally the cDNA was diluted with 91µl of H_2O and stored at -20°C.

To load the samples cocktail into the 96 well plate of the PCR array, an experimental cocktail was prepared in a multi-channel reservoir as the following; 1350µl of RT^2 qPCR Master Mix, 102µl of diluted cDNA and 1248µl of RNase free water (total volume 2700µl). 25µl of the cocktail was added to the 96 well plates by using a multi-channel pipette. The plate was sealed, centrifuged and placed in the real-time PCR instrument (ABI 7500 Fast) following the manufacturer's cycling conditions. To analyse the data, the RT^2 Profiler PCR Array Data Analysis (version 3.5) was used on the base of delta-delta Ct fold-change calculations method.

5.5 Results

5.5.1 Alteration in gene expression in 6 month-old- GENA348 mice

HO GENA348 mice developed significant cardiac hypertrophy with diastolic dysfunction at 6 months, which progressed to dilatation of the left ventricle and systolic dysfunction at 12 months. It was interesting to study the alteration in the gene expression of the heart between the two age groups of mice to understand the metabolic changes that occur in the heart.

In order to investigate this, the Mouse Diabetes RT² *Profiler*™ PCR Array plates were used and WT mice were used as a control. These plates were designed around genes involved in the early onset of diabetes and its complications. In 6-month-old GENA348 mice, it appeared that the majority of genes examined were expressed in the heart as shown in figure 5.2.

There were six up-regulated genes and ten down-regulated genes, which showed greater than a 2-fold change. The relative fold expression data is presented in two different formats. Firstly: a table, which classifies the genes on the basis of their functional groupings (Table 5.1). Secondly, a scatter plot to compare the normalised expression of every gene on the array between HO mutant mice and WT control groups by plotting them against one another to visualise large gene expression changes (Figure 5.3).

The most apparent observation was that the majority of altered genes were down-regulated in 6-month-old GENA348 mice. In addition, among the six functional categories, receptors, transports and channels, and signal transductions were the most altered groups in 6-month-old GENA mice. The complete list of genes in this PCR Array is shown in the appendix of this thesis.

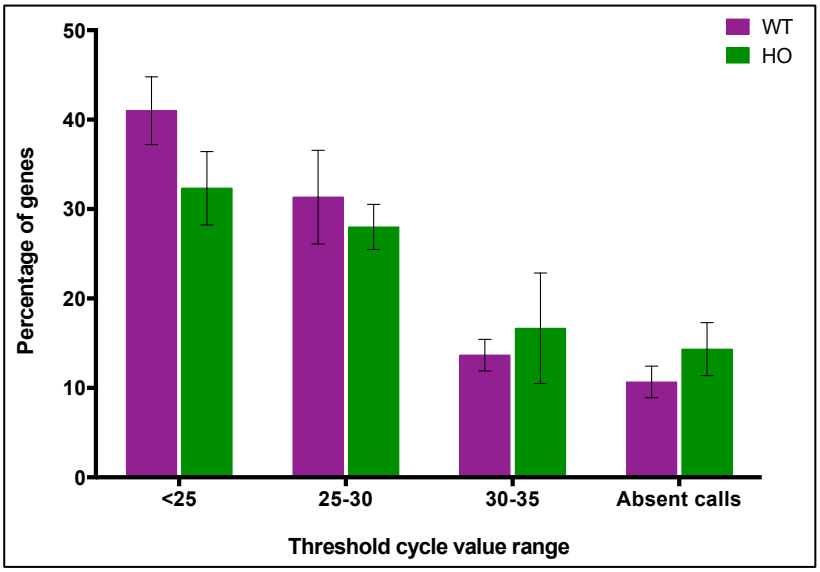

Figure 5.2 Distribution of Ct values in 6 month-old- GENA348 mice.

The figure shows that the majority of genes examined in 6-month-old GENA348 mice were expressed in the heart. Absent calls means that the Ct values are greater than 35 which represent no expression of the target gene in the tissue. (WT n=3, HO n=3). Data are expressed as mean±SEM,

N	Gene symbol	Gene name	Functional gene groupings	Fold change
1	Aqp2	Aquaporin 2	Receptors, Transports and Channels	4.31
2	Ctla4	Cytotoxic T-lymphocyte-associated protein 4		2.84
3	Gcgr	Glucagon receptor		3.82
4	Rab4a	RAB4A, member RAS oncogene family.		3.10
5	Adra1a	Adrenergic receptor, alpha 1a		-2.28
6	Tnfrsf1b	Tumor necrosis factor receptor superfamily, member 1b		-2.10
7	Vamp2	Vesicle-associated membrane protein 2		-2.61
8	Pdx1	Pancreatic and duodenal homeobox1	Transcription Factors	2.13
9	Hnf4a	Hepatic nuclear factor 4, alpha		-3.37
10	Pck1	Phosphoenolpyruvate carboxykinase 1, cytosolic	Metabolic Enzymes	3.48
11	Gpd1	Glycerol-3-phosphate dehydrogenase 1 (soluble)		-2.20
12	Ifng	Interferon gamma	Secreted Factors	-2.14
13	Pik3cd	Phosphatidylinositol 3-kinase catalytic delta polypeptide	Signal Transduction	-2.68
14	Pik3r1	Phosphatidylinositol 3-kinase, regulatory subunit, polypeptide 1 (p85 alpha),		-2.44
15	Ptpn1	Protein tyrosine phosphatase, non-receptor type 1,		-3.97
16	Pparg	Peroxisome proliferator activated receptor gamma,	Nuclear Receptors	-10.03

Table 5.1 Altered gene expressions in 6-month-old GENA348 mice.

The lists of the genes that had altered expression in the diabetic mice compared to controls. Green: up regulated, Red: down regulated. (WT n= 3, HO n= 3).

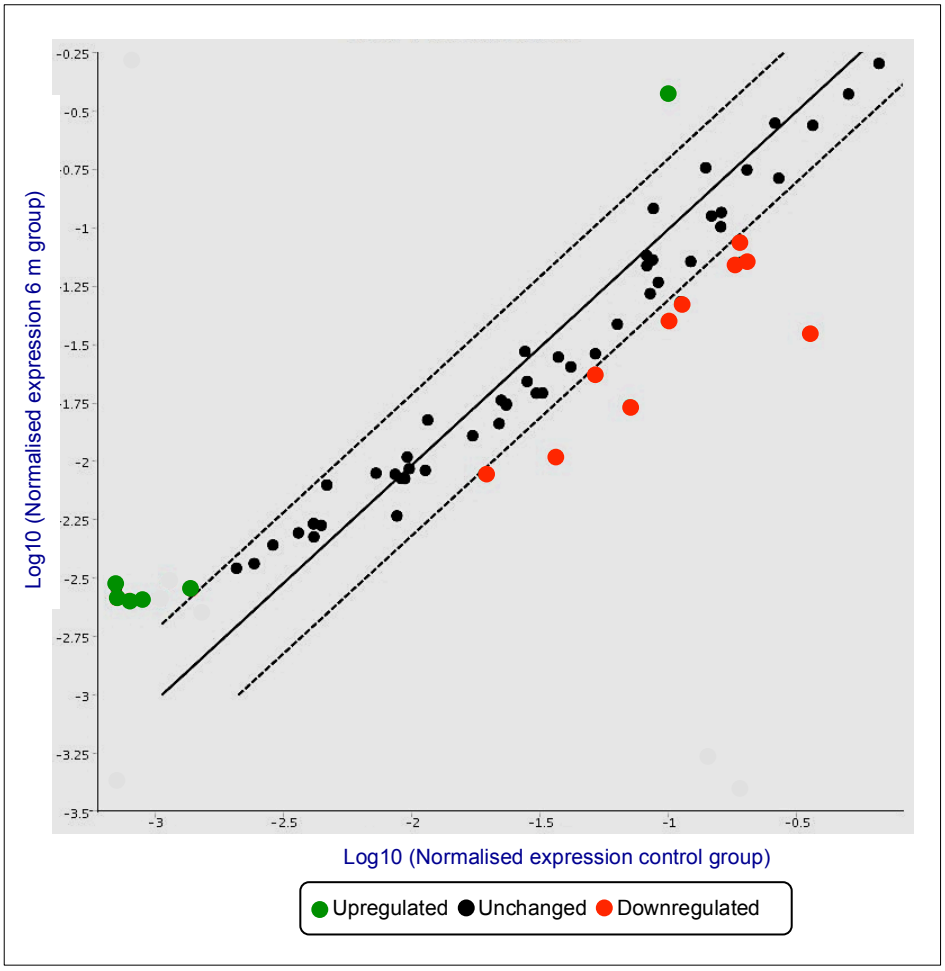

Figure 5.3 Scatter plot of the target genes examined in the PCR array plate in 6-month-old GENA348 mice.

The scatter plot compares the normalised expression of every gene on the array between HO mutant mice and WT control groups by plotting them against one another to visualise large gene expression changes. The central line indicates unchanged gene expression. Whole heart tissue was used (WT n=3, HO n=3).

5.5.2. Alteration in gene expression in 12 month-old- GENA348 mice

In the 12-month-old GENA348 mice, it emerged that the majority of genes examined were expressed in the heart as shown in figure 5.4. There were twelve up-regulated genes that showed greater than a 2-fold change. The relative fold expression data is presented as previously described. Firstly: a table, which classifies the genes on the basis of their functional groupings (Table 5.2). Secondly, a scatter plot (Figure 5.5). The most apparent observation was that the majority of the altered genes were up-regulated at 12 months. In addition, among the six functional categories, the metabolic enzymes were the most altered group. Interestingly, there were three up-regulated genes that appeared in the 6-month-old mice as well as in the 12 month old mice, which could provide potential new avenues to explore, and these are highlighted in table 5.3.

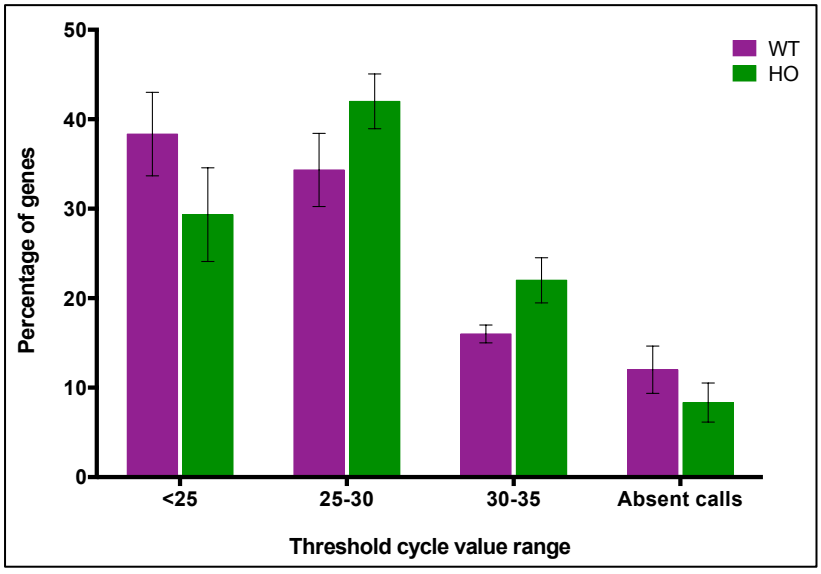

Figure 5.4 Distribution of Ct values in 12 month-old-GENA348 mice.

The figure shows that the majority of genes examined in 12-month-old GENA348 mice were expressed in the heart. Absent calls means that the Ct values are greater than 35 which represent no expression of the target gene in the tissue. (WT n=3, HO n=3).

N	Gene symbol	Gene name	Functional gene groupings	Fold change
1	**Adrb3**	Adrenergic receptor, beta 3	**Receptors, Transports and Channels**	**5.45**
2	**Rab4a**	RAB4A, member RAS oncogene family.		**2.65**
3	**Cebpa**	CCAAT/enhancer binding protein (C/EBP), alpha	**Transcription Factors**	**2.95**
4	**Pdx1**	Pancreatic and duodenal homeobox1		**2.99**
5	**G6pc**	Glucose-6-phosphatase, catalytic	**Metabolic Enzymes**	**2.86**
6	**Parp1**	Poly (ADP-ribose) polymerase family, member 1,		**2.06**
7	**Pygl**	Liver glycogen phosphorylase,		**2.44**
8	**Pck1**	Phosphoenolpyruvate carboxykinase 1, cytosolic		**7.31**
9	**Retn**	Resistin	**Secreted Factors**	**2.85**
10	**Tnf**	Tumor necrosis factor,		**2.97**
11	**Il12b**	Interleukin 12B		**2.97**
12	**Ucp2**	Uncoupling protein 2 (mitochondrial, proton carrier)	**Others**	**2.21**

Table 5.2 Altered gene expressions in 12-month-old GENA348 mice.

The lists of the genes that had altered expression in the diabetic mice compared to controls. Green: up regulated (WT n= 3, HO n= 3).

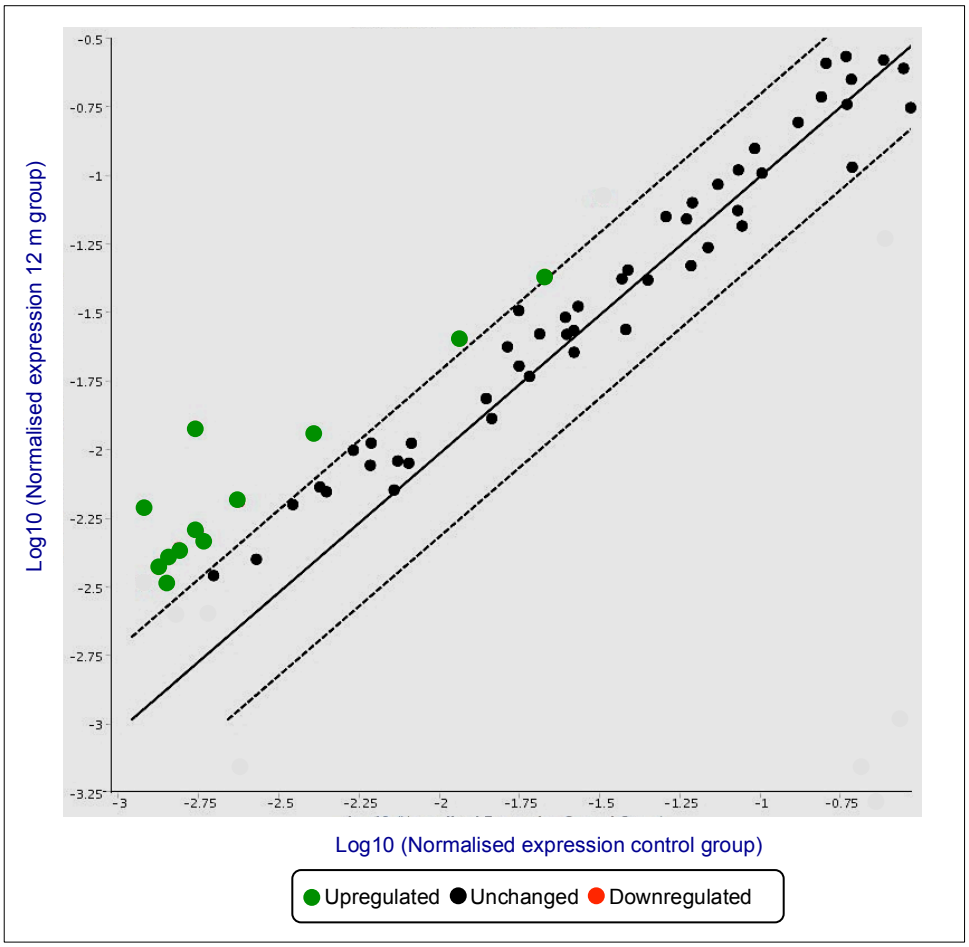

Figure 5.5 Scatter plot of the target genes examined in the PCR array plate in 12-month-old GENA348 mice.

The scatter plot compares the normalised expression of every gene on the array between HO mutant mice and WT control groups by plotting them against one another to quickly visualise large gene expression changes. The central line indicates unchanged gene expression. Whole heart tissue was used (WT n=3, HO n=3).

N	Gene symbol	Function	Fold change (6 m)	Fold change (12m)
1	**Pck1**	Involved in the regulation of gluconeogenesis	**3.48**	**7.31**
2	**Pdx1**	Involved in the early pancreatic development of and plays a main role in the regulation of insulin gene.	**2.13**	**2.99**
3	**Rab4a**	Involved in endocytosis and biosynthetic protein transport	**3.10**	**2.65**

Table 5.3 Altered gene expressions in both 6- and 12-month-old GENA348 mice that showed greater than a 2-fold change and their main functions

The lists of the genes that had altered expression in both 6- and 12-month HO mice compared to controls.1-(Bouche et al., 2004), 2(Marshak et al., 2000),3- (Imamura et al., 2003). (WT n= 3, HO n= 3).

5.5.3 Validation of the diabetes PCR array results by using RT-PCR

As with all array technology, the first step would be to verify the hits in the assay with RT-PCR. The validation was done with different set of samples. Almost all genes with the highest fold change were examined (Figure 5.6 and 5.7). It was found that no significant changes were observed in most of the examined genes. However, only two up-regulated genes, Phosphoenolpyruvate carboxykinase 1 (Pck1) (~8-fold increase) and Glucose-6-Phosphatase, Catalytic Subunit (G6pc) (~3-fold increase) showed a comparable pattern as the array results (Figure 5.8). Pck1 and G6pc are the main enzymes that play a key role in gluconeogenesis regulation.

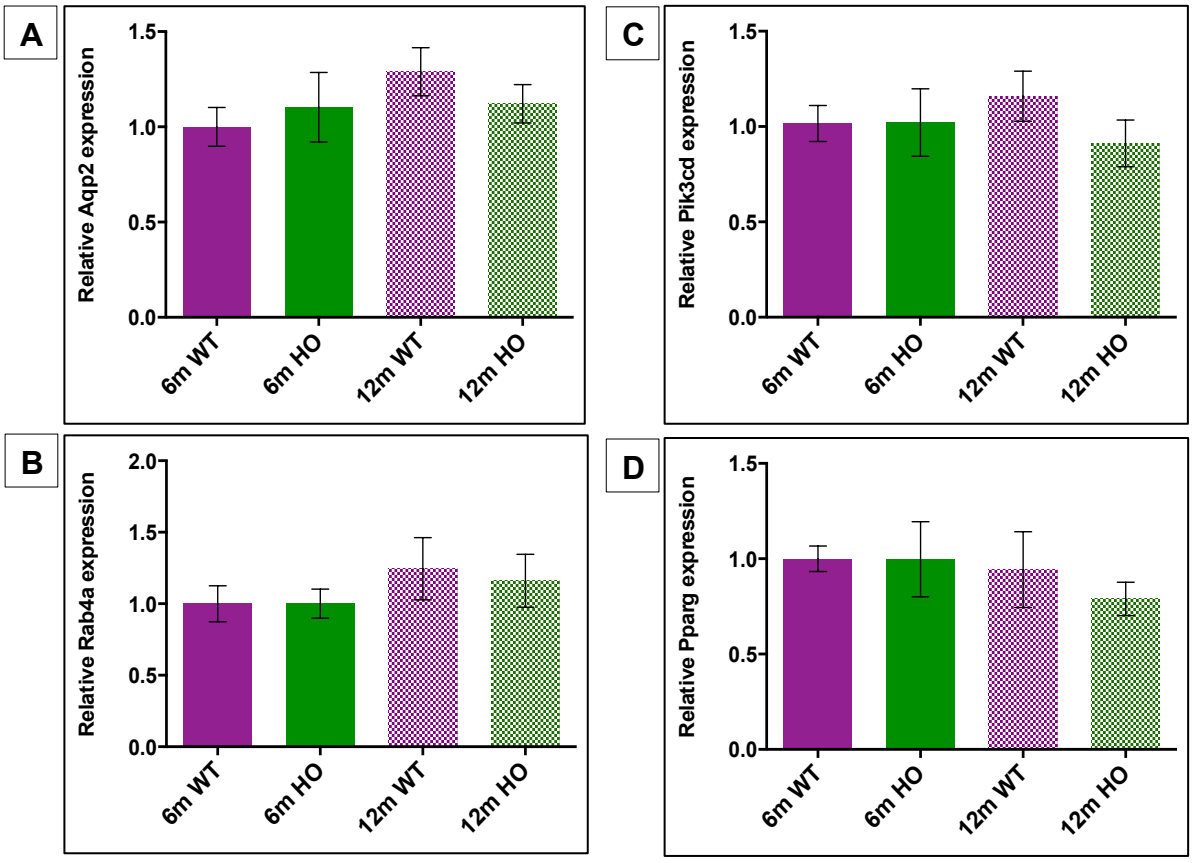

Figure 5.6 A number of genes with the highest fold change from the PCR array plates that were examined.

Q-PCR quantification of A- Aqp2, B-Rab4a, C-Pik3cd, and D-Pparg genes indicated that there were no significant changes in the expression of these genes. Data are expressed as mean±SEM, N=6.

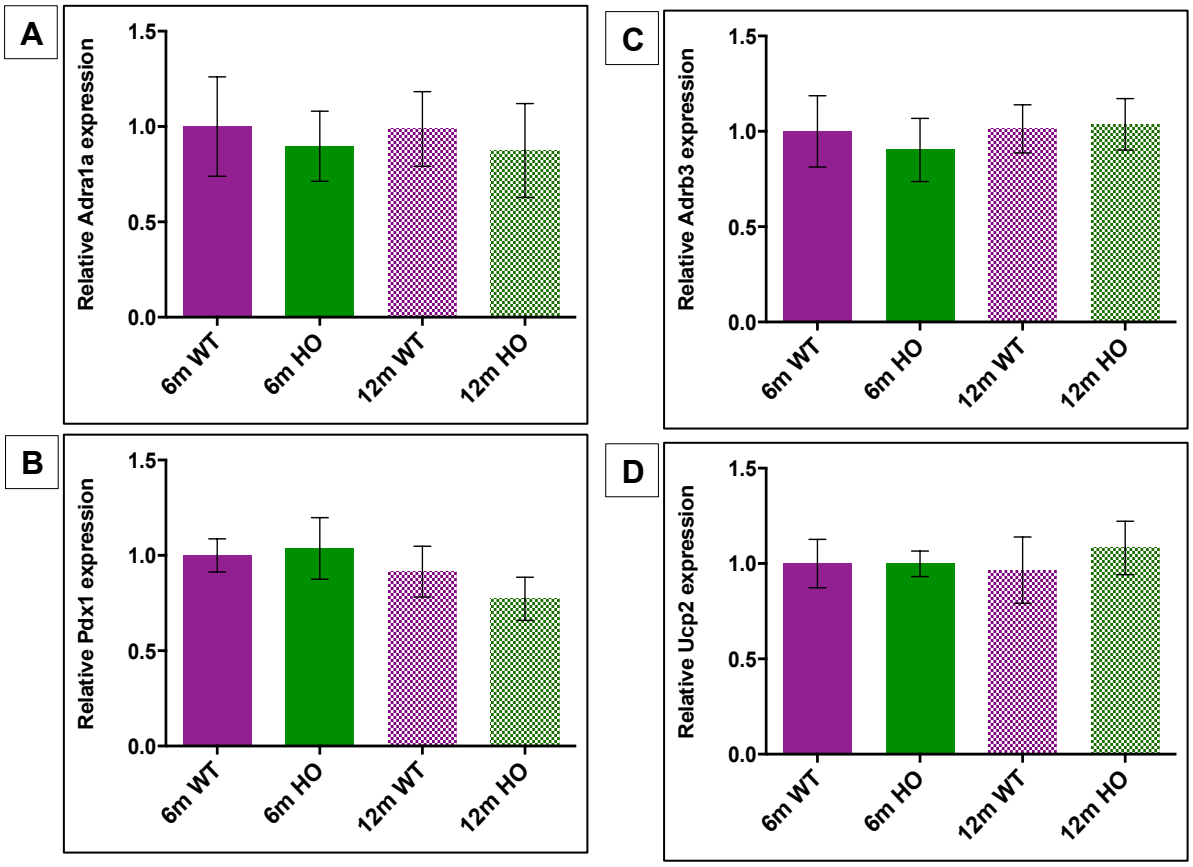

Figure 5.7 A number of genes with the highest fold change from the PCR array plates that were examined.

Q-PCR quantification of A- Adra1a, B-Pdx1, C-Adrb3 and D-Ucp2 genes indicated that there were no significant changes in the expression of these genes. Data are expressed as mean±SEM. N=6.

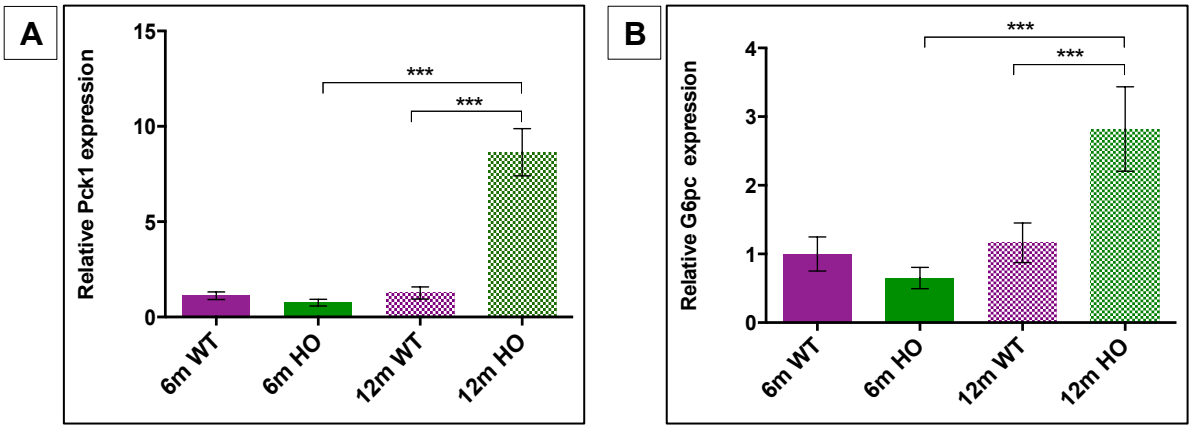

Figure 5.8 Both Pck1 and G6pc are up-regulated genes in 12-month-old GENA348 mice.

Q-PCR quantification of A- Pck1 and B- G6pc genes indicated there was a significant increase in the expression of both genes in the HO mice at 12 month compared to WT controls. The data confirmed the results from the diabetes PCR array plates. Data are expressed as mean±SEM, *** P<0.001, N=6

5.5.4. Regulation of gluconeogenesis through FoxO activation

Gluconeogenesis is required for survival especially during starvation or prolonged fasting. However, it is inappropriately triggered in diabetes mellitus Among FoxO family members, FoxO1 is one of the main transcriptional components known to have a fundamental physiological role in contributing to the regulation of gluconeogenesis. It was established that FoxO1 can bind directly to the promoters of the main gluconeogenic genes (Pck1 and G6pc) and stimulate glucose production (Hall et al., 2000; Nakae et al., 2002).

Since FoxO1 can bind to the promoters of the gluconeogenic genes and trigger glucose production, the protein expression level of FoxO1 was examined in both 6 and 12 month old GENA348 HO mice. In the HO mice, there was a significant 2.8±0.3 fold increase ($P<0.001$) in the phosphorylation of FoxO at 6-months, an indication of its inactive state. However, at 12 months, there was a significant 1.3±0.05 fold reduction in the phosphorylation of FoxO ($P<0.001$), which is indirectly suggestive of its activation (Figure 5.9.). A decreased phosphorylation of pFoxO1 proteins is an indication of increased nuclear localisation of FoxO1 (Battiprolu et al., 2012).

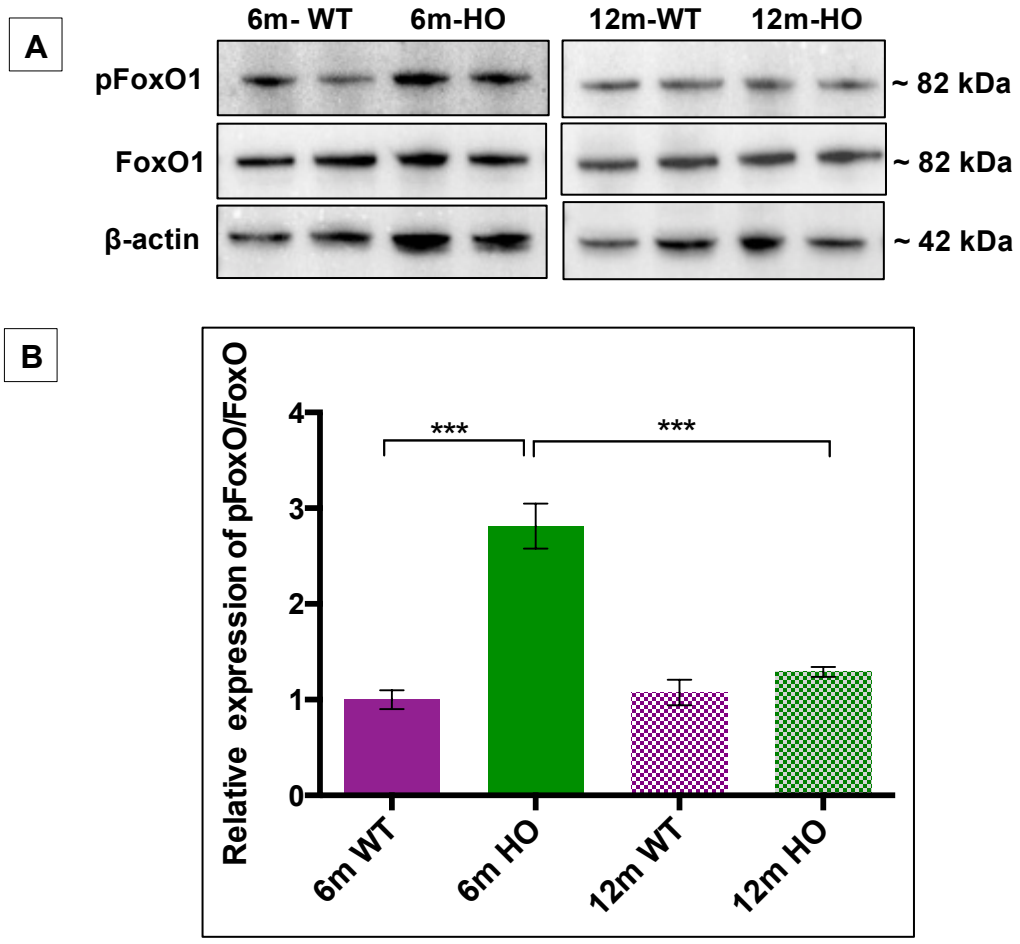

Figure 5.9 FoxO1 protein expression in 6 and 12 month old GENA348 mice

A- Representative immunoblots performed on protein extracted from heart tissue of 6 and 12 GENA348 mice showing that FoxO1 expression increased at 6 months, an indication of its inactive state. However, at 12 months, there was a significant decrease in FoxO1 expression compared to the 6 month old HO mice which, indirectly suggestive of its activation. Data are presented as mean ±SEM, *** P<0.00. N=4.

5.6 Discussion

Hyperglycaemia is one of the hallmark features of diabetes mellitus. However, the independent effect of hyperglycaemia that contributes to the development of cardiomyopathy is still unknown. Other rodent diabetic models that are frequently used to study this disease have altered insulin levels and obesity in addition to elevated blood glucose. Previous findings in our group have shown that GENA348 mice developed chronic hyperglycaemia and cardiac hypertrophy with diastolic dysfunction at 6 months, which progressed to dilatation of the left ventricle and systolic dysfunction at 12 months.

It was interesting to study the changes in the gene expression of the heart between the two age groups of mice to identify molecular and cellular signalling, and genes that may contribute to the changes seen in the cardiac metabolism. The aim of this study was initially directed to identify the underlying alteration in the gene expression in the heart of GENA348 mice.

5.6.1 Altered gene expression observed in this study.

In order to investigate the effect of hyperglycaemia on altered gene expression of the heart of 6 and 12 month old GENA348 mice, the Mouse Diabetes RT² Profiler™ PCR Array was used.

The most apparent observation, and after the validation of the PCR array results, was that only two up-regulated genes, Phosphoenolpyruvate carboxykinase 1 (Pck1) (~8-fold increase) and Glucose-6-Phosphatase, Catalytic Subunit (G6pc) (~3-fold increase) have shown a comparable pattern as the array results.

Under normal physiological conditions, insulin triggers glycolysis enzymes and suppresses gluconeogenesis enzymes activity in order to accomplish

homeostatic regulation of blood glucose (Wang et al., 1994). However, during diabetes, starvation and prolonged fasting, gluconeogenesis enzymes are activated and are involved in the generation of glucose from non-carbohydrate substrates such as pyruvate, lactate, glycerol and glucogenic amino acids to provide glucose to other organs. Gluconeogenesis is controlled over the long term mainly by changes in the expression of two major gluconeogenic enzymes: Pck1 and G6pc (Bouche et al., 2004). Whereas Pck1 is the rate-limiting enzyme that phosphorylates oxaloacetate to form phosphoenolpyruvate, G6pc catalyses the dephosphorylation of glucose-6-phosphate to glucose as the final step in glycogenolysis and gluconeogenesis. In several animal models of diabetes and obesity, gluconeogenesis and mRNA expression of Pck1 and G6pc genes are augmented by 2-3 fold compared to controls (Friedman et al., 1997). This increase in the gluconeogenic enzymes is assumed to participate in the increase of hepatic glucose production associated with diabetes (Friedman et al., 1997).

5.6.2 Regulation of gluconeogenesis through FoxO activation

In a variety of tissues, including the liver, gluconeogenesis is required for survival during starvation or prolonged fasting. However, it is activated in uncontrolled diabetes. FoxO1 is one of the main transcriptional components known to have a vital physiological role in participating to the regulation of gluconeogenesis. It was establish that FoxO1 can bind directly to the promoters of gluconeogenic genes and stimulate glucose production (Hall et al., 2000; Nakae et al., 2002).

In our project, protein expression level of FoxO1 was examined in both 6 and 12 month old GENA348 HO mice. In the HO mice, there was a significant

2.8±0.3 fold increase (P<0.001) in the phosphorylation of FoxO at 6-months, an indication of its inactive state. However, at 12 months, there was a significant 1.3±0.05 fold decrease in the phosphorylation of FoxO (P<0.001), which is indirectly suggestive of its activation. Alteration of FoxO activity between 6 and 12 month old GENA348 mice was evident in our model of mice.

Activation of Foxo1 was also reported in literature, it was found that in transgenic mice which express a constitutively active form of FoxO1 in the liver result in augmented expression of the gluconeogenic genes (Pck1 and G6pc), which eventually leads to elevated plasma glucose levels (Zhang et al., 2006). Furthermore, in the case of insulin resistance and diabetes mellitus, the inhibition of FoxO1, which is activated by Akt as a result of feeding or insulin stimulation, is unregulated. Therefore, the dephosphorylation of Foxo1 at the conserved Akt phosphorylation sites (T24, S256, and S319) increases Foxo1 activity, which then triggers gluconeogenesis and leads to increased glucose production. Elevated nuclear dephosphorylated FoxO1 levels were identified in the liver and heart of diabetic mice (Altomonte et al., 2003; Battiprolu et al., 2012). These data support our results as the main gluconeogenic enzymes are up regulated. This indicates increased FoxO activity and as a consequence an increase in glucose production. Our metabolomics data support these results as we found that there was a significant 5.9 and 3.6 fold increase in glucose and glucose-6-phosphate, respectively in 12-month-old HO GENA348 mice compared to WT controls.

On the other hand, suppression of FoxO1 has also been reported in literature. In db/db mice and L-DKO mice, the hepatic deletion of Foxo1 decreases glucose production and improves diabetes (Zhang et al., 2012). Furthermore, it was found that in mice with diet induced obesity and through using an antisense

oligonucleotide-mediated approach to reduce FoxO1 in both liver and white adipose tissue, there was a decrease in fasting glucose levels and a reduction in the expression of both Pck1 and G6pc (Samuel et al., 2006). Consistent with these studies, adenoviral administration of dominant-inhibitory FoxO1 in mice also displays a decrease in fasting blood glucose levels through suppressing the expression of the gluconeogenic genes Pck1 and G6pc (Altomonte et al., 2003). It has also been shown in the Liver-Specific FoxO1 Knockouts mice that, chronic deletion of hepatic FoxO1 leads to reduced glucose production in in the liver (Matsumoto et al., 2007). Collectively, the data presented here indicate that FoxO1 is required as a main transcription factor for controlling gluconeogenesis.

Zhang and colleagues found that FoxO1 could decrease the expression of glucokinase, which is the major enzyme responsible for the oxidation of glucose (Zhang et al., 2006). In HO GENA348 mice, a reduction in the expression level of glucokinase was reported in the liver (Gibbons, 2011) and in the pancreas (Toye et al., 2004). The reduction in the utilization of glucose could contribute to the ability of the body to produce newly synthesized glucose especially when insulin levels are low and when gluconeogenic genes and FoxO proteins are active.

There are some questions that remain to be answered, is there any association between the increase in the level of the gluconeogenic genes and the cardiac phenotype in GENA348 mice? Does gluconeogenesis influence the heart function in this model of diabetes?

5.7 Limitations and future work:

It would be interesting to define the molecular alterations before and after the onset of hyperglycaemia. Since hyperglycaemia developed in the mice at 3 months, samples could be collected and examined before GENA348 mice reach 3 months of age. In addition, our study assessed transcription alterations in whole hearts; therefore, additional studies are necessary to outline the impact of single cardiomyocytes or fibroblasts to the influence of hyperglycemia on cardiac metabolism.

More experimental evidence is warranted in order to confirm the activity of FoxO1 as these were the last findings I made and I would go on to look at the localisation of FoxO1 by using subcellular fractionation. Furthermore, it would be interesting to examine which signalling pathway is involved in the activation of FoxO1.

5.8 Conclusion

Alterations in gene expression play an important role in the pathophysiological changes, which arise in response to diabetes. In order to examine the effect of hyperglycaemia in the alteration of the gene expression in the hearts of 6 and 12 month old GENA348 HO mice, the Mouse Diabetes RT² *Profiler*™ PCR Array plates were used. It was clear that hyperglycaemia as a result of genetic mutation in the glucokinase gene results in altered gene expression in the 12 months old HO mice. After the validation of the results that were obtained from the PCR array plates, it was found that there are only two up regulated genes, Pck1 and G6pc, which showed a similar pattern. FoxO1 is known to have a vital physiological role in participating to the regulation of gluconeogenesis. FoxO1 was examined at protein levels and preliminary data illustrated that there was a significant increase in the phosphorylation level of FoxO1 in 6-month-old GENA348 mice and there was a significant decrease in the phosphorylation level of FoxO1 in 12-month-old GENA348 mice. The precise mechanism behind this phenomenon is unclear. Although, accumulating evidence suggests that this alteration of the cardiac metabolism plays a significant role in the development of cardiomyopathy, a better understanding of the dysregulation of the cardiac metabolism during the development of hyperglycaemia might offer knowledge as prospective targets for the treatment of cardiomyopathy. Also, it could provide novel therapies designed to help the rapidly growing cohort of diabetic patients.

Chapter 6 General conclusion

The role of hyperglycaemia in the pathogenesis of cardiovascular complications of diabetes has not yet been fully understood. This is mainly due to the lack of suitable animal models that accurately replicate the human condition. However, GENA348 represents a human relevant model to investigate the complexities behind cardiovascular complications of diabetes.

GENA348 mouse was generated through ENU mutagenesis resulting in a point mutation in the glucokinase gene. Glucokinase is a glucose sensor that regulates insulin secretion. As a result of abnormal glucose regulation, the HO mice developed progressive hyperglycaemia. At 6 months, the mice developed a diabetic cardiomyopathy equivalent to that seen in clinical practice with the development of cardiac hypertrophy and diastolic dysfunction, which progressed to dilatation of the left ventricle and systolic dysfunction at 12 months.

The overall aim of the project was to examine the molecular and pathophysiological mechanisms that contribute to development of the cardiac phenotype in diabetic GENA348 mice in the setting of hypertension and at baseline.

Diabetic patients often present with comorbidities, which can have an additive effect on cardiovascular complications. To simulate this, 6-month old-GENA348 HO and WT mice were subjected to ANG II infusion stress. Following ANG II infusion, HO and WT GENA348 mice exhibited a significant increase in systolic and diastolic blood pressure compared to untreated controls. Even though the HO mice were hypertrophic, in the first place before the ANG II treatment and after ANG II treatment the hypertrophy only went up to the same absolute level as WT mice. The diastolic function was generally preserved in WT and HO mice

following the ANG II treatment. However, systolic function was improved following ANG II treatment in the HO mice. Our data indicates that the HO mice have had a blunted hypertrophic response to the hypertension induced by ANG II. This possibly is in part as a result of the reduction in the ANG II receptor type 1 as a consequence of chronic ANG II infusion.

At baseline, two hypothesis-generating methods were used. Firstly, metabolomics were used on 12-month-old GENA348 mice heart and serum samples. Secondly, diabetes PCR array plates were used on 6- and 12-month-old GENA348 mice heart samples. For the metabolomics, there were 43 differences in metabolites from tissue samples and 93 from serum samples. The main altered metabolites from tissue samples were sugars and fatty acids. However, fatty acids, phospholipids and sphingolipids were the main altered metabolites from serum samples.

Following the validation of the array plates the most evident observation was that only two up-regulated genes, Phosphoenolpyruvate carboxykinase 1 (Pck1) and Glucose-6-Phosphatase, Catalytic Subunit (G6pc) revealed a similar pattern as the array results. Pck1 and G6pc are the main enzymes that play a key role in gluconeogenesis regulation. We also looked at the expression level of one of the main transcriptional regulators of gluconeogenesis, Forkhead box protein O1 (FoxO1). It was found that the expression was changed at 12 months.

The data suggest that hyperglycaemia altered gene expression and the metabolites profiles in 12 month old HO mice, with apparent changes detected in genes and metabolites involved in the metabolic regulation of the heart. In addition, this study may provide initial insights into the pathophysiological

alterations in the cardiac metabolism that may contribute to the development of diabetic cardiomyopathy.

Cardiac metabolism is a promising target for a novel therapeutic intervention in maintaining the cardiovascular health in diabetes. Restoring the balance between lipids–glucose and preventing metabolic lockdown of the diabetic heart should be applied as approaches to reverse cardiomyopathy in diabetes.

7 References

ADA. (2002). *Report of the Expert Committee on the Diagnosis and Classification of Diabetes Mellitus* (Vol. 25, pp. 5-20).

Abdi, H., & Williams, L. J. (2010). Principal component analysis. *Wires Computational Statistics*, *2*, 433-459.

Alberti, K. G., & Zimmet, P. Z. (1998). Definition, diagnosis and classification of diabetes mellitus and its complications. Part 1: diagnosis and classification of diabetes mellitus. Provisional report of a WHO consultation. *Diabetic medicine*, *15*, 539–553.

Altomonte, J., Richter, A., Harbaran, S., Suriawinata, J., Nakae, J., Thung, S. N., Meseck, M., et al. (2003). Inhibition of Foxo1 function is associated with improved fasting glycemia in diabetic mice. *American Journal of Physiology. Endocrinology and Metabolism*, *129*, 718-728.

Altshuler, D., Hirschhorn, J., & Klannemark, M. (2000). The common PPARγ Pro12Ala polymorphism is associated with decreased risk of type 2 diabetes. *Nature genetics*, *26*, 76-80.

An, D., & Rodrigues, B. (2006). Role of changes in cardiac metabolism in development of diabetic cardiomyopathy. *American Journal of Physiology. Heart and Circulatory Physiology*, *291*, H1489-H1506.

Armoni, M., Harel, C., Bar-yoseph, F., Milo, S., & Karnieli, E. (2005). Free Fatty Acids Repress the GLUT4 Gene Expression in Cardiac Muscle via Novel Response Elements. *The Journal of biological Chemistry*, *280*, 34786-34795.

Attiya, K., & Sahar, F. (2012). Maturity-onset Diabetes of the Young (MODY) Genes: Literature Review. *Clinical Practice*, *1*, 4-11.

Avogaro, A., Nosadini, R., Doria, A., Fioretto, P., Velussi, M., Vigorito, C., Sacca, L., et al. (1990). Myocardial metabolism in insulin-deficient humans without coronary artery disease. *The American Journal of Physiology Endocrinology and Metabolism*, *258*, E606-E618.

Basu, R., Oudit, G. Y., Wang, X., Zhang, L., Ussher, J. R., Lopaschuk, G. D., & Kassiri, Z. (2009). Type 1 diabetic cardiomyopathy in the Akita (Ins2 WT / C96Y) mouse model is characterized by lipotoxicity and diastolic dysfunction with preserved systolic function. *American Journal of Physiology. Heart and Circulatory Physiology*, *297*, 2096-2108.

Battiprolu, P. K., Hojayev, B., Jiang, N., Wang, Z. V., Luo, X., Iglewski, M., Shelton, J. M., et al. (2012). Metabolic stress – induced activation of FoxO1

triggers diabetic cardiomyopathy in mice. *The Journal of Clinical Investigation*, *122*, 1109-1118.

Bauters, C., Lamblin, N., Mc Fadden, E. P., Van Belle, E., Millaire, A., & de Groote, P. (2003). Influence of diabetes mellitus on heart failure risk and outcome. *Cardiovascular diabetology*, *2*, 1.

Begley, P., Francis-mcintyre, S., Dunn, W. B., Broadhurst, D. I., Halsall, A., Tseng, A., Knowles, J., et al. (2009). Development and Performance of a Gas Chromatography-Time-of-Flight Mass Spectrometry Analysis for Large-Scale Nontargeted Metabolomic Studies of Human Serum. *Analytical Chemistry*, *81*, 7038-7046.

Bilsen, M. V., Daniels, A., Brouwers, O., Janssen, B. J. A., Derks, W. J. A., Brouns, A. E., Munts, C., et al. (2014). Hypertension Is a Conditional Factor for the Development of Cardiac Hypertrophy in Type 2 Diabetic Mice. *PLoS ONE*, *9*, 1-10.

Black, M., Amore, A. D., Auden, A., Stamp, L., Osicka, T., Panagiotopoulos, S., & Jerums, G. (2010). Chronic type 1 diabetes in spontaneously hypertensive rats leads to exacerbated cardiac fibrosis. *Cardiovascular Pathology*, *19*, 361-370.

Borradaile, N., & Schaffer, J. (2005). Lipotoxicity in the heart. *Current Hypertension Report*, *7*, 412-7.

Bouche, C., Serdy, S., Kahn, C. R., Bouche, C., & Goldfine, A. B. (2004). The Cellular Fate of Glucose and Its Relevance in Type 2 Diabetes. *Endocrine Reviews*, *25*, 807-830.

Boudina, S., & Abel, E. D. (2007). Diabetic cardiomyopathy revisited. *Circulation*, *115*, 3213-3223.

Brown, M., Dunn, W. B., Dobson, P., Patel, Y., Winder, C. L., Francis-mcintyre, S., Begley, P., et al. (2009). Mass spectrometry tools and metabolite-specific databases for molecular identification in metabolomics. *Analyst*, *134*, 1322-1332.

Brownlee, M. (2005). The pathobiology of Diabetic complications. *Diabetes*, *54*, 1615-1625.

Brutsaert, D., & Housmans, P. (1980). Dual control of relaxation. Its role in the ventricular function in the mammalian heart. *Circulation research*, *47*, 637-652.

Buchanan, J., Mazumder, P. K., Hu, P., Chakrabarti, G., Roberts, M. W., Yun, U. J., Cooksey, R. C., et al. (2005). Reduced Cardiac Efficiency and Altered Substrate Metabolism Precedes the Onset of Hyperglycemia and Contractile Dysfunction in Two Mouse Models of Insulin Resistance and Obesity. *Endocrinology*, *146*, 5341-5349.

Camps, M., Castello, A., Munoz, P., Monfar, M., Testar, X., Palacin, M., & Zorzano, A. (1992). Effect of diabetes and fasting on GLUT-4 (muscle/fat) glucose-transporter expression in insulin-sensitive tissues. *Biochemistry Journal*, *282*, 765-772.

Carroll, R., Carley, A. N., Dyck, J. R. B., Severson, D. L., Carley, A. N., & Dyck, J. R. B. (2005). Metabolic effects of insulin on cardiomyocytes from control and diabetic db / db mouse hearts. *American Journal of Physiology. Endocrinology and Metabolism*, *288*, 900-906.

Chang, D., & Talamini, M. (2011). A review for clinical outcomes research: hypothesis generation, data strategy, and hypothesis-driven statistical analysis. *Surgical endoscopy*, *25*, 2254-60.

Chen, D., & Coffman, T. M. (2015). ScienceDirect AT 1 Angiotensin receptors - vascular and renal epithelial pathways for blood pressure regulation. *Current Opinion in Pharmacology*, *21*, 122-126.

Cohen-solal, A., Beauvais, F., & Logeart, D. (2008). Heart Failure and Diabetes Mellitus : Epidemiology and Management of an Alarming Association. *Journal of Cardiac Failure*, *14*, 615-626.

Daniels, A., Linz, D., Bilsen, M. V., Ru, H., Sadowski, T., Ruf, S., Juretschke, H.-paul, et al. (2012). Long-term severe diabetes only leads to mild cardiac diastolic dysfunction in Zucker diabetic fatty rats. *European journal of heart failure*, *14*, 193-201.

Diabetes UK. (2014). Diabetes: facts and stats. *UK*. Retrieved from https://www.diabetes.org.uk/Documents/Position statements/Facts and stats June 2015.pdf

Doria, A., Nosadini, R., Avogaro, A., Fioretto, P., & Crepaldi, G. (1991). Myocardial Metabolism in Type 1 Diabetic Patients Without Coronary Artery Disease. *Diabetic medicine*, *8*, S104–S107.

Du, X., Matsumura, T., Edelstein, D., Rossetti, L., Zsengellér, Z., Szabó, C., & Brownlee, M. (2003). Inhibition of GAPDH activity by poly (ADP-ribose) polymerase activates three major pathways of hyperglycemic damage in endothelial cells. *Journal of Clinical Investigation*, *112*, 1049-1057.

Dunn, W. B., Broadhurst, D., Begley, P., Zelena, E., Francis-mcintyre, S., Anderson, N., Brown, M., et al. (2011a). Procedures for large-scale metabolic profiling of serum and plasma using gas chromatography and liquid chromatography coupled to mass spectrometry. *Nature Protocols*, *6*, 1060-1083.

Dunn, W. B., Broadhurst, D. I., Atherton, H. J., Goodacre, R., & Griffin, J. L. (2011b). Systems level studies of mammalian metabolomes : the roles of mass spectrometry and nuclear magnetic resonance spectroscopy. *Chemical Society Reviews*, *40*, 387-426.

Dunn, W. B., Goodacre, R., Neyses, L., & Mamas, M. (2011c). Integration of metabolomics in heart disease and diabetes research : current achievements and future outlook. *Bioanalysis*, *3*, 2205-2222.

Dunn, W. B., Lin, W., Broadhurst, D., Begley, P., Brown, M., Zelena, E., Vaughan, A. A., et al. (2014). Molecular phenotyping of a UK population : defining the human serum metabolome. *Metabolomics*, *11*, 9-26.

Dyntar, D., Eppenberger-eberhardt, M., Maedler, K., Pruschy, M., Eppenberger, H. M., Spinas, G. A., & Donath, M. Y. (2001). Glucose and Palmitic Acid Induce Degeneration of Myofibrils and Modulate Apoptosis in Rat Adult. *Diabetes*, *50*, 2105-2113.

Ehtisham, S., Hattersley, A., Dunger, D., & Barrett, T. (2004). First UK survey of paediatric type 2 diabetes and MODY. *Archives of Disease in Childhood*, *89*, 526-529.

Factor, S., Minase, T., & Sonnenblick, E. (1980). Clinical and morphological features of human hypertensive-diabetic cardiomyopathy. *American Heart Journal*, *99*, 446-458.

Fajans, S., Bell, G., & Polonsky, K. (2001). MOLECULAR MECHANISMS AND CLINICAL PATHOPHYSIOLOGY OF MATURITY ONSET DIABETES OF THE YOUNG. *The New England Journal of Medicine*, *345*, 971-980.

Fang, Z. Y., Prins, J. B., & Marwick, T. H. (2004). Diabetic cardiomyopathy: evidence, mechanisms, and therapeutic implications. *Endocrine reviews*, *25*, 543-567.

Farooqi, I. S., Wangensteen, T., Collins, S., Kimber, W., Matarese, G., Keogh, J. M., Lank, E., et al. (2007). Clinical and molecular genetic spectrum of congenital deficiency of the leptin receptor. *The New England journal of medicine*, *356*, 237-47.

Feng, M., Whitesall, S., Zhang, Y., Beibel, M., Alecy, L. D., & Dipetrillo, K. (2008). Validation of Volume – Pressure Recording Tail-Cuff Blood Pressure Measurements. *American Journal of Hypertension*, *21*, 6-9.

Finck, B., Lehman, J., & Leone, T. (2002). The cardiac phenotype induced by PPARalpha overexpression mimics that caused by diabetes mellitus. *The Journal of Clinical Investigation*, *109*, 121-130.

Finehout, E., & Lee, K. (2004). An Introduction to Mass Spectrometry Applications in Biological Research. *Biochemistry and Molecular Biology Education*, *32*, 93-100.

Friedman, J. E., Sun, Y., Ishizuka, T., Farrell, C. J., Mccormack, S. E., Herron, L. M., Hakimi, P., et al. (1997). Phosphoenolpyruvate Carboxykinase (GTP) Gene Transcription and Hyperglycaemia Are Regulated by Glucocorticoids in Genetically Obese db / db Transgenic Mice. *The Journal of Biological Chemistry*, *272*, 31475-31481.

Fuentes-Antrás, J., Picatoste, B., Ramírez, E., Egido, J., Tuñón, J., & Lorenzo, Ó. (2015). Targeting metabolic disturbance in the diabetic heart. *Cardiovascular Diabetology*, *17*, 1-11.

Gibbons, S. (2011). *Insights into the cardiovascular complications of a novel mouse model of Diabetes Mellitus: a mechanistic view*.

Gil, A., Silvan, G., Illera, M., & Illera, J. (2004). he effects of anesthesia on the clinical chemistry of New Zealand White rabbits. *Contemporary Topics in Laboratory Animal Science*, *43*, 25-29.

Golfman, L. S., Wilson, C. R., Sharma, S., Burgmaier, M., Young, M. E., Guthrie, P. H., Arsdall, M. V., et al. (2005). Activation of PPARg enhances myocardial glucose oxidation and improves contractile function in isolated working hearts of ZDF rats. *American journal of Physiology. Endocrinology and Metabolism*, *1*, 328-336.

Grossman, E. (2009). Should We Treat Prehypertension in Diabetes? *Diabetes Care*, *32*, 0-3.

Grossman, E., & Messerli, F. (2008). Hypertension and Diabetes. *Advanced cardiology*, *45*, 82-106.

Guo, X., & Lankmayr, E. (2012). Hyphenated Techniques in Gas Chromatography. *Advanced Gas Chromatography - Progress in Agricultural, Biomedical and Industrial Applications*, *21*, 3-26.

Gurusamy, N., Watanabe, K., Ma, M., Zhang, S., Muslin, A. J., Kodama, M., & Aizawa, Y. (2005). Inactivation of 14-3-3 protein exacerbates cardiac hypertrophy and fibrosis through enhanced expression of protein kinase C beta 2 in experimental diabetes. *Biological & pharmaceutical bulletin*, *28*, 957-962.

Halket, J. M., Waterman, D., Przyborowska, A. M., Patel, R. K. P., & Fraser, P. D. (2005). Chemical derivatization and mass spectral libraries in metabolic profiling by GC / MS and LC / MS / MS. *Journal of experimental Botany*, *56*, 219-243.

Hall, R. K., Yamasaki, T., Kucera, T., Waltner-law, M., Brien, R. O., & Granner, D. K. (2000). Regulation of Phosphoenolpyruvate Carboxykinase and Insulin-like Growth Factor-binding Protein-1 Gene Expression by Insulin. *The Journal of Biological Chemistry*, *275*, 30169-30175.

Hayat, S. a, Patel, B., Khattar, R. S., & Malik, R. a. (2004). Diabetic cardiomyopathy: mechanisms, diagnosis and treatment. *Clinical science*, *107*, 539-557.

IDF. (2009). The economic impacts of diabetes. *International Diabetes Federation*.

IDF. (2015). International Diabetes Federation. *Diabetes Atlas* (7th ed.). Brussels, Belgium.

Ivosev, G., Burton, L., & Bonner, R. (2008). Dimensionality Reduction and Visualization in Principal Component Analysis. *Analytical Chemistry*, *80*, 4933-4944.

Jagasia, D., Whiting, J. M., Concato, J., Pfau, S., & Mcnulty, P. H. (2001). Effect of Non – Insulin-Dependent Diabetes Mellitus on Myocardial Insulin Responsiveness in Patients With Ischemic Heart Disease. *Circulation*, *103*, 1734-1739.

Jessup, M., Abraham, W. T., Casey, D. E., Feldman, A. M., Francis, G. S., Ganiats, T. G., Konstam, M. a, et al. (2009). ACCF/AHA Guidelines for the Diagnosis and Management of Heart Failure in Adults: a report of the American College of Cardiology Foundation/American Heart Association Task Force on Practice Guidelines. *Circulation*, *119*, 1977-2016.

Jung, O., Brandes, R. P., Kim, I.-H., Schweda, F., Schmidt, R., Hammock, B. D., Busse, R., et al. (2005). Soluble epoxide hydrolase is a main effector of angiotensin II-induced hypertension. *Hypertension*, *45*, 759-765.

Justice, M. J. (2000). Capitalizing on large-scale mouse mutagenesis screens. *Nature reviews. Genetics*, *1*, 109-115.

Kannel, WB. (2000). Incidence and epidemiology of heart failure. *Heart Failure Reviews*, *5*, 167-173.

Kannel, William. (2009). Hypertension: Reflections on Risks and Prognostication. *Medical Clinics of North America*, *93*, 1-23.

Kanwal, A., Fazal, S., & Ismail, M. (2011). A narrative insight to maturity-onset diabetes of the young. *Clinical Reviews and Opinions*, *3*, 6-13.

Karnieli, E., & Armoni, M. (2008). Transcriptional regulation of the insulin-responsive glucose transporter GLUT4 gene : from physiology to pathology. *American journal of physiology. Endocrinology and Metabolism*, *295*, 38-45.

Kell, D., & Oliver, S. (2004). Here is the evidence, now what is the hypothesis? The complementary roles of inductive and hypothesis-driven science in the post-genomic era. *Bioessays*, *26*, 99-105.

Koek, M. M., Muilwijk, B., Werf, J. V. D., & Hankemeier, T. (2006). Microbial Metabolomics with Gas Chromatography / Mass Spectrometry. *Analytical Chemistry*, *78*, 1272-1281.

Kopka, J., Schauer, N., Krueger, S., Birkemeyer, C., Usadel, B., Bergmüller, E., Dörmann, P., et al. (2005). Systems biology: the Golm Metabolome Database. *Bioinformatics*, *21*, 1635-1638.

Lassegue, B., Alexander, A., Nickenig, G., Clark, M., & Griendling, K. (1995). Angiotensin II Down-regulates the Vascular Smooth Muscle AT1 Receptor by Transcriptional and Post-transcriptional Mechanisms : Evidence for

Homologous and Heterologous Regulation. *Molecular Pharmacology*, *48*, 601-609.

Lavrentyev, E. N., Estes, A. M., & Malik, K. U. (2007). Mechanism of High Glucose – Induced Angiotensin II Production in Rat Vascular Smooth Muscle Cells. *Circulation Research*, *101*, 455-464.

Ledermann, H. (1995). Is maturity onset diabetes at young age (MODY) more common in Europe than previously assumed? *Lancet*, *11*, 648.

Liu, J., Jahn, L. A., Fowler, D. E., Barrett, E. J., & Cao, W. (2011). Free Fatty Acids Induce Insulin Resistance in Both Cardiac and Skeletal Muscle Microvasculature in Humans. *Journal of Clinical Endocrinology and Metabolism*, *96*, 438-446.

Liu, W., Zi, M., Jin, J., Prehar, S., Oceandy, D., Kimura, T. E., Lei, M., et al. (2009). Cardiac-specific deletion of mkk4 reveals its role in pathological hypertrophic remodeling but not in physiological cardiac growth. *Circulation research*, *104*, 905-914.

Livak, K. J., & Schmittgen, T. D. (2001). Analysis of Relative Gene Expression Data Using Real- Time Quantitative PCR and the 2-DeltaDelta CT Method Method. *Methods*, *408*, 402-408.

Luiken, J. J. F. P., Koonen, D. P. Y., Willems, J., Zorzano, A., Becker, C., Fischer, Y., Tandon, N. N., et al. (2002). Insulin Stimulates Long-Chain Fatty Acid Utilization by Rat Cardiac Myocytes Through Cellular Redistribution of FAT/CD36. *Diabetes*, *51*, 3113-3119.

Marieb, E., & Hoehn, K. (2005). *Human Anatomy & Physiology* (7th ed.). San Francisco, USA: Pearson Benjamin Cummings.

Matsumoto, M., Pocai, A., Rossetti, L., Depinho, R. A., & Accili, D. (2007). Article Impaired Regulation of Hepatic Glucose Production in Mice Lacking the Forkhead Transcription Factor Foxo1 in Liver. *Cell Metabolism*, *6*, 208-216.

McMurray, J. J., & Stewart, S. (2000). Epidemiology, aetiology, and prognosis of heart failure. *Heart British Cardiac Society*, *83*, 596-602.

Meyer, C., Stumvoll, M., Nadkarni, V., Dostou, J., Mitrakou, A., & Gerich, J. (1998). Abnormal Renal and Hepatic Glucose Metabolism in Type 2 Diabetes Mellitus. *Journal of Clinical Investigation*, *102*, 619-624.

Monassier, L., Combe, R., & Fertak, L. (2006). Mouse models of hypertension. *Drug Discovery Today: Disease Models*, *3*, 273-281.

Morrish, N., Wang, S.-L., Stevens, L., & Fuller, J. (2001). Mortality and causes of death in the WHO Multinational Study of Vascular Disease in Diabetes. *Diabetologia*, *44*, S14-S21.

Munoz, P., Chillaron, J., Camps, M., Castello, A., Furriols, M., Testar, X., Palucin, M., et al. (1996). Evidence for Posttranscriptional Regulation of GLUT4 Expression in Muscle and Adipose Tissue from Streptozotocin-Induced Diabetic and Benfluorex-Treated Rats. *Biochemical Pharmacology*, *52*, 1665-1673.

Murarka, S., & Movahed, M. R. (2010). Diabetic cardiomyopathy. *Journal of Cardiac Failure*, *16*, 971-979.

Murphy, D. (2002). Gene expression studies using microarrays: principles, problems, and prospects. *Advances in Physiology Education*, *26*, 256-270.

Nakae, J., Iii, W. H. B., Kitamura, T., Cavenee, W. K., Wright, C. V. E., Arden, K. C., & Accili, D. (2002). Regulation of insulin action and pancreatic β-cell function by mutated alleles of the gene encoding forkhead transcription factor Foxo1. *Nature Genetics*, *32*, 245-253.

Nishino, N., Tamori, Y., & Kasuga, M. (2007). Insulin Efficiently Stores Triglycerides in Adipocytes by Inhibiting Lipolysis and Repressing PGC-1α Induction . *Kobe Journal of Medical Sciences*, *53*, 99-106.

Novakova, L., Matysov, L., & Solich, P. (2006). Advantages of application of UPLC in pharmaceutical analysis. *Talanta*, *68*, 908-918.

Ong, F. S., Lin, C. X., Campbell, D. J., Okwan-Duodu, D., Chen, X., Blackwell, W.-L. B., Shah, K. H., et al. (2012). Increased angiotension II induced hypertrophy and inflammatory cytokines in mice lacking angiotensin converting enzyme n domain activity. *Hypertension*, *59*, 283-290.

Osbak, K. K., Colclough, K., Saint-martin, C., Beer, N. L., Bellanne, C., Ellard, S., & Gloyn, A. L. (2009). Update on Mutations in Glucokinase (GCK), Which Cause Maturity-Onset Diabetes of the Young , Permanent Neonatal Diabetes , and Hyperinsulinemic Hypoglycemia. *Human Mutation*, *1*, 1512-1526.

Park, T.S., & Goldberg, I. (2012). Sphingolipids, Lipotoxic Cardiomyopathy, and Cardiac Failure. *Heart Failure Clinics*, *8*, 633-641.

Park, T.-sik, Hu, Y., Noh, H.lim, Drosatos, K., Okajima, K., Buchanan, J., Tuinei, J., et al. (2008). Ceramide is a cardiotoxin in lipotoxic cardiomyopathy. *Journal of Lipid Research*, *49*, 2101-2112.

Park, T.-sik, Yamashita, H., Blaner, W. S., & Goldberg, I. J. (2007). Lipids in the heart : a source of fuel and a source of toxins. *Current Opinion in Lipidology*, *18*, 277-282.

Peterson, L. R., Herrero, P., Schechtman, K. B., Racette, S. B., Waggoner, A. D., Kisrieva-ware, Z., Dence, C., et al. (2004). Effect of Obesity and Insulin Resistance on Myocardial Substrate Metabolism and Efficiency in Young Women. *Circulation*, *109*, 2191-2197.

Poornima, I. G., Parikh, P., & Shannon, R. P. (2006). Diabetic cardiomyopathy: the search for a unifying hypothesis. *Circulation research*, *98*, 596-605.

Reece, E. A., Ji, I., & Wu, Y.-king. (2006). Characterization of differential gene expression profiles in diabetic embryopathy using DNA microarray analysis. *American Journal of Obstetrics and Gynecology*, *195*, 10-15.

Regan, T. J., Lyons, M. M., Ahmed, S. S., Levinson, G. E., Oldewurtel, H. a, Ahmad, M. R., & Haider, B. (1977). Evidence for cardiomyopathy in familial diabetes mellitus. *The Journal of clinical investigation*, *60*, 884-899.

Rockman, M. V., & Kruglyak, L. (2006). Genetics of global gene expression. *Nature*, *7*, 862-872.

Roglic, G., Unwin, N., Bennett, P., & Mathers, C. (2005). The Burden of Mortality Attributable to Diabetes. *Diabetes*, *28*, 2130-2135.

Rubler, S., Dlugash, J., Yuceoglu, Y. Z., Kumral, T., Branwood, a W., & Grishman, A. (1972). New type of cardiomyopathy associated with diabetic glomerulosclerosis. *The American journal of cardiology*, *30*, 595-602.

Ruggenenti, M. P., & Iliev, M. I. (2008). Preventing Left Ventricular Hypertrophy by ACE Inhibition in Hypertensive Patients With Type 2 Diabetes. *Diabetes Care*, *31*, 1629-1634.

Saito, F., Kawaguchi, M., Izumida, J., Asakura, T., Maehara, K., & Maruyama, Y. (2003). Alteration in haemodynamics and pathological changes in the cardiovascular system during the development of Type 2 diabetes mellitus in OLETF rats. *Diabetologia*, *46*, 1161-1169.

Samuel, V. T., Choi, C. S., Phillips, T. G., Romanelli, A. J., Geisler, J. G., Bhanot, S., Mckay, R., et al. (2006). Targeting Foxo1 in Mice Using Antisense Oligonucleotide Improves Hepatic and Peripheral Insulin Action. *Diabetes*, *55*, 2042-2050.

Schannwell, C., Schneppenheim, M., & Perings, S. (2002). Left Ventricular Diastolic Dysfunction as an Early Manifestation of Diabetic Cardiomyopathy. *Cardiology*, 33-39.

Semeniuk, L. M., Kryski, A. J., Severson, D. L., Lisa, M., Kryski, A. J., & David, L. (2002). Echocardiographic assessment of cardiac function in diabetic db / db and transgenic db / db-hGLUT4 mice. *American Journal of Physiology. Heart and Circulatory Physiology*, *1*, 976-982.

Shulman, G. I., & others. (2000). Cellular mechanisms of insulin resistance. *Journal of Clinical Investigation*, *106*, 171–176.

Singh, R., Barden, A., Mori, T., & Beilin, L. (2001). Advanced glycation end-products : a review. *Diabetologia*, *44*, 129-146.

Slonim, D. K., & Yanai, I. (2009). Getting Started in Gene Expression Microarray Analysis. *PLOS Computational Biology*, *5*, 3-6.

Sowers, J. R., & Epstein, M. (1995). Diabetes Mellitus and Associated Hypertension, Vascular Disease, and Nephropathy An Update. *Hypertension*, *26*, 869-879.

Steck, A. K., & Winter, W. E. (2011). Review on monogenic diabetes. *Current opinion in endocrinology, diabetes, and obesity*, *18*, 252-258.

Stride, A., & Hattersley, A. (2002). Different genes, different diabetes: lessons from maturity-onset diabetes of the young. *Annals of Medicine*, *34*, 207-216.

Suhre, K., Altmaier, E., Belcredi, P., Meisinger, C., Do, A., Chang, D., Milburn, M. V., et al. (2010). Metabolic Footprint of Diabetes : A Multiplatform Metabolomics Study in an Epidemiological Setting. *PLOS ONE*, *5*, 1-11.

Summers, S. A. (2006). Ceramides in insulin resistance and lipotoxicity. *Progress in lipid research*, *45*, 42-72.

Tanaka, Y., Konno, N., & Kako, K. J. (1992). Mitochondrial dysfunction observed in situ in cardiomyocytes of rats in experimental diabetes. *Cardiovascular research*, *26*, 409-414.

Tautenhahn, R., Böttcher, C., & Neumann, S. (2008). Highly sensitive feature detection for high resolution LC/MS. *BMC Bioinformatics*, *16*, 1-16.

Thanabalasingham, G., & Owen, K. R. (2011). Diagnosis and management of maturity onset diabetes of the young (MODY). *British Medical Journal*, *343*,

Touyz, R., He, G., Deng, L., & Schiffrin, E. (1999). Role of Extracellular Signal-Regulated Kinases in Angiotensin II – Stimulated Contraction of Smooth Muscle Cells From Human Resistance Arteries. *Circulation*, *99*, 392-399.

Toye, A., Moir, L., Hugill, A., & Bentley, L. (2004). A new mouse model of type 2 diabetes, produced by N-ethyl-nitrosourea mutagenesis, is the result of a missense mutation in the glucokinase gene. *Diabetes*, *53*, 1577-1583.

Tremblay, F., Dubois, M., & Marette, A. (2003). Regulation of GLUT4 traffic and function by insulin and contraction in skeletal muscle. *Frontiers in Bioscience*, *8*, d1072-1084.

Ugarte, M., Brown, M., Hollywood, K. A., Cooper, G. J., Bishop, P. N., & Dunn, W. B. (2012). Metabolomic analysis of rat serum in streptozotocin-induced diabetes and after treatment with oral triethylenetetramine (TETA). *Genome Medicine*, *4*, 1-15.

Utriainen, T., Takala, T., Luotolahti, M., Laine, H., Ruotsalainen, U., Haaparanta, M., & Nuutila, P. (1998). Insulin resistance characterizes glucose uptake in skeletal muscle but not in the heart in NIDDM. *Diabetologia*, *41*, 555-559.

Velho, G., Blanché, H., Vaxillaire, M., Bellanné-Chantelot, C., Pardini, V. C., Timsit, J., Passa, P., et al. (1997). Identification of 14 new glucokinase mutations and description of the clinical profile of 42 MODY-2 families. *Diabetologia*, *40*, 217-224.

WHO. (2004). diabetes action now. *World Health Organization*.

WHO. (2006). Definition and diagnosis of diabetes mellitus and intermediate hyperglycaemia. *World Health Organisation*.

WHO. (2012). Hypertension Fact sheet. *World Health Organization.*

WHO. (2013). A global brief of Hypertension. *World Health Organization.*

Wada, J., Zhang, H., Tsuchiyama, Y., Hiragushi, K., Hida, K., Shikara, K., Kanwar, Y., et al. (2001). Gene expression profile in streptozotocin-induced diabetic mice kidneys undergoing glomerulosclerosis. *Kidney International*, *59*, 1363-1373.

Wang, R., Bouwens, L., & Kloppel, G. (1994). Beta-cell proliferation in normal and streptozotocin-treated newborn rats: site, dynamics and capacity. *Diabetologia*, *37*, 1088-1096.

Williams, G., & Pickup, J. (2004). Handbook of Diabetes (3rd ed.). Oxford: Blackwell Publishing.

Wilson, P. W. F., D'Agostino, R. B., Levy, D., Belanger, A. M., Silbershatz, H., & Kannel, W. B. (1998). Prediction of Coronary Heart Disease Using Risk Factor Categories. *Circulation*, *97*, 1837–1847. Am Heart Assoc.

Wold, L. E., Ceylan-isik, A. F., & Ren, J. (2005). Oxidative stress and stress signaling : menace of diabetic cardiomyopathy. *Acta Pharmacologica Sinica*, *26*, 908-917.

Wu, P., Sato, J., Zhao, Y., Jaskiewicz, J., Popov, K. M., & Harris, R. A. (1998). Starvation and diabetes increase the amount of pyruvate dehydrogenase kinase isoenzyme 4 in rat heart. *Biochemistry Journal*, *201*, 197-201.

Yagyu, H., Chen, G., Yokoyama, M., Hirata, K., Augustus, A., Kako, Y., Seo, T., et al. (2003). Lipoprotein lipase (LpL) on the surface of cardiomyocytes increases lipid uptake and produces a cardiomyopathy. *The Journal of Clinical Investigation*, *111*, 419-427.

Yan, R., Shan, H., Lin, L., Zhang, M., Diao, Y., Zhu, Y., & Wei, J. (2016). Changes of cardiac structure and Ang II in streptozotocin-induced diabetic cardiomyopathy rats. *Journal of Xi'an Jiaotong University*, *37*, 199-203.

Zhang, K., Li, L., Qi, Y., Zhu, X., Gan, B., Depinho, R. A., Averitt, T., et al. (2012). Hepatic Suppression of Foxo1 and Foxo3 Causes Hypoglycemia and Hyperlipidemia in Mice. *Endocrinology*, *153*, 631-646.

Zhang, W., Patil, S., Chauhan, B., Guo, S., Powell, D. R., Le, J., Klotsas, A., et al. (2006). FoxO1 Regulates Multiple Metabolic Pathways in the Liver. *The Journal of Biological Chemistry*, *281*, 10105-10117.

Zhang, X., & Chen, C. (2012). A new insight of mechanisms, diagnosis and treatment of diabetic cardiomyopathy. *Endocrine Practice*, *18,* 146-151.

Zhou, Y.-ting, Grayburn, P., Karim, A., Shimabukuro, M., Higa, M., Baetens, D., Orci, L., et al. (2000). Lipotoxic heart disease in obese rats : Implications for human obesity. *Proceedings of the National Academy of Sciences*, *97*, 1784-1789.

van Hoeven, K., & Factor, S. M. (1990). A Comparison of the Pathological Spectrum of Hypertensive , Diabetic , and Hypertensive-Diabetic Heart Disease. *Circulation*, *82*, 848-856.